AD-A067 035 TRACOR INC AUSTIN TEX F/G 17/1
LONG RANGE UPGRADING OF THE AN/SQS-26.(U)
AUG 67 C H HAYES NOBSR-95149
UNCLASSIFIED TRACOR-67-693-C NL

1 OF 2
AD A
067035

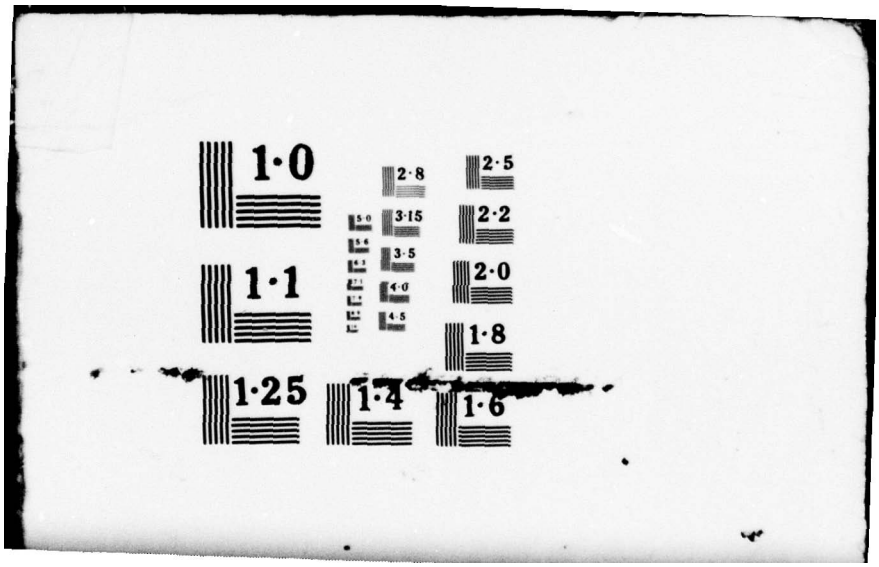
1·0
1·1
1·25
1·4
1·6
1·8
2·0
2·2
2·5
2·8
3·15
3·5
4·0
4·5

MOST Project I

LEVEL II

(1)

Contract NObsr-95149
Project Serial SS041-001
Tasks 8156, 8193
TRACOR Project 002 019 09
Document Number 67-693-C

SUMMARY REPORT

LONG RANGE UPGRADING OF THE AN/SQS-26(U)

by

Charles H. Hayes

Submitted to:

Commander,
Naval Ship Systems Command
Department of the Navy
Washington, D. C. 20360
Attention: Code PMS-87

30 August 1967

TRACOR

6500 Tracor Lane, Austin, Texas 78721, AC 512/926-2800

UNCLASSIFIED
~~CONFIDENTIAL~~

TRACOR, INC. 6500 TRACOR LANE, AUSTIN, TEXAS 78721

(15) Contract NObsr-95149
Project Serial SS041-001
Tasks 8156, 8193
TRACOR Project 002 019 09
Document Number 67-693-C

(14) TRACOR-67-693-C

(16) SS041

(17) SS041001

SUMMARY REPORT

(6) LONG RANGE UPGRADING OF THE AN/SQS-26(U).

by

(10) Charles H. Hayes

(9) Final repts. Submitted to: (12) 110p.

Commander,
Naval Ship Systems Command
Department of the Navy
Washington, D. C. 20360
Attention: Code PMS-87

(11) 30 August ~~1st~~ 1967

Approved by

E. A. Tucker
E. A. Tucker
Program Manager

Submitted by

C. H. Hayes
C. H. Hayes
Project Director

UNCLASSIFIED
~~CONFIDENTIAL~~

352 100

TRACOR 6500 TRACOR LANE, AUSTIN, TEXAS 78721

ABSTRACT AND ACKNOWLEDGEMENTS

This is the final report on Task 2 of Contract NObsr-95149, whose purpose was to generate ideas and concepts which could lead to a long range upgrading of the AN/SQS-26 Sonar.

Echo energy splitting, often erroneously called correlation loss, arises because the returning echo consists of a coherent sum of a number of discrete echoes from different scattering centers, spread out in time and Doppler shift. A technique for measuring the extent of echo energy splitting, and two techniques for building processors whose gains approximate those of full coherent processing with reduced sensitivity to energy splitting are described.

The use of linear matched filter techniques to normalize the output of a temporal processor without sacrifice of processing gain is described. The relative invariance of the ratio of the mean to the standard deviation of the unnormalized correlator output makes such techniques practicable.

The use of signal processing techniques that enhance the signal-to-noise ratio of a return prior to display was investigated as a means of improving precision bearing measurements on the Sector Scan Indicator (SSI).

Analyses of AN/SQS-26(BX) data were made, primarily to check the signal processor gain, the uniformity of the A Scan, and the minimum detectable signal levels.

The efforts of a number of people are reflected in this report. In addition to the work of Peter Brown on the overall task the author wishes to acknowledge, in particular, the considerable assistance of Hugh Reeder, who prepared Chapter 4, and of Bill Butler and Worth Duderstadt, who prepared Chapter 5.

TRACOR 6500 TRACOR LANE, AUSTIN, TEXAS 78721

TABLE OF CONTENTS

TRACOR 6500 TRACOR LANE, AUSTIN, TEXAS 78721

TABLE OF CONTENTS (cont'd.)

TRACOR 6500 TRACOR LANE, AUSTIN, TEXAS 78721

LIST OF ILLUSTRATIONS

TRACOR 6500 TRACOR LANE, AUSTIN, TEXAS 78721

1. INTRODUCTION

The purpose of this task was to generate and investigate ideas and concepts which could lead to a long range upgrading of the AN/SQS-26 Sonar. The techniques to be investigated could involve analog and digital means anywhere throughout the system. Although this task charter is extremely broad, efforts were made to restrict the work somewhat to consideration of portions of the system where the problems seemed more severe and where the concepts to be investigated could provide relatively rapid fallout. The emphasis in this task has been placed on the "back end" of the system. This includes portions of the receiver starting at the input to the processor. Several areas have been investigated which seem to provide many of the major problems and fundamental limitations which still remain in modern sonar systems.

One problem area which involves both the signal processor and the pulse code has been called echo energy splitting. When real sonar echoes are processed by a linear correlator, a degradation of correlation performance from the theoretical value is often observed. Although this phenomenon is frequently called "correlation loss" it is entirely explainable in terms of multiple returns. It results in a time-spreading in the correlator output in excess of that produced by a perfectly coherent, single signal and causes a fundamental limitation to the processing gain which may be achieved with a given pulse using fully coherent signal processing. This effect gives rise to approximately 2 dB of degradation in the present SQS-26 and very effectively restricts the maximum values of bandwidth and pulse duration which could be employed. Two techniques are investigated and reported here which could lead to processing gains very close to that achievable with a full coherent processor and yet result in a processor which is fairly insensitive to the splitting effects. Successful implementation of this sort of processor could lead to the use of much larger bandwidth time (BT) products, with the associated increased processing gain.

A second area of weakness in modern sonar systems is in achieving proper temporal normalization. This is a quite serious problem since it very grossly affects the dynamic range required in the display. Indeed, in some of the earlier sonar systems the normalization was so poor that during the early part of an echo cycle the screen would be totally painted and during the later portion of an echo cycle the threshold would be effectively so far above the noise mean that the probability of a signal marking the display was quite low. This meant that only a very narrow range interval was usefully displayed. Normalization may be obtained, of course, with clipping techniques. However, linear matched processing seems to offer enough significant gains to be worth implementing, and techniques of obtaining suitably normalized outputs from linear processors are investigated and included in this report.

A third major problem area in present sonars is that of designing adequate displays. Many display design problems arise primarily from the need of supplying ping-to-ping integration on a multiplicity of data channels. Some of the work done on this task indicates that it may be somewhat simpler from an engineering point of view to resort to computer systems in ping-to-ping integration and display the final results in a form somewhat different from the conventional B Scan rather than to attempt to match the receiver-display-operator system in the conventional manner through a series of degrading and perhaps disastrous engineering compromises.

A large portion of the work carried out on this task was done in direct cooperation with and at the direction of the U. S. Navy Underwater Sound Laboratory. Many of the specific questions answered in connection with this work fall directly into the above mentioned areas and the results are therefore included in these discussions. Chapter 5 of this report contains a summary of analyses of AN/SQS-26 BX data. These analyses were primarily performed in order to check the processor gain, the uniformity of the A Scan, and the minimum detectable signal levels.

TRACOR 6500 TRACOR LANE, AUSTIN, TEXAS 78721

2. ECHO ENERGY SPLITTING

2.1 GENERAL DISCUSSION OF ECHO ENERGY SPLITTING

When matched filter or replica correlator techniques are used to process sea data a phenomenon occurs which has been called by many "correlation loss." This phenomenon may be described as follows. A signal is transmitted into the water and an exact copy of that transmitted signal is used as a reference in the correlator. If the total energy at the input is measured and compared with the processor output, the S/N_o produced by this incoming energy is less than that predicted by theory.

Two basically different phenomena could account for this effect. First, the returning echo may have suffered loss of internal phase coherence, so that it no longer properly matches the replica. Second, the returning echo may consist of a coherent sum of a number of discrete echoes from different scattering centers, with the internal phase of each remaining intact. These component returns may differ either in time or in Doppler shift. The second explanation can be verified by measurements. If the input signal-to-noise ratio is corrected to reflect only the signal energy in the largest arrival, the output signal-to-noise ratio agrees quite well with the theory. Since this "echo energy splitting" is sufficient to account for the observed degradation, it is felt that loss of phase coherence is not an important factor and that the term "correlation loss" is somewhat misleading.

Since the resolution of a pulse in time is inversely proportional to the bandwidth, and the resolution in Doppler is inversely proportional to the time duration of the signal, it follows that going to larger BT values using correlators to process the data increases the amount of degradation incurred due to echo energy splitting. With the present signal parameters in the SQS-26 the degradation amounts to about to 2dB. Energy splitting thus limits the useful maximum BT product for coherent processing and prevents one from taking advantage of the signal processing gains which could be had using larger BT values.

TRACOR 6500 TRACOR LANE, AUSTIN, TEXAS 78721

In this chapter the measurement technique for echo energy splitting, and two different techniques for building processors whose gains approximate full coherent processing but which are greatly reduced in sensitivity to echo energy splitting will be described. Since adequate sea data with appropriate variations in signal parameters are not available, a model was developed to generate simulated sea echoes. With this model any required number of signals with various degrees of echo energy splitting and various signal parameters may be generated. These echoes are used to compare some of the processors and their sensitivities to echo energy splitting.

2.2. ECHO ENERGY SPLITTING MEASUREMENTS

The extent of echo energy splitting for FM slides, whether caused by multiple time delay or multiple Doppler, may be measured by the following approach:

In Fig. 2-1, S_1 represents a section of a correlogram, one portion of which contains an echo. The entire echo is contained in the interval S_2. Sections S_3 contain noise only, and S_4 is a resolution interval centered on the signal peak.

Assuming that the average noise power in S_3 is the same as in S_2, the noise can be subtracted out to obtain the total signal energy in S_2. The energy of the largest resolvable arrival, in S_4, can be found by the same means.

An energy splitting factor may be defined as 10 times the logarithm of the ratio of the signal energy in the largest resolvable arrival to the total signal. If no splitting occurred, the ratio would be 1, giving a 0 dB energy splitting factor. For most real echoes splitting occurs, and the ratio would be less than 1, giving a negative energy splitting factor.

The evaluation of processing gain for the linear correlation process depends upon obtaining a meaningful measurement of both input and output (S/N). The input (S/N) is measured

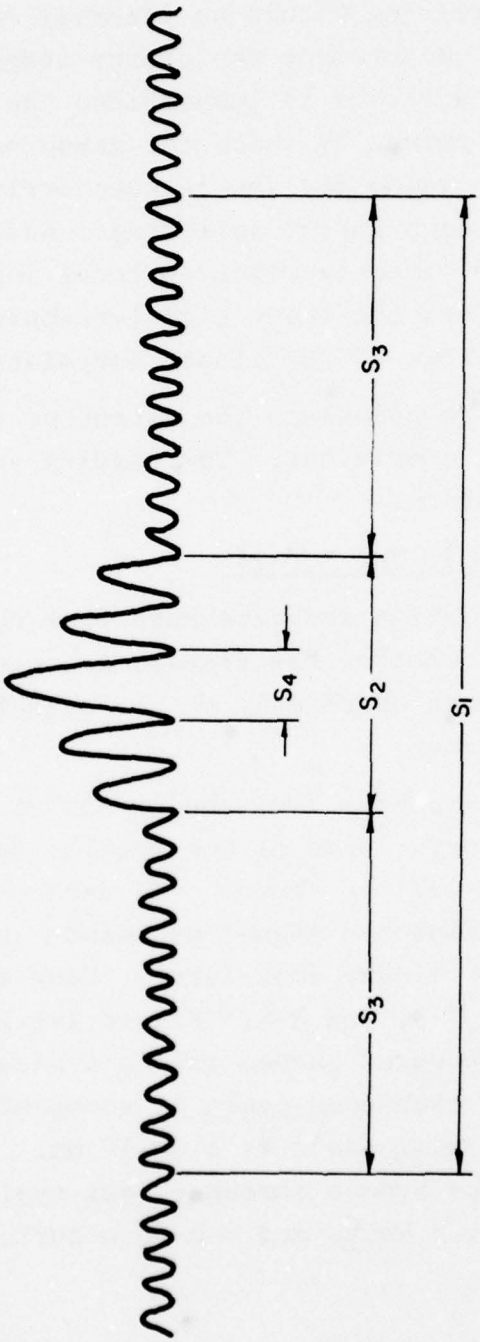

FIG. 2-1 -CORRELOGRAM WITH ECHO

TRACOR, INC. 1 DWG. 6-13-1962
AUSTIN, TEXAS 9-14-66 WITTENBORN/SL

in terms of the echo energy arriving within an interval equal to the pulse length. In this measurement the energy associated with any overlapped, separate arrivals is lumped into the value of input (S/N) obtained. The amount by which the measured value of (S/N) differs from the true value for the largest arrival is proportional to the degree of echo energy splitting. Adding the energy splitting factor to the directly measured total input signal-to-noise ratio in dB gives the input signal-to-noise ratio associated with the largest output of the linear correlator.

This method was used to calculate the extent of echo energy splitting under various conditions. The results are described in the following section.

2.3 ECHO ENERGY SPLITTING IN THE SQS-26

Since the output statistics and data rate from the processor will remain the same whether the signals are clean or structured performance curves based only on the signal-to-noise ratio will be adequate here.

Numerous bottom bounce echoes from the AN/SQS-26 have been processed at this laboratory. Some of the results for ½ second 100 Hz FM slide signals will be shown. The data were recorded at the input to the shipboard signal processor and processed using an ideal 12-bit linear correlator. Four echo cycles are shown in Figs. 2-2, 2-3, and 2-4. Figure 2-2 shows two echo cycles containing structured echoes from a typical bottom bounce run. The raw data from each echo cycle is shown with the correlator outputs below. The time scale is 1 mm=10 ms. Figures 2-3 and 2-4 show two echo cycles from a somewhat less typical run. Here, the target was closing at 8 knots and the structuring is seen to be severe.

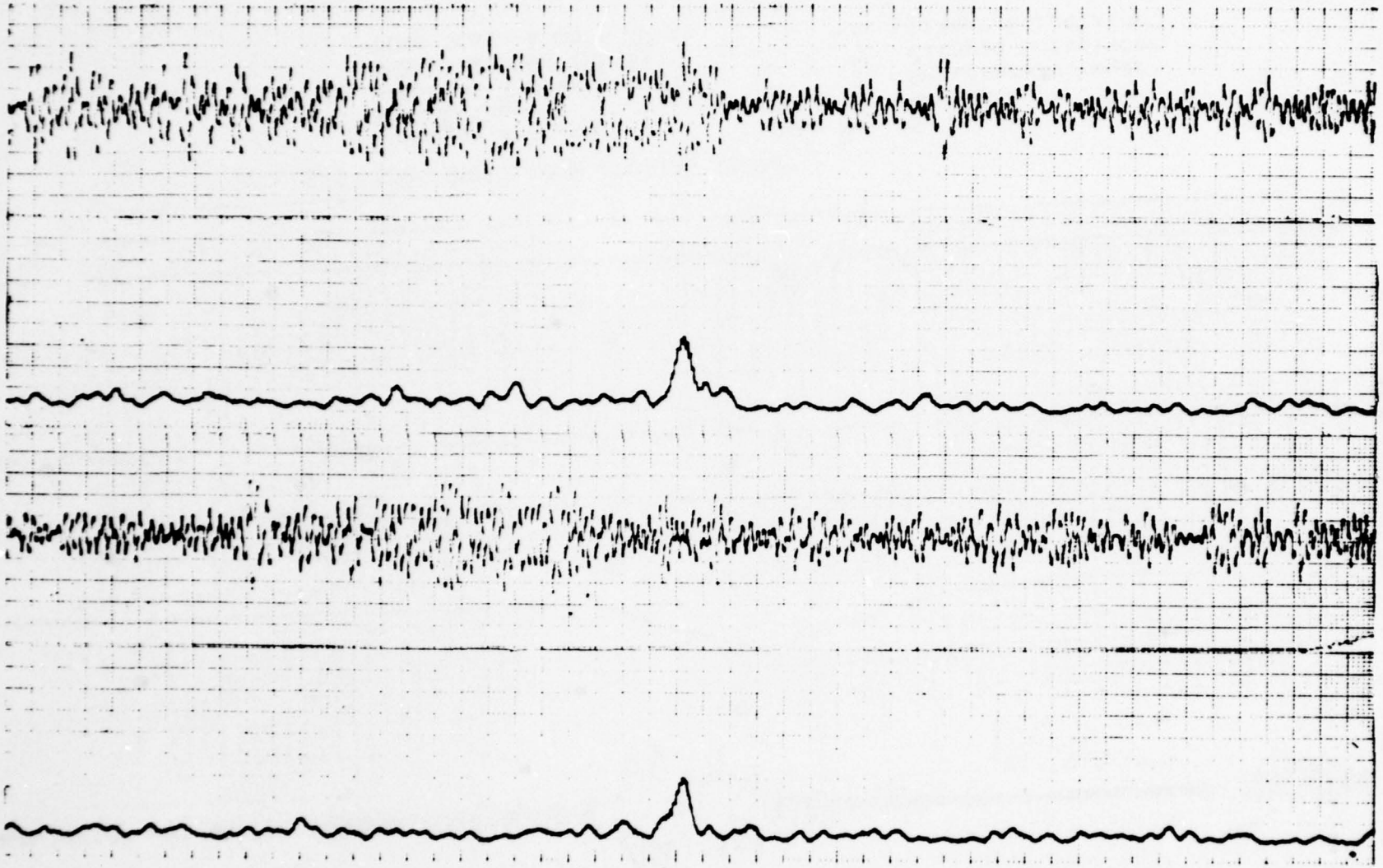

CONFIDENTIAL

FIG. 2-2 TWO TYPICAL ECHOES FROM THE AN/SQS-26.

Time Scale: 1 mm = 10 ms
Trace 1. Raw Data
2. Detected Correlator

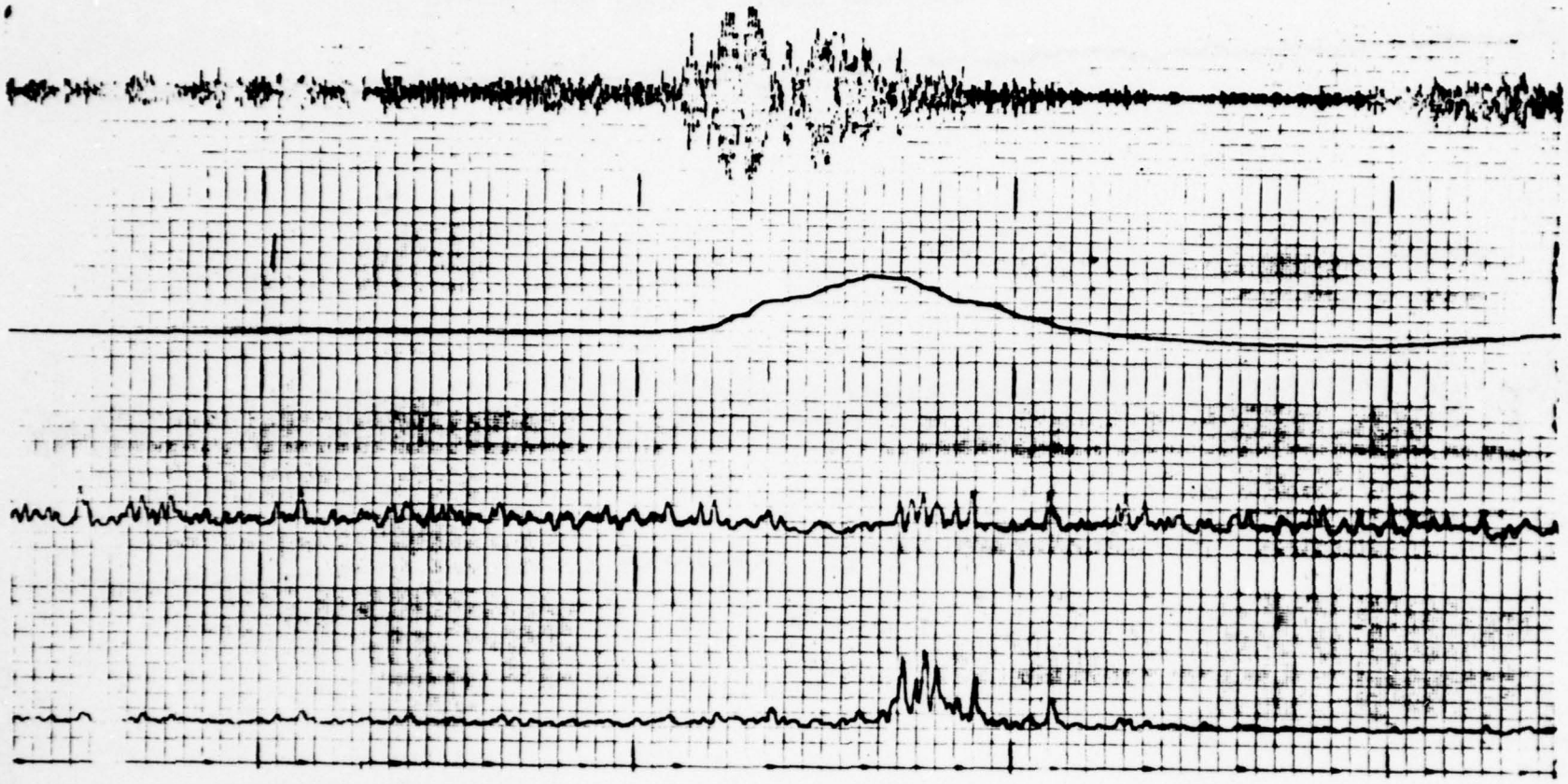

FIG. 2-3 ECHO CYCLE WITH CLOSING TARGET.

Computer Run 100
Analog Tape 11
Recorded 3 December 1963
USS WILKINSON (DL 5)
Time Scale 1 mm = 10 ms

Echo No. 26
Trace 1. Raw Data
2. Detector-Averager
3. Clipped Correlator
4. Linear Correlator

CONFIDENTIAL

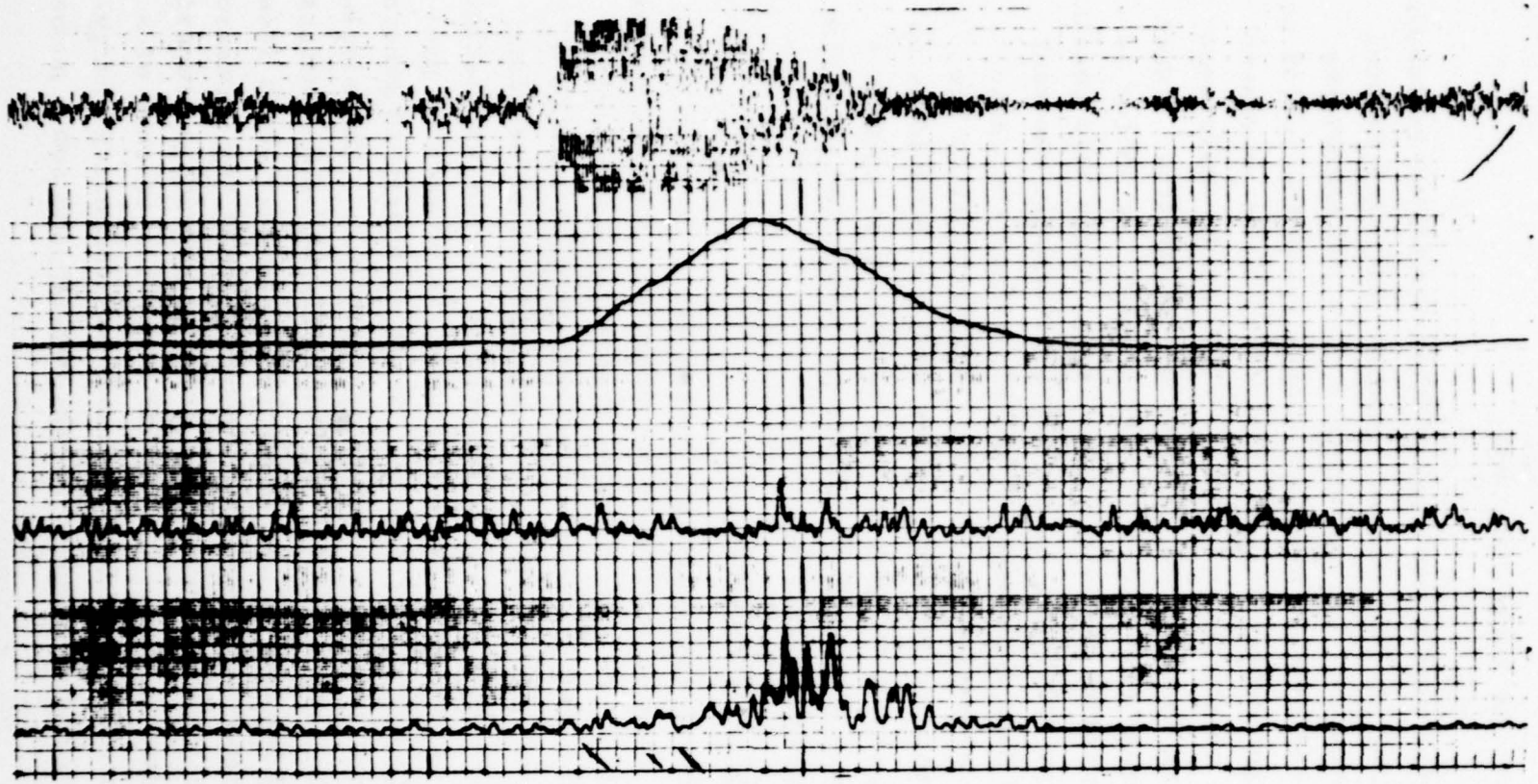

FIG. 2-4 ECHO CYCLE WITH CLOSING TARGET.

Computer Run 100
Analog Tape 11
Recorded 3 December 1963
USS WILKINSON (DL 5)
Time Scale 1 mm = 10 ms

Echo No. 46
Trace 1. Raw Data
2. Detector-Averager
3. Clipped Correlator
4. Linear Correlator

CONFIDENTIAL

Both target aspect and transmission bandwidth influence the energy splitting in real echoes. Energy splitting factors have been calculated for various aspect angles and bandwidths. Figure 2-5 shows the average measured energy splitting factor as a function of target aspect angle. The dotted lines represent confidence limits on the measurements. Very little difference in energy splitting is noted for various aspect angles. Figure 2-6 shows the average measured echo energy splitting factor as a function of transmission bandwidth with aspect angle held constant at 90^{o}. The energy splitting factor stays relatively constant out to 200 Hz and then increases at 400 Hz. Since the range resolution of the processor is inversely proportional to the bandwidth, this leads to the conclusions that for bandwidths up to 200 Hz on beam aspect targets energy splitting is largely a Doppler phenomenon. Above 200 Hz the range resolution gets fine enough to cause further splitting.

2.4 SIMULATION OF SEA ECHOES

Since echo energy splitting losses are a function of signal parameters such as bandwidth and duration, the performance of processors designed to discriminate against energy splitting losses compared to the fully coherent processor will also be a function of these signal parameters. Large amounts of sea data with a sufficient variety of signal parameters are not available. Thus, in order to investigate more fully the performance of processors designed to avoid these losses, it is necessary to generate or simulate sea echoes using a variety of parameters. The simplest echo to generate is referred to as an "ideal signal" and consists merely of a scaled replica of the transmitted signal. These ideal signals were generated and processed through each of the processors described in the following sections in order to provide a comparison between the performance of the individual processor to that of a fully coherent processor. A first approach at generating energy-split or structured signals was to merely overlap and sum a number

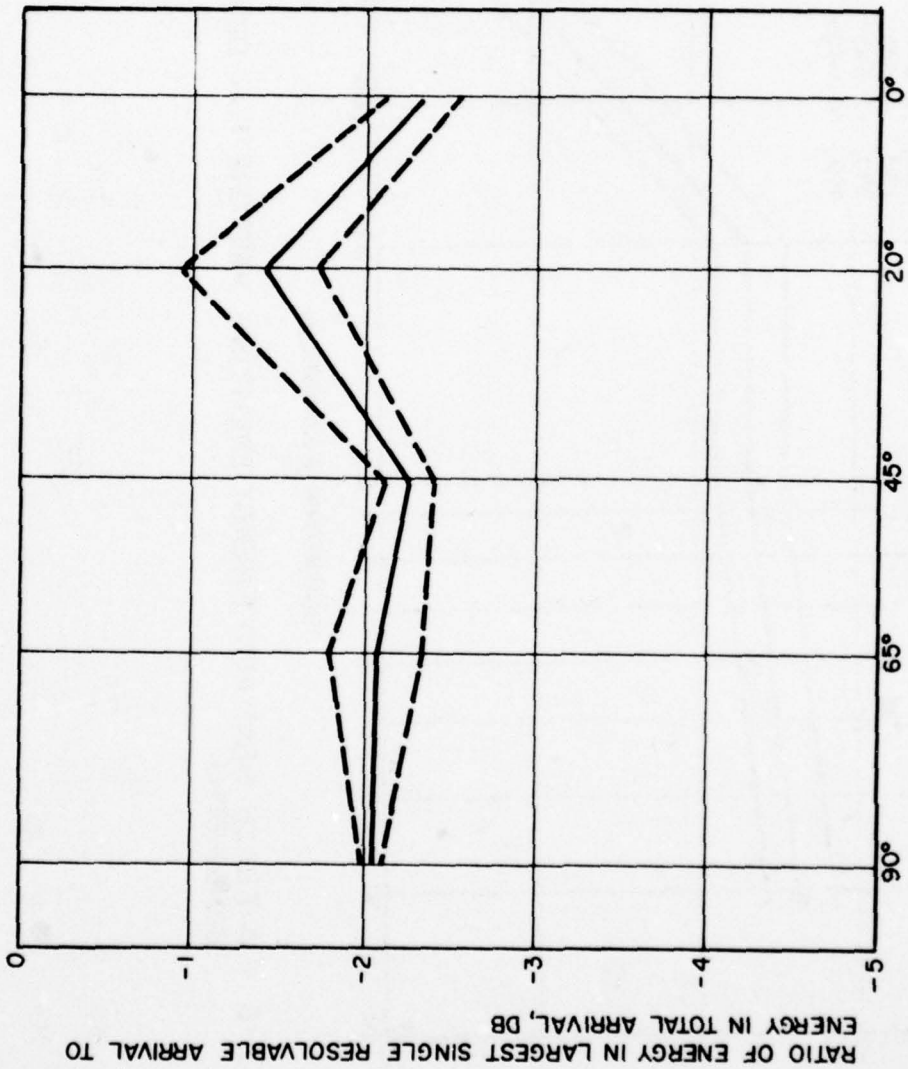

FIG. 2-5 - AVERAGE MEASURED ENERGY SPLITTING FACTORS FOR DIFFERENT TARGET ASPECTS

TRACOR, INC. AUSTIN, TEXAS 1 DWG. 6-13-1961 9-14-66 WITTENBORN/SL

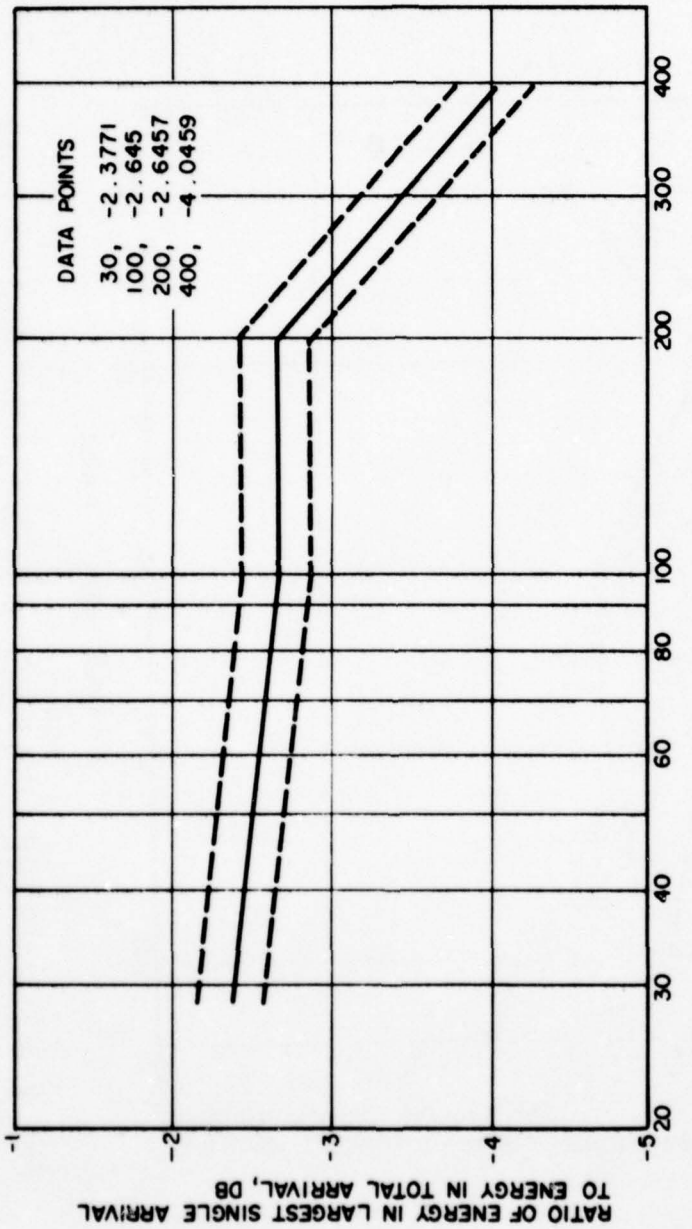

FIG. 2-6 - AVERAGE MEASURED ENERGY SPLITTING FACTORS FOR DIFFERENT BANDWIDTHS

TRACOR, INC. 1 DWG. 6-13-1960
AUSTIN, TEXAS 9-14-66 WITTENBORN/SL

of ideal signals delayed in time. A much more realistic and complex model of echoes was then constructed and a large group of signals were generated using this model. The remainder of this chapter is devoted to describing the signal models and the performance of several signal processors operating on the generated signals.

2.4.1 Ideal Signals

The conventional simulated echo consists of a scaled replica of the transmitted signal superimposed on noise. In the remainder of this report, such a signal will be termed an "ideal" signal. Although such signals are now known to be inadequate simulations of real echoes, they will be useful in making comparisons between different processors.

2.4.2 Ideal Triplets

An initial approach at simulated echo energy splitting in the echo was a signal formed by adding three overlapped ideal signals with 20 ms delay between components. Such signals are referred to as "ideal triplets".

2.4.3 Jittered Signals

In order to study the performance degradations caused by echo energy splitting, a statistical model was designed to simulate a sonar echo composed of multipath returns from a single target. The model assumes that such a structured echo consists of the summation of several ideal signals which have been shifted in Doppler and time and scaled in amplitude. The Doppler, the time delay, and the intensity in dB are all assumed to obey Gaussian distributions which are truncated at $\pm 3\sigma$. Any number of composite signals are normalized to have the same total power. For the present study, signals were generated having 6 components. The standard deviation of the Doppler shifts was 3Hz, the standard deviation of the time shifts was 20 milliseconds, and the standard deviation of the amplitude distribution was 3dB.

Four typical examples of 2 sec, 200 Hz FM slide signals generated in this way are shown in Fig. 2-7. Below each signal is a correlogram of the signal which resulted by linearly correlating the generated signal with an ideal FM slide. Table 2-I shows actual values of time and Doppler shift for each component of these four signals as well as the fraction of the signal power contained in that component and the expected peak shift after the signal is correlated. So far only FM slide type signals have been generated. These signals were added to noise at various signal-to-noise ratios and passed through several processors. The results are described below. The signals generated as described above will be referred to as "jittered signals".

2.5 PERFORMANCE COMPARISON OF SELECTED SIGNAL PROCESSORS

Several processors are investigated in this chapter. Their performances are compared with both ideal signals and energy-split signals.

These processors are best compared on a basis which includes both the output statistics and the data rates. These comparisons are based on what are referred to as modified ROC curves, which give probability of detection vs threshold crossing rate. A family of these curves, one for each input signal-to-noise ratio, is required to describe each signal processor. Although the modified ROC curves give a complete comparison of processors they are rather difficult to evaluate at a glance. Therefore, one further curve is included for each of the signal processors. This curve gives the required input signal-to-noise ratio for 0.5 probability of detection as a function of threshold crossing rate and may be obtained from the set of modified ROC curves by plotting the threshold crossing rate which corresponds to 0.5 probability of detection for each member of the set vs the input signal-to-noise ratio which appears on that curve.

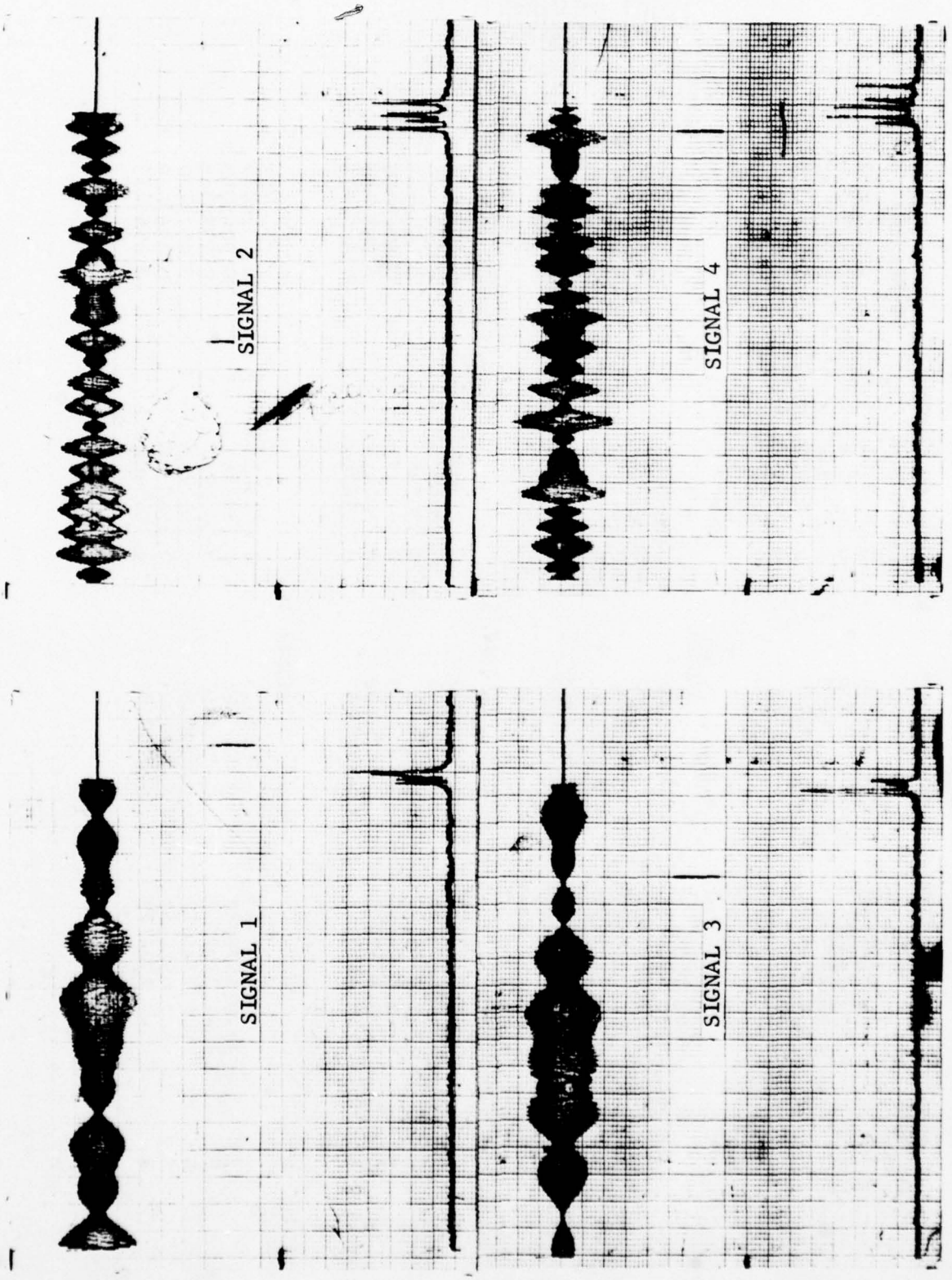

FIG. 2-7 SOME TYPICAL "JITTERED" 200 CPS FM SLIDE SIGNALS OF 2 SEC DURATION AND THEIR CORRELOGRAMS

TRACOR, INC. DWG. A6-13-2000
AUSTIN, TEXAS 1-26-67 BROWN/SL

TRACOR, INC. 6500 TRACOR LANE, AUSTIN, TEXAS 78721

TABLE 2-I

CHARACTERISTICS OF JITTERED SIGNALS

SIGNAL 1

COMPONENT	DOPPLER SHIFT (Hz)	TIME SHIFT (sec)	FRACTION OF POWER IN COMPONENT	PEAK SHIFT AT CORRELATOR OUTPUT
1	0.0561832	0.0193864	0.0967401	0.0199482
2	-0.7257411	-0.0111936	0.2497188	-0.0184510
3	2.2877507	-0.0191208	0.0999354	0.0037567
4	0.0936560	-0.0073755	0.0392629	-0.0064389
5	-2.3553818	0.0115866	0.1214475	-0.0119673
6	-2.6389537	-0.0002913	0.3928952	-0.0266808

SIGNAL 2

1	-5.5865114	0.0057891	0.1000302	-0.0500760
2	2.9892023	0.0333049	0.2327274	0.0631969
3	1.0528831	-0.0035592	0.1411158	0.0069697
4	0.5847853	0.0221042	0.0482932	0.0279521
5	-0.8945057	-0.0062256	0.1026044	-0.0027194
6	-3.0939513	-0.0171062	0.3752290	-0.0480457

SIGNAL 3

1	0.0062413	-0.0185995	0.1073864	-0.0185371
2	0.5338761	0.0212036	0.2694975	0.0265424
3	2.3724769	-0.0036439	0.3302984	0.0200809
4	-0.0436958	0.0230520	0.0677257	0.0226150
5	5.4506465	-0.0247578	0.1684017	0.0297487
6	-0.3442747	-0.0037287	0.0566904	-0.0071715

SIGNAL 4

1	-0.0062413	-0.0323425	0.0628026	-0.0324049
2	-0.4578087	0.0000416	0.2688863	-0.0045365
3	-4.3277443	0.0045810	0.1050963	-0.0386965
4	2.7325012	0.0339920	0.0807773	0.0613170
5	2.6574563	0.0101343	0.3168894	0.0367089
6	-8.2396178	-0.0140497	0.1655481	-0.0964459

2.5.1 Linear Correlation of FM Slide Signals of 2 Seconds Duration and 200 Hz Bandwidth

The processor used here consists of a linear correlator with its reference matched to the transmitted signal, followed by a linear rectifier and an averager.

2.5.1.1 Ideal Signals. In this case the averaging time is the reciprocal of the input bandwidth. The modified ROC curves for this process are shown in Fig. 2-8. Since only a single Doppler channel output is provided with this processor, Doppler shifted returns will cause a slight degradation in its performance. For a given Doppler return, either positive or negative, a new set of modified ROC curves may be obtained from Fig. 2-8 by adding a small amount to the input signal-to-noise ratio which appears on each of the curves. The required increase in input signal-to-noise ratio may be obtained from Fig. 2-9 for Dopplers up to 12 knots. Figure 2-10 gives the required input signal-to-noise ratio for 0.5 probability of detection as a function of the threshold crossing rate. This curve was obtained from Fig. 2-8 by the procedure mentioned above.

2.5.1.2 Ideal FM Slide Triplets. The processor consists of a linear correlator with an ideal FM slide signal as a reference followed by a linear rectifier and a perfect averager. The averaging time was 50 milliseconds in order to taken advantage of the energy contained in all three of the signals in a triplet. The modified ROC curves for this process are shown in Fig. 2-11. The input signal-to-noise ratios shown are in terms of the total energy contained in all three of the triplet components. Figure 2-12 was obtained from Fig. 2-11 and gives required input signal-to-noise ratio for 0.5 probability of detection vs the threshold crossing rate.

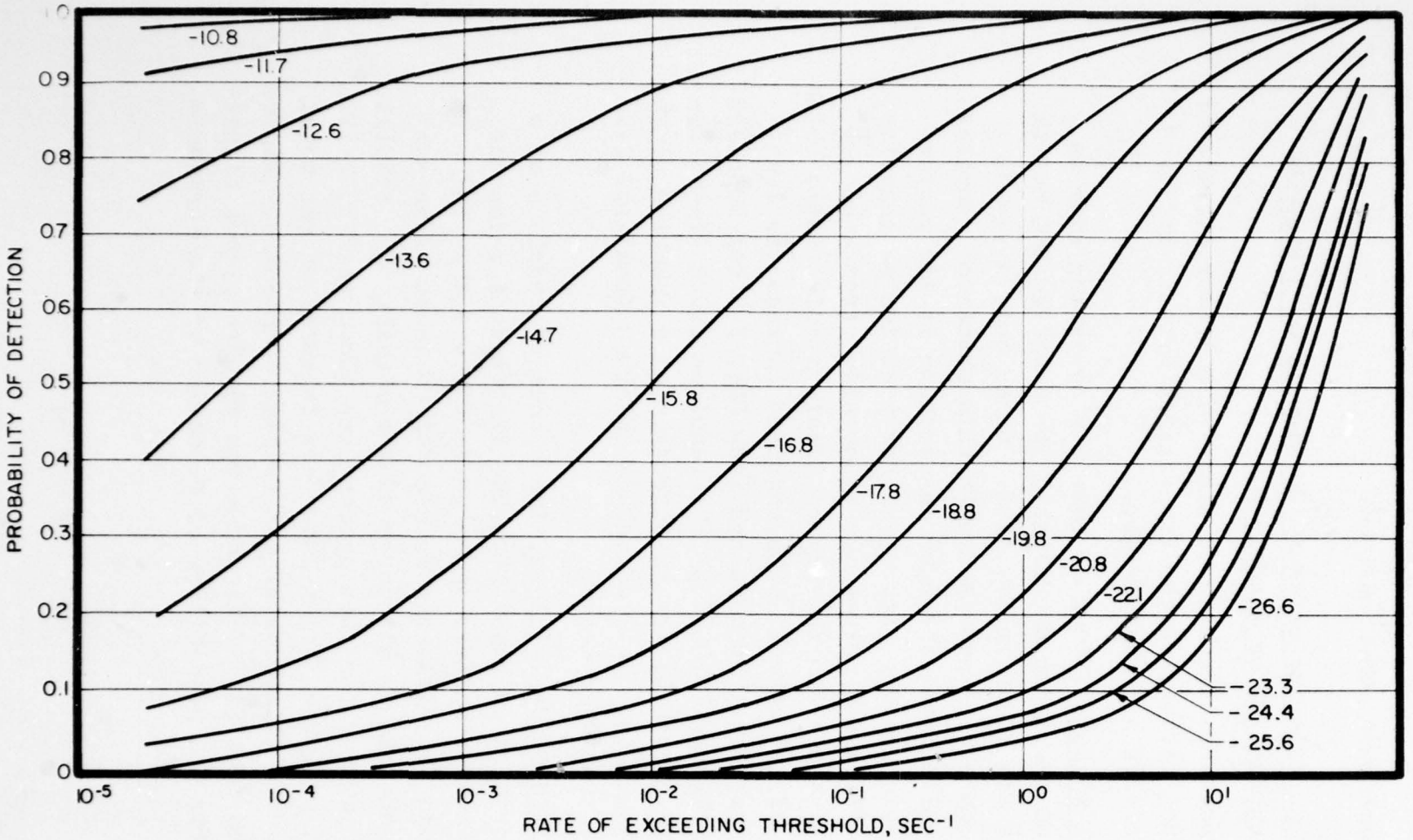

FIG. 2-8 — PROBABILITY OF DETECTION VS RATE OF EXCEEDING THRESHOLD FOR FULLY COHERENT CORRELATION OF 200 Hz FM SLIDES OF 2 SEC DURATION. THE INPUT SIGNAL-TO-NOISE RATIOS ARE INDICATED FOR EACH CURVE IN DB

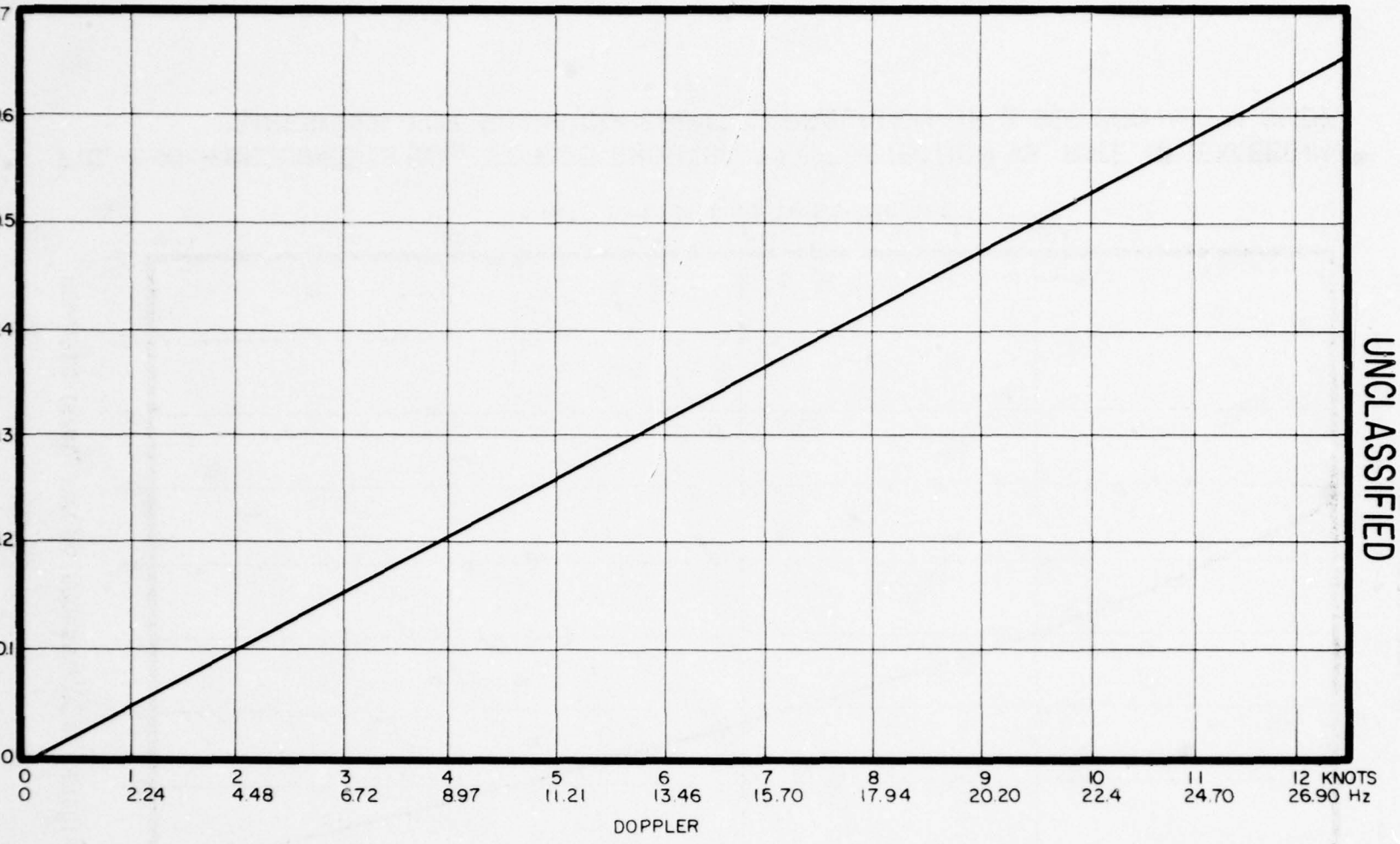

TRACOR, INC. AUSTIN, TEXAS 9-5-67 HAYES/SL DWG A6-13-2189

FIG. 2-9 — REQUIRED INCREASE OF $(S/N)_{IN}$ AS A FUNCTION OF DOPPLER FOR 200 Hz FM SLIDE. A DOPPLER SCALE IN KNOTS IS SHOWN FOR 3.5 KC CENTER FREQUENCY

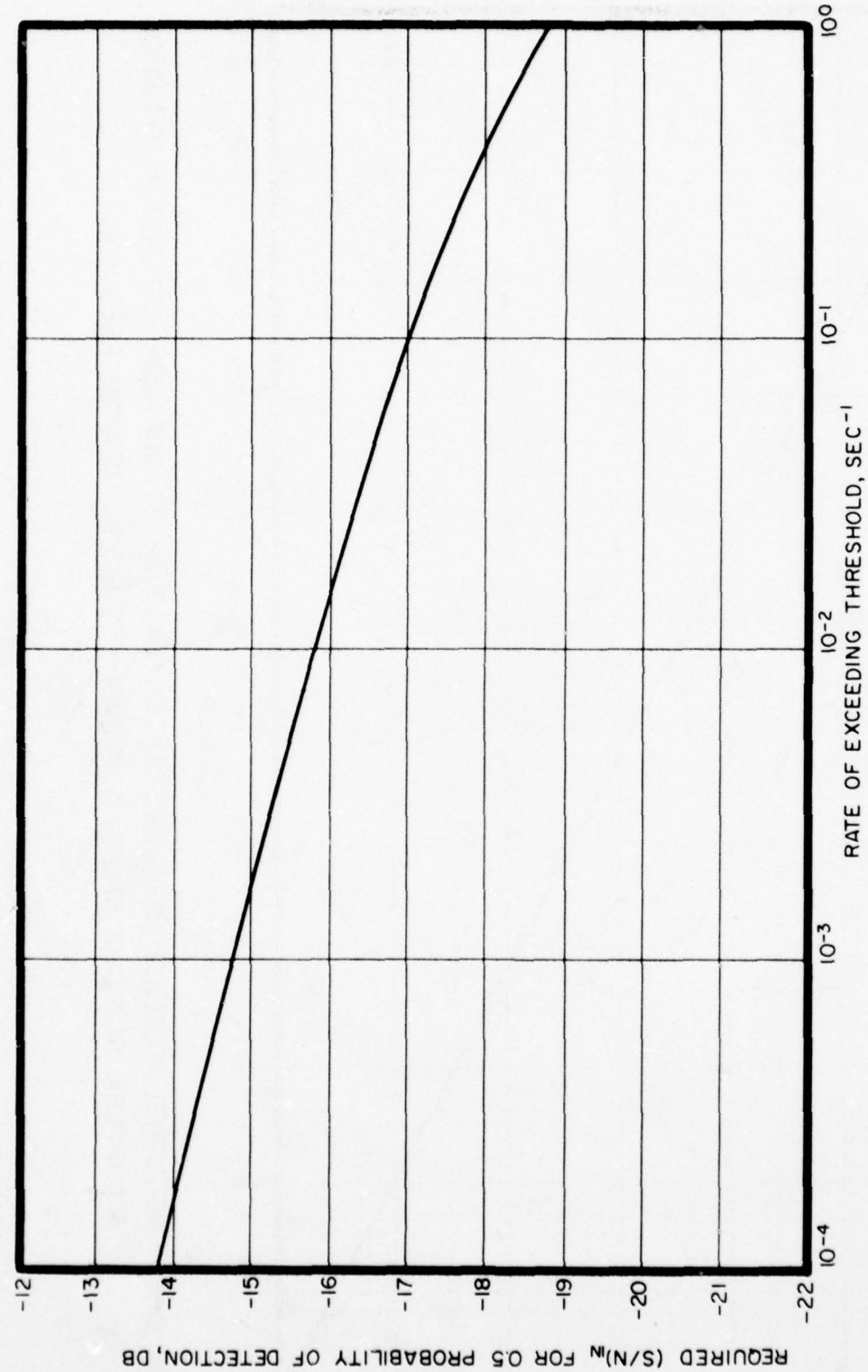

FIG. 2-10 – REQUIRED $(S/N)_{IN}$ FOR 0.5 PROBABILITY OF DETECTION VS RATE OF EXCEEDING THRESHOLD FOR FULLY COHERENT CORRELATION OF 2 SEC 200 Hz FM SLIDE

TRACOR, INC. AUSTIN, TEXAS DWG. A6-13-2193 9-5-67 HAYES/SL

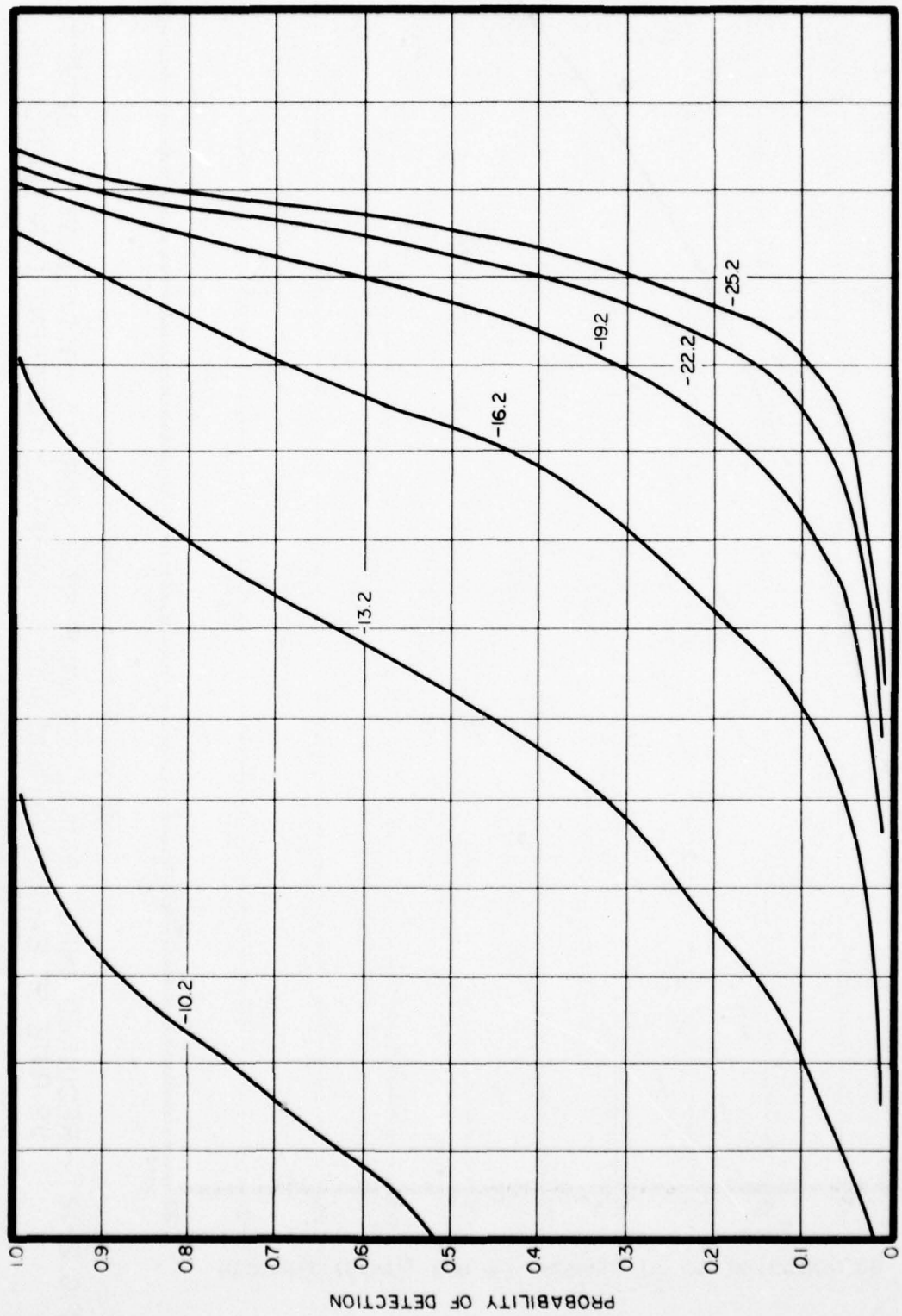

FIG. 2-11 – PROBABILITY OF DETECTION VS RATE OF EXCEEDING THRESHOLD FOR FULLY COHERENT CORRELATION OF 2 SEC 200 Hz FM TRIPLETS. THE INPUT SIGNAL-TO-NOISE RATIOS ARE INDICATED FOR EACH CURVE IN DB

TRACOR, INC. AUSTIN, TEXAS 9-5-67 DWG A6-13-2199 HAYES/SL

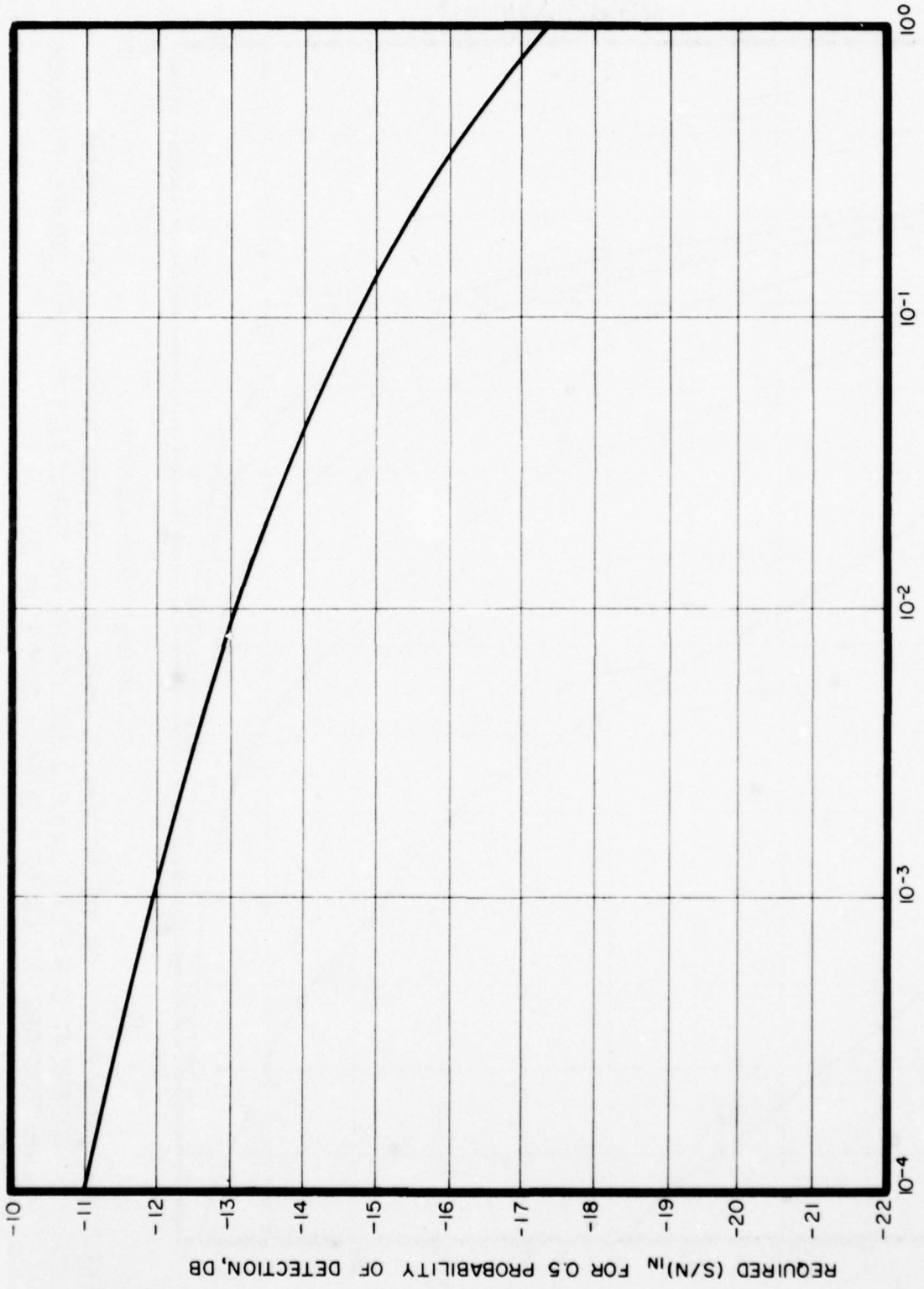

FIG. 2-12 – REQUIRED INPUT SIGNAL-TO-NOISE RATIO FOR 0.5 PROBABILITY OF DETECTION VS RATE OF EXCEEDING THRESHOLD FOR FULLY COHERENT CORRELATION OF 2 SEC 200 Hz FM SLIDE TRIPLETS

2.5.1.3 Jittered FM Slide Signals The effects of the simulated energy splitting on this processor are significant. The processor is the same as that described before for use on ideal signals and ideal triplets, a linear replica correlator followed by a linear rectifier and perfect averager. Two sets of modified ROC curves were obtained. The first set, shown in Fig. 2-13, describes the process when a five millisecond averaging time is used. The second set of modified ROC curves, shown in Fig. 2-14, describes the process of a 50 millisecond averaging time. There is very little apparent difference in the two sets of curves although the over-averaging seems to give a very slight advantage at the small signal-to-noise ratios. Figure 2-15 was obtained from Figs. 2-13 and 2-14. This figure is the required input signal-to-noise ratio for 0.5 probability of detection as a function of the threshold crossing rate for the two processes described in Figs. 2-13 and 2-14.

2.5.2 Correlation by Partial Sums of 200 Hz Linear FM Slide Signals of 2 Seconds Duration

2.5.2.1 Ideal Signals

Correlation by partial sums uses two or more correlators, each having a reference that corresponds to part of the signal. For two-piece partial sums correlation, for example, two correlators are used. Each of these correlators uses one-half the signal as a reference. For this example, one correlator contained a reference which consisted of a 1 second long FM slide running from 200 to 300 Hz. The other correlator used a reference which was 1 second long and consisted of an FM slide running from 300 to 400 Hz. The output of each of these correlators was rectified and averaged for 10 milliseconds. When a signal is correlated a peak occurs from the first correlator one second before the peak from the second correlator. The first peak is

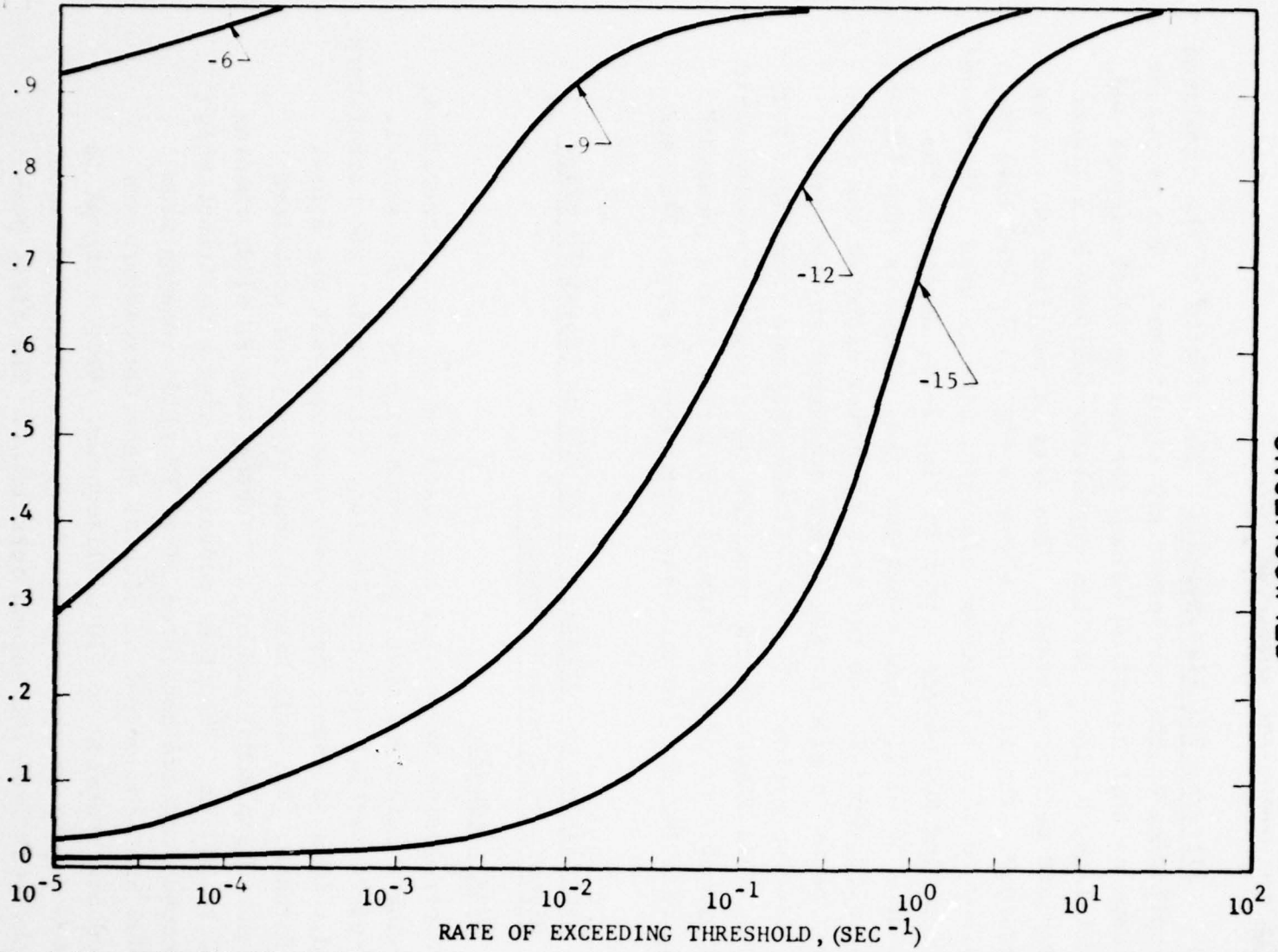

FIG. 2-13 PROBABILITY OF DETECTION VS RATE OF EXCEEDING THRESHOLD FOR FULL CORRELATION OF JITTERED FM SLIDE SIGNALS WITH 200 HZ BANDWIDTH AND 2 SECOND DURATION. THE AVERAGING TIME USED IS 5 MILLISECONDS. THE INPUT SIGNAL-TO-NOISE RATIOS ARE INDICATED FOR EACH CURVE IN dB.

TRACOR, INC
AUSTIN, TEXAS
1 DWG 6-13-302
5 16 66 BROWN/SL

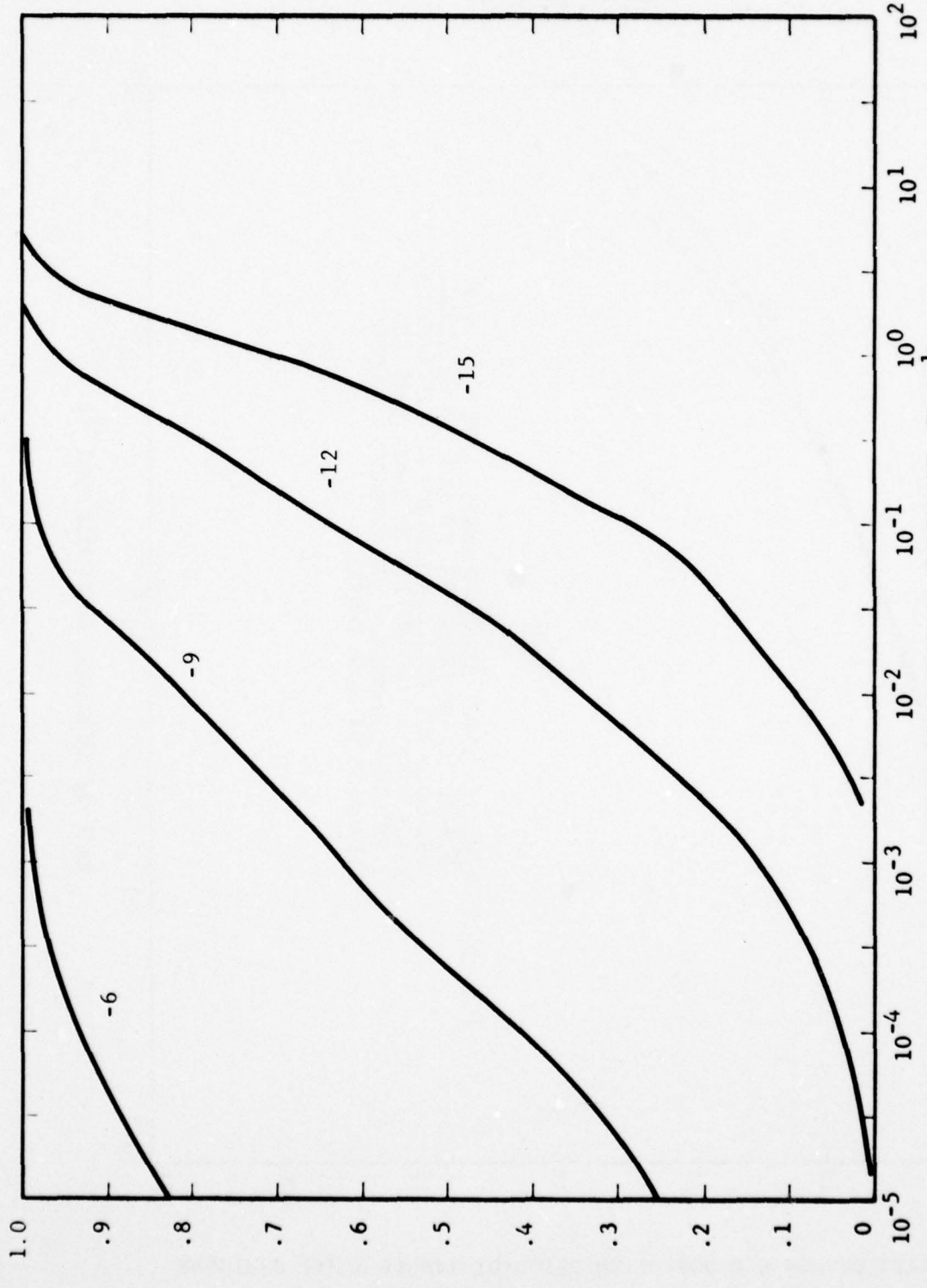

FIG. 2-14 PROBABILITY OF DETECTION VS RATE OF EXCEEDING THRESHOLD FOR FULL CORRELATION OF JITTERED FM SLIDE SIGNALS WITH 200 HZ BANDWIDTH AND 2 SECOND DURATION. THE AVERAGING TIME USED WAS 50 MILLISECONDS. THE INPUT SIGNAL-TO-NOISE RATIOS ARE INDICATED FOR EACH CURVE IN dB.

TRACOR, INC. AUSTIN, TEXAS | DWG. 6-13-317 | 3-16-66 BROWN/SL

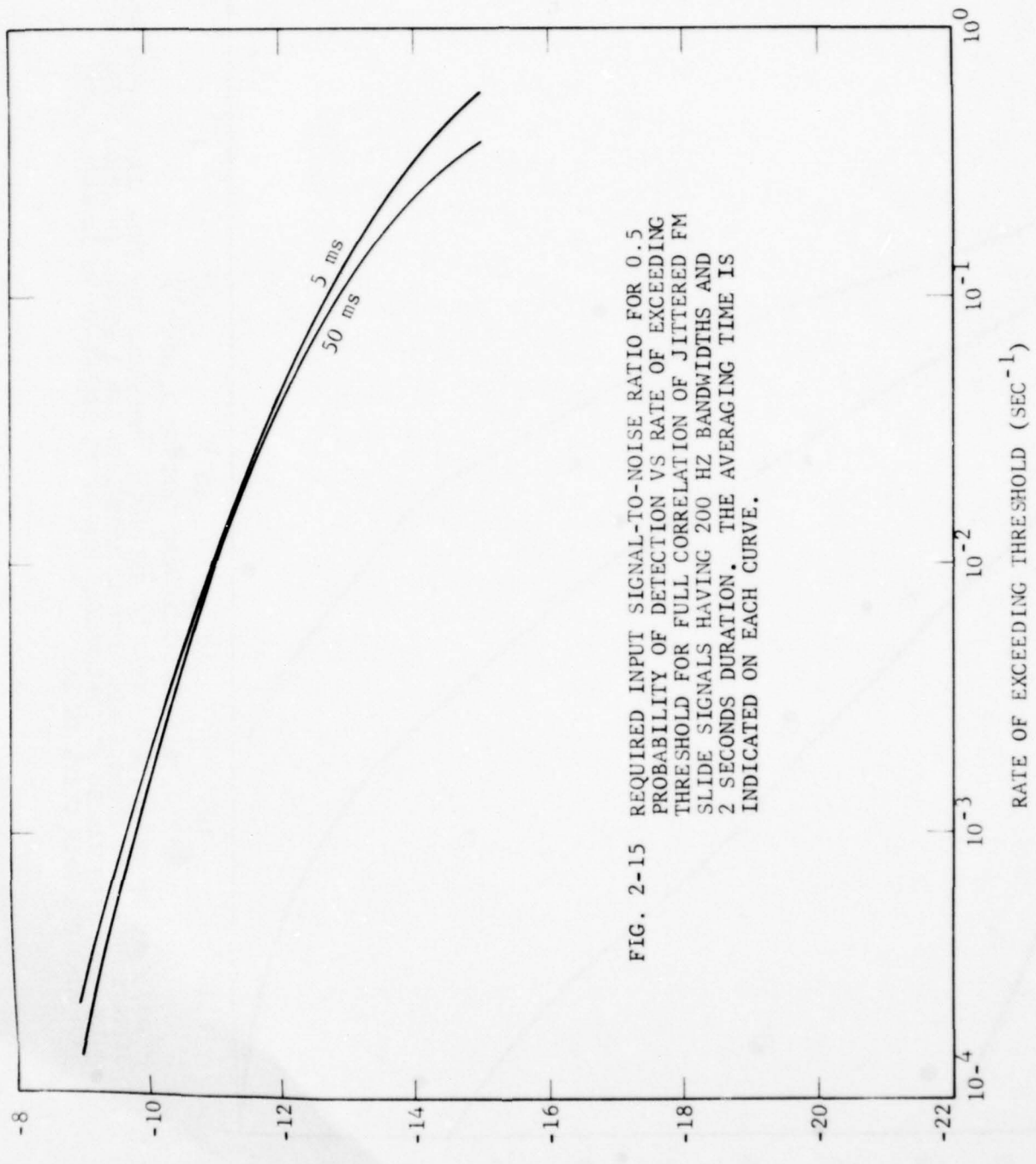

FIG. 2-15 REQUIRED INPUT SIGNAL-TO-NOISE RATIO FOR 0.5 PROBABILITY OF DETECTION VS RATE OF EXCEEDING THRESHOLD FOR FULL CORRELATION OF JITTERED FM SLIDE SIGNALS HAVING 200 HZ BANDWIDTHS AND 2 SECONDS DURATION. THE AVERAGING TIME IS INDICATED ON EACH CURVE.

TRACOR, INC. AUSTIN, TEXAS | DWG. 6-13-294 | 3-15-66 | BROWN/SL

delayed by one second so that the two peaks line up, and the two channels are then added. Modified ROC curves are shown for this process in Fig. 2-16. Figure 2-17 is obtained from Fig. 2-16 and gives the required input signal-to-noise ratio for 0.5 probability of detection as a function of the threshold crossing rate.

2.5.2.2 Ideal FM Slide Triplets This process is carried out in a manner similar to that for ideal signals. The correlator references are copies of a single component of the triplets. The averaging time used in this process is 50 milliseconds for each correlator. Figure 2-18 gives the modified ROC curves for this process and Fig. 2-19 gives the required input signal-to-noise ratio for 0.5 probability of detection as a function of the threshold crossing rate.

2.5.2.3 Jittered FM Slide Signals

Partial sums correlation was performed for the jittered FM slide signals by both two-piece and eight-piece partial sums correlators.

Two sets of modified ROC curves were obtained using two-piece partial sums correlation. The set shown in Fig. 2-20 is the result of using the ideal 10 ms averaging time on each channel, and the set shown in Fig. 2-21 was obtained by using a 50 ms time constant on each channel. The set of modified ROC curves shown in Fig. 2-22 represents the results of partial sums correlation with eight references of 25 Hz bandwidth and 250 ms duration. In this case the averaging time was 40 ms.

Figure 2-23 was obtained from Figs. 2-20, 2-21 and 2-22. This figure gives the required input signal-to-noise ratio for 0.5 probability of detection as a function of the threshold crossing rate for the three partial sums processors described.

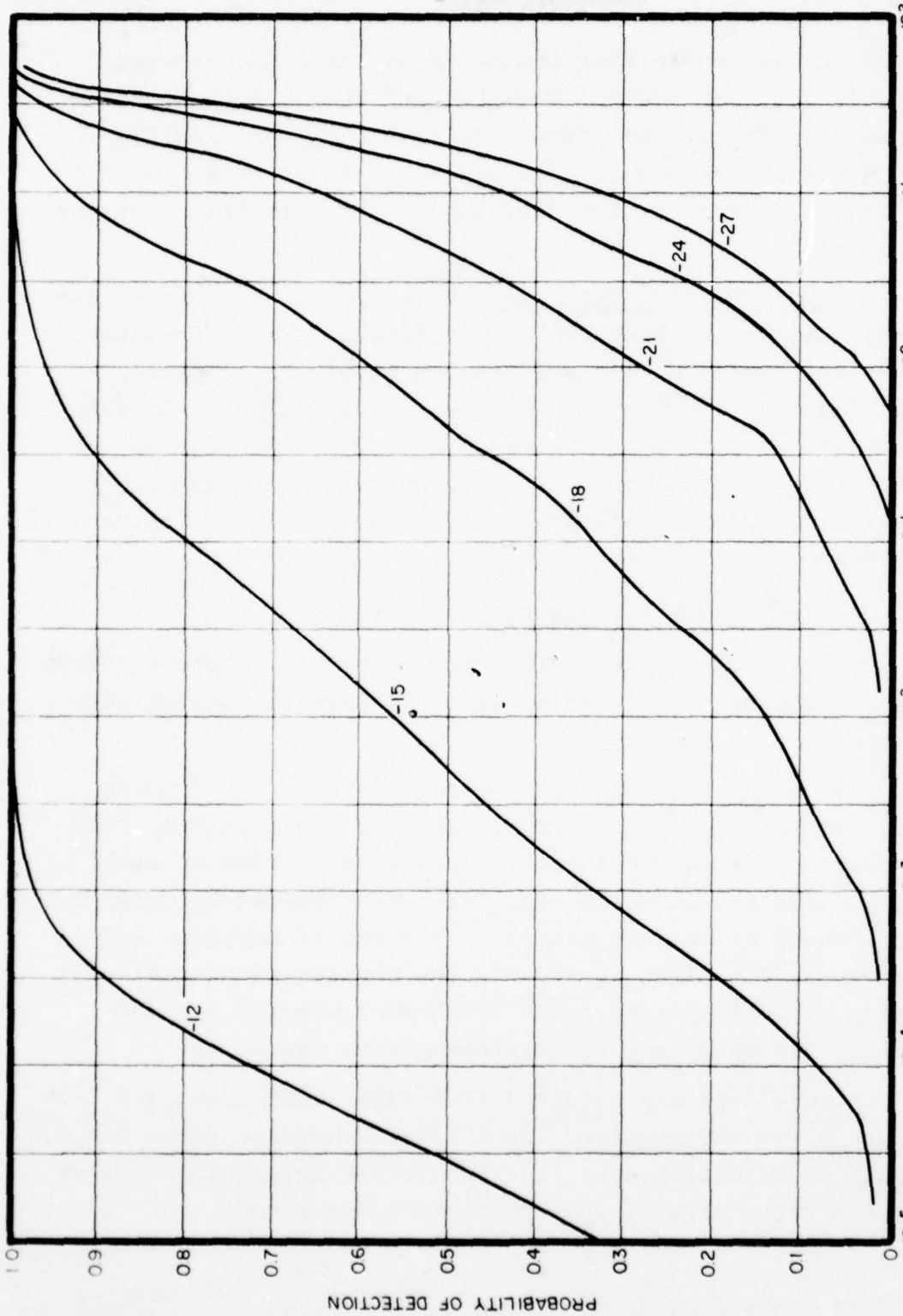

FIG. 2-16 — PROBABILITY OF DETECTION VS RATE OF EXCEEDING THRESHOLD FOR CORRELATION BY PARTIAL SUMS OF 200 Hz FM SLIDES OF 2 SEC DURATION. THE INPUT SIGNAL-TO-NOISE RATIOS ARE INDICATED FOR EACH CURVE IN DB

TRACOR, INC. DWG A6-13-2198
AUSTIN, TEXAS 9 5 67 HAYES/SL

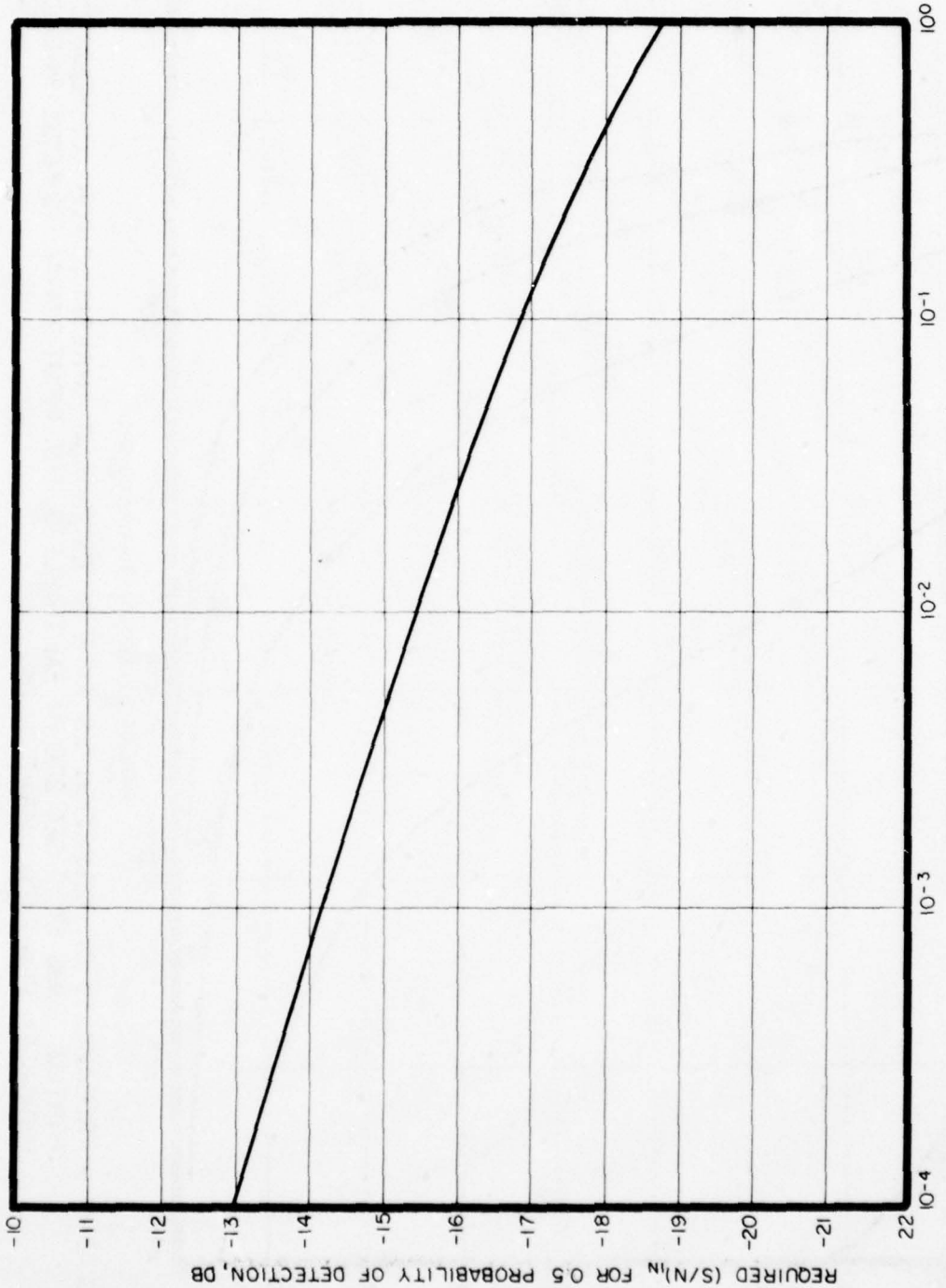

FIG. 2-17 — REQUIRED INPUT SIGNAL-TO-NOISE RATIO FOR 0.5 PROBABILITY OF DETECTION VS RATE OF EXCEEDING THRESHOLD FOR CORRELATION BY PARTIAL SUMS OF 2 SEC 200 Hz FM SLIDE SIGNALS

TRACOR, INC. AUSTIN, TEXAS 9-5-67 DWG A6-13-2191 HAYES/SL

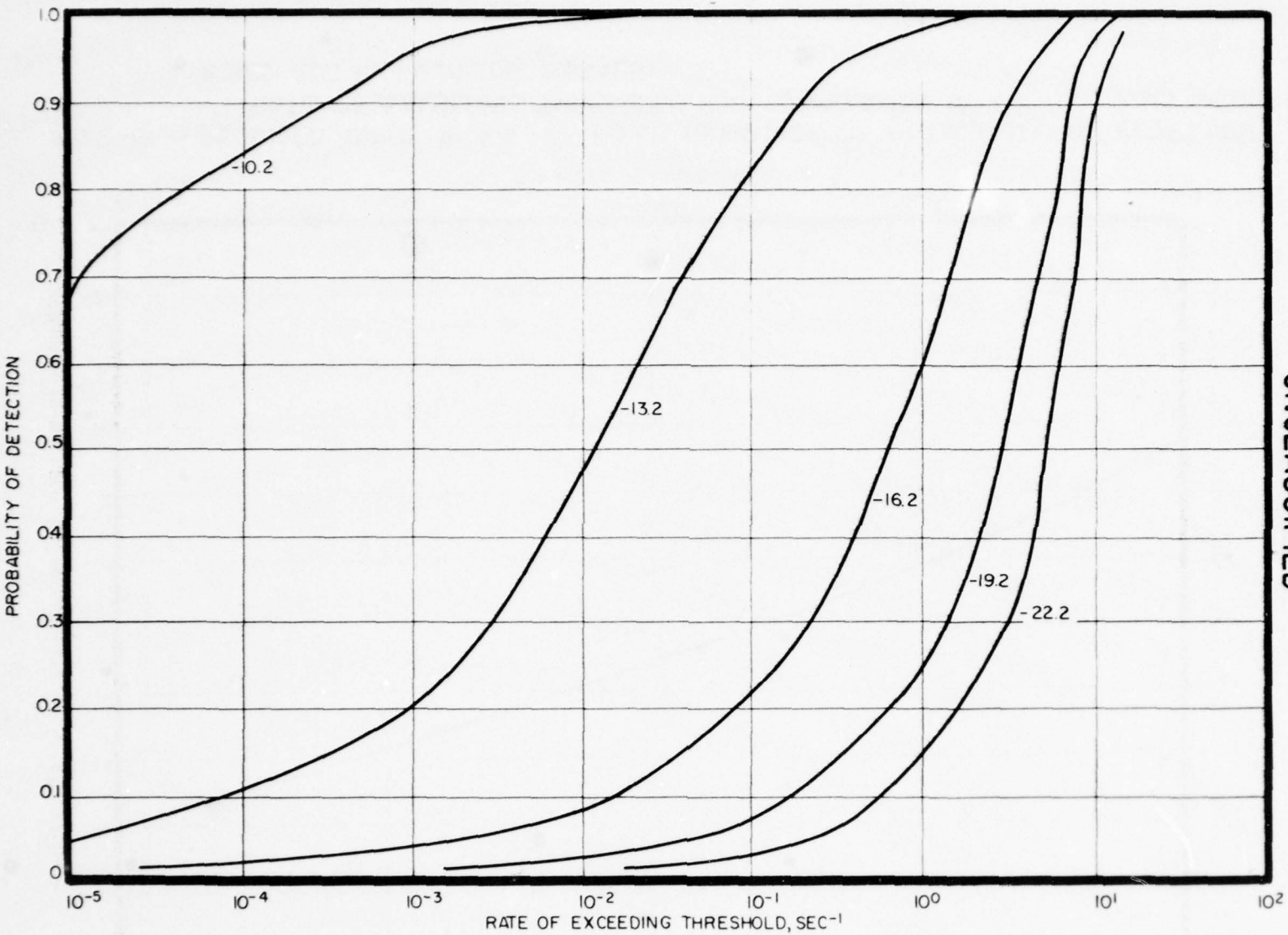

FIG. 2-18 — PROBABILITY OF DETECTION VS RATE OF EXCEEDING THRESHOLD FOR CORRELATION BY PARTIAL SUMS OF 2 SEC 200 Hz FM TRIPLETS. THE INPUT SIGNAL-TO-NOISE RATIOS ARE INDICATED FOR EACH CURVE IN DB

TRACOR, INC.
AUSTIN, TEXAS
9-5-67
DWG. A6-13-2197
HAYES/SL

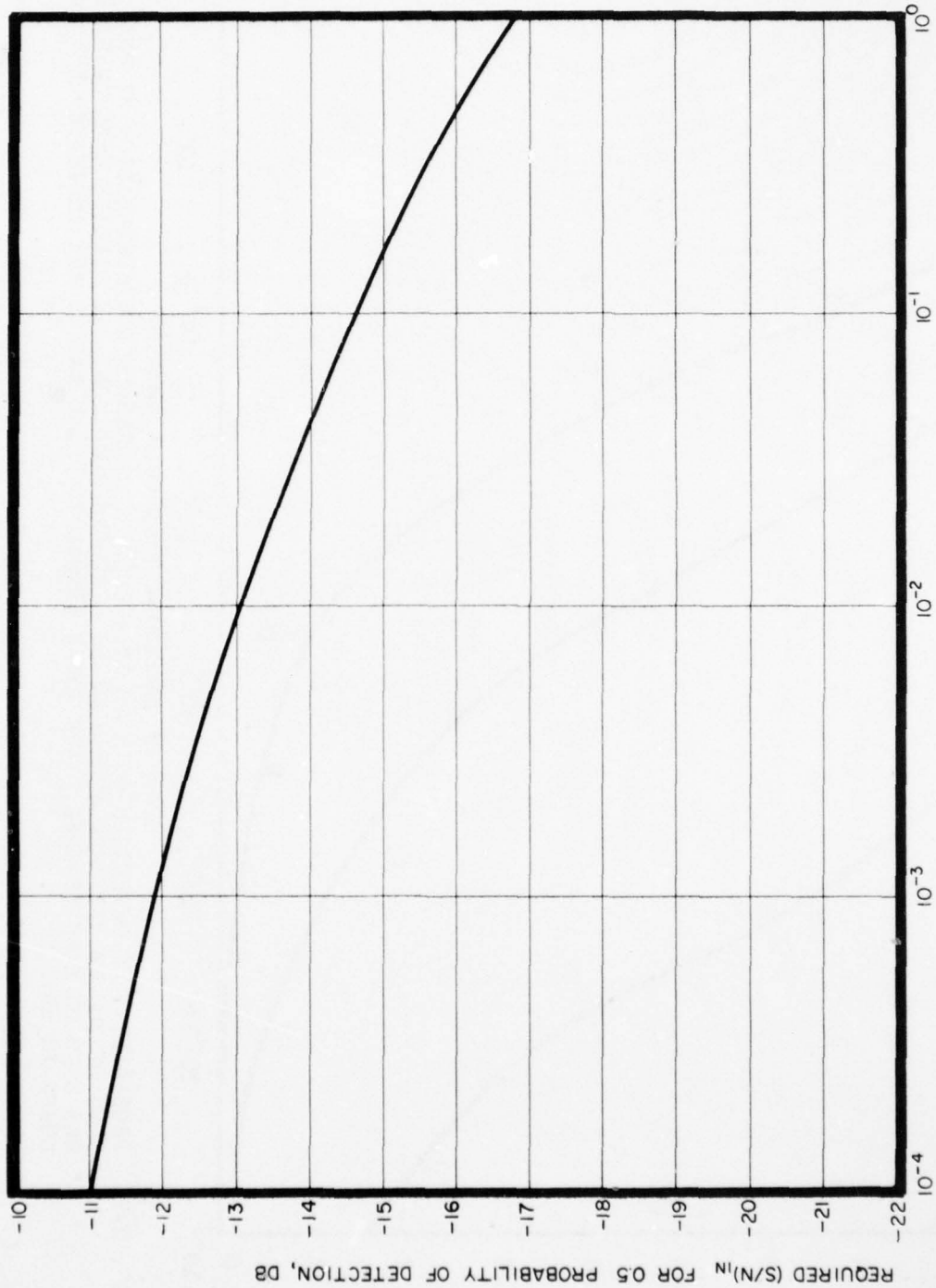

FIG. 2-19— REQUIRED INPUT SIGNAL-TO-NOISE RATIO FOR 0.5 PROBABILITY OF DETECTION VS RATE OF EXCEEDING THRESHOLD FOR CORRELATION BY PARTIAL SUMS OF 2 SEC 200 Hz FM SLIDE TRIPLETS

TRACOR, INC. DWG A6-13-2190
AUSTIN, TEXAS 9-5-67 HAYES/SL

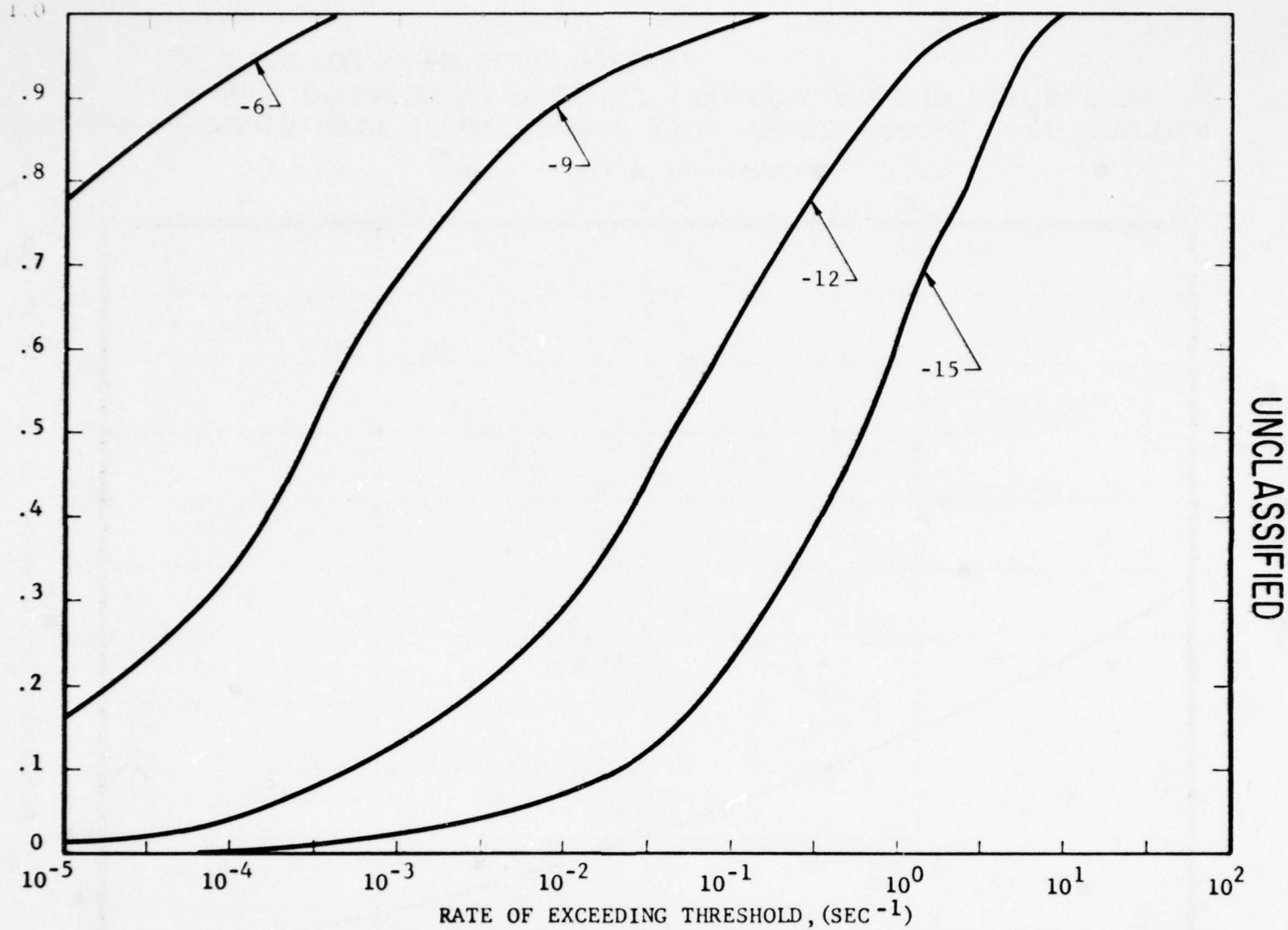

FIG. 2-20 PROBABILITY OF DETECTION VS RATE OF EXCEEDING THRESHOLD FOR CORRELATION BY PARTIAL SUMS OF 200 HZ JITTERED FM SLIDES OF 2 SECOND DURATION. 10 MILLISECONDS AVERAGING WAS USED ON EACH CHANNEL. THE INPUT SIGNAL-TO-NOISE RATIOS ARE INDICATED FOR EACH CURVE IN dB.

TRACOR, INC. AUSTIN, TEXAS | DWG. 6-13-304 | 3-16-66 BROWN/SL

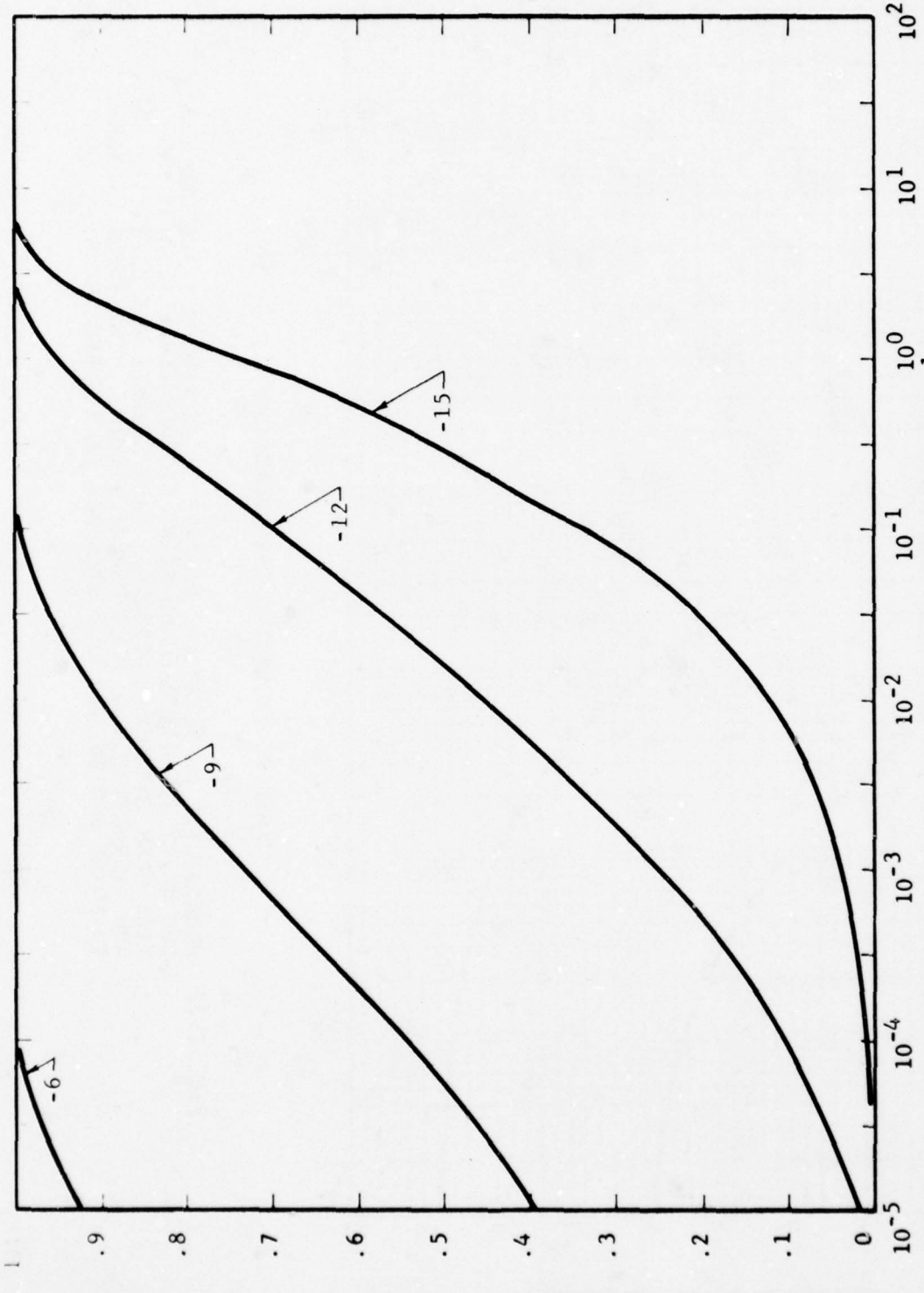

FIG. 2-21 PROBABILITY OF DETECTION VS RATE OF EXCEEDING THRESHOLD FOR CORRELATION BY PARTIAL SUMS OF 200 HZ JITTERED FM SLIDES OF 2 SECOND DURATION. 50 MILLISECONDS AVERAGING WAS USED ON EACH CHANNEL. THE INPUT SIGNAL-TO-NOISE RATIOS ARE INDICATED FOR EACH CURVE IN dB.

TRACOR, INC. AUSTIN, TEXAS | DWG 6-13-301 | 3-18-66 | BROWN/SL

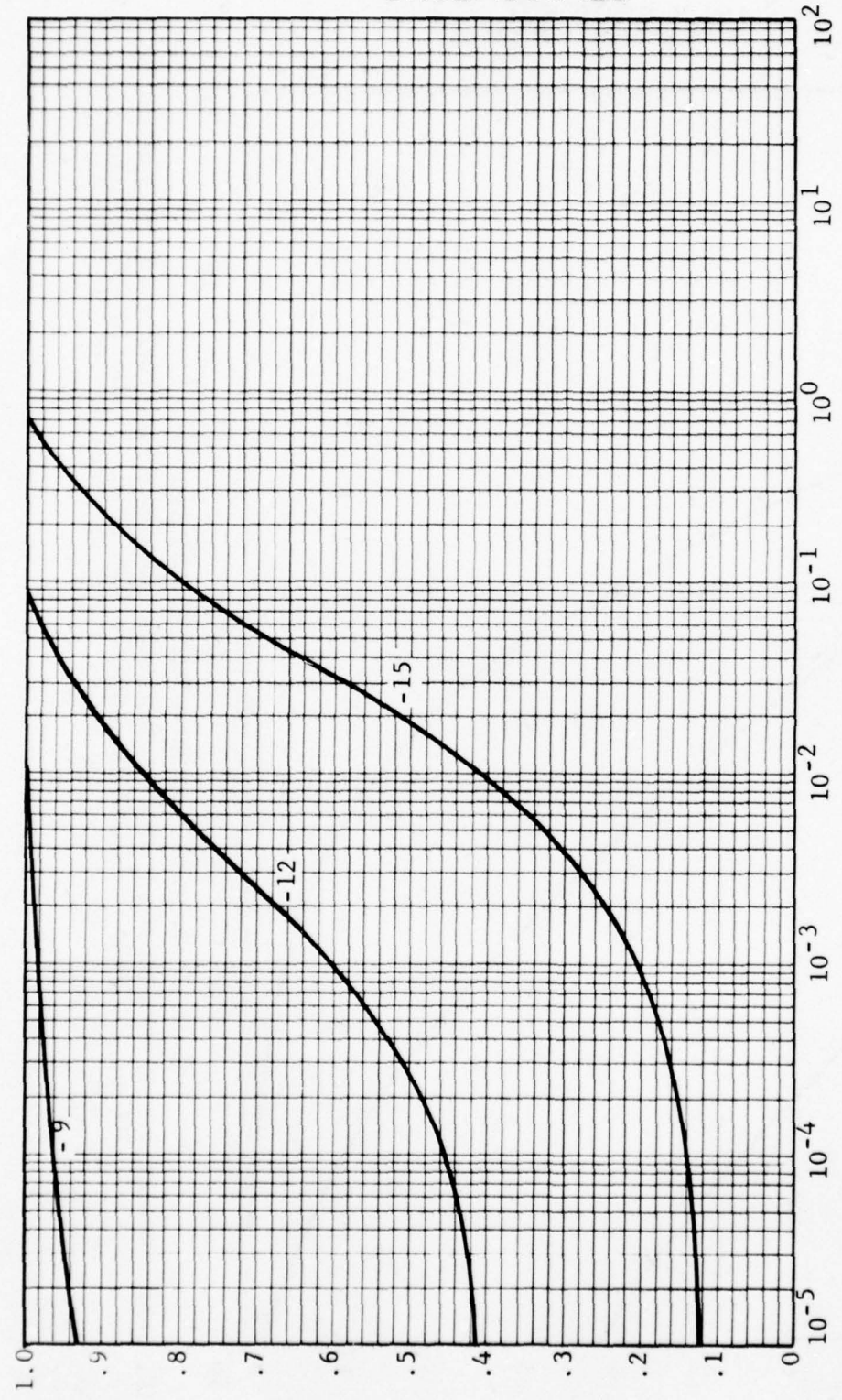

FIG. 2-22 PROBABILITY OF DETECTION VS RATE OF EXCEEDING THRESHOLD FOR 200 HZ, 2 SEC JITTERED FM SLIDE SIGNALS CORRELATED BY PARTIAL SUMS IN EIGHT SECTIONS. EACH CHANNEL WAS RECTIFIED AND AVERAGED FOR 40 MSEC BEFORE SUMMING. THE INPUT SIGNAL-TO-NOISE RATIOS ARE INDICATED FOR EACH CURVE IN dB.

TRACOR, INC. DWG. A6-13-2005
AUSTIN, TEXAS 1-26-67 BROWN/SL

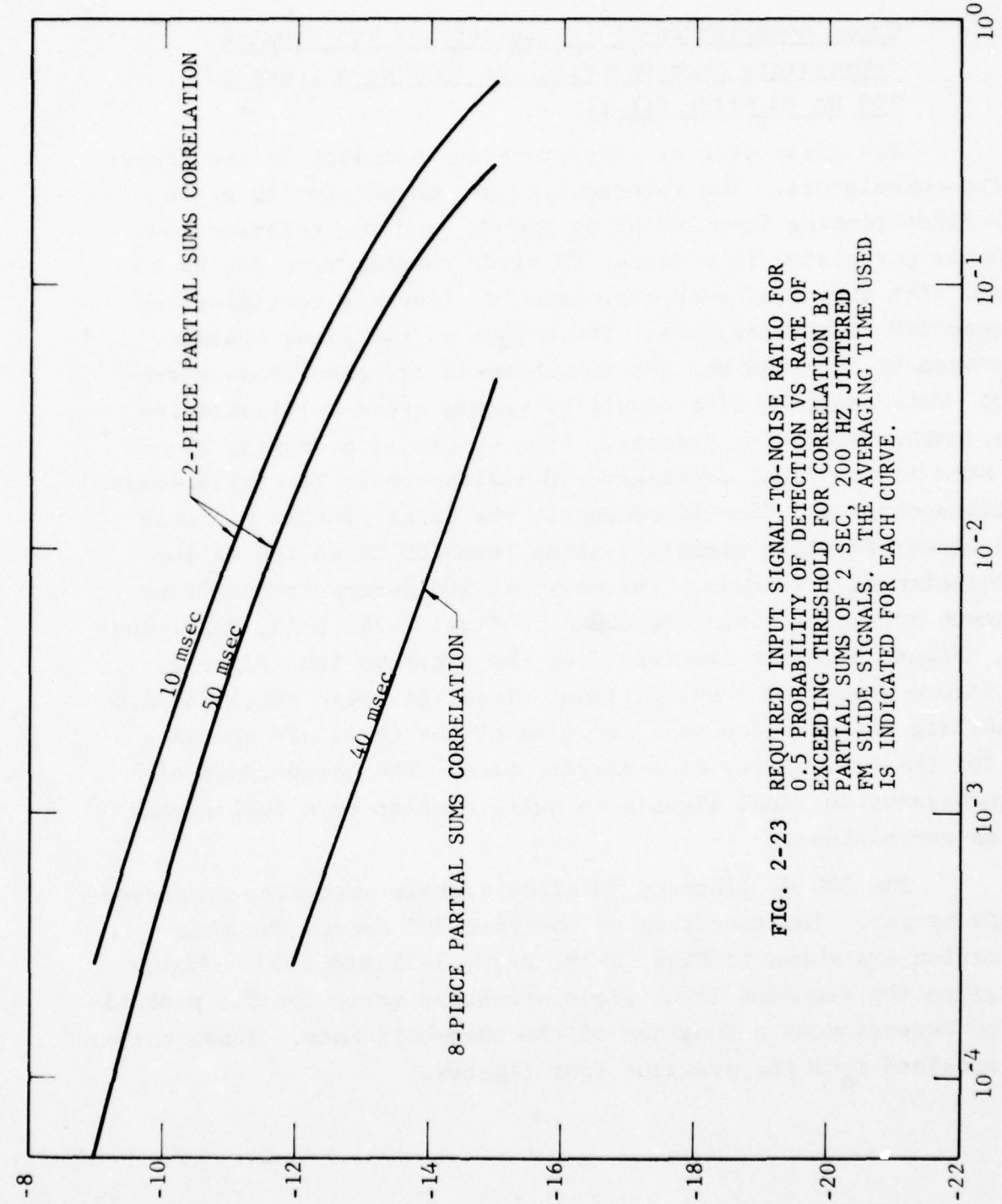

FIG. 2-23 REQUIRED INPUT SIGNAL-TO-NOISE RATIO FOR 0.5 PROBABILITY OF DETECTION VS RATE OF EXCEEDING THRESHOLD FOR CORRELATION BY PARTIAL SUMS OF 2 SEC, 200 HZ JITTERED FM SLIDE SIGNALS. THE AVERAGING TIME USED IS INDICATED FOR EACH CURVE.

TRACOR, INC AUSTIN, TEXAS DWG A6-13-2010 1-26-67 BROWN/SL

2.5.3 Cross Correlation of the Outputs of Two Replica Correlators Each Operating on Half of a 2 Second 200 Hz FM Slide Signal

The first part of this processor consists of two linear replica correlators. The reference on one correlator is a 100 Hz FM slide running from 200 Hz to 300 Hz, and the reference on the other correlator is a linear FM slide running from 300 Hz to 400 Hz. The output of each correlator is linearly rectified and averaged for 10 milliseconds. The output of the first averager is delayed by 1 second and the two channels are then cross correlated. This consists of a sample by sample cross multiplication and a further averaging process. Four values of averaging time were used in the final averager: 10 milliseconds, 20 milliseconds, 40 milliseconds and 80 milliseconds. The first signals run were ideal linear FM slide signals running from 200 Hz to 400 Hz for the duration of 2 seconds. The modified ROC curves for the four different averaging times are shown in Figs. 2-24, 2-25, 2-26, and 2-27. Figure 2-28 was obtained from the previous four figures. This figure gives the required input signal-to-noise ratio for 0.5 probability of detection as a function of the threshold crossing rate for the four values of averaging time. The performance of this processor on ideal signals is quite similar to a full linear replica correlation.

The 200 Hz jittered FM slide signals were also processed in this manner. The four sets of modified ROC curves for this application are shown in Figs. 2-29, 2-30, 2-31, and 2-32. Figure 2-33 gives the required input signal-to-noise ratio for 0.5 probability of detection as a function of the threshold rate. These curves were obtained from the previous four figures.

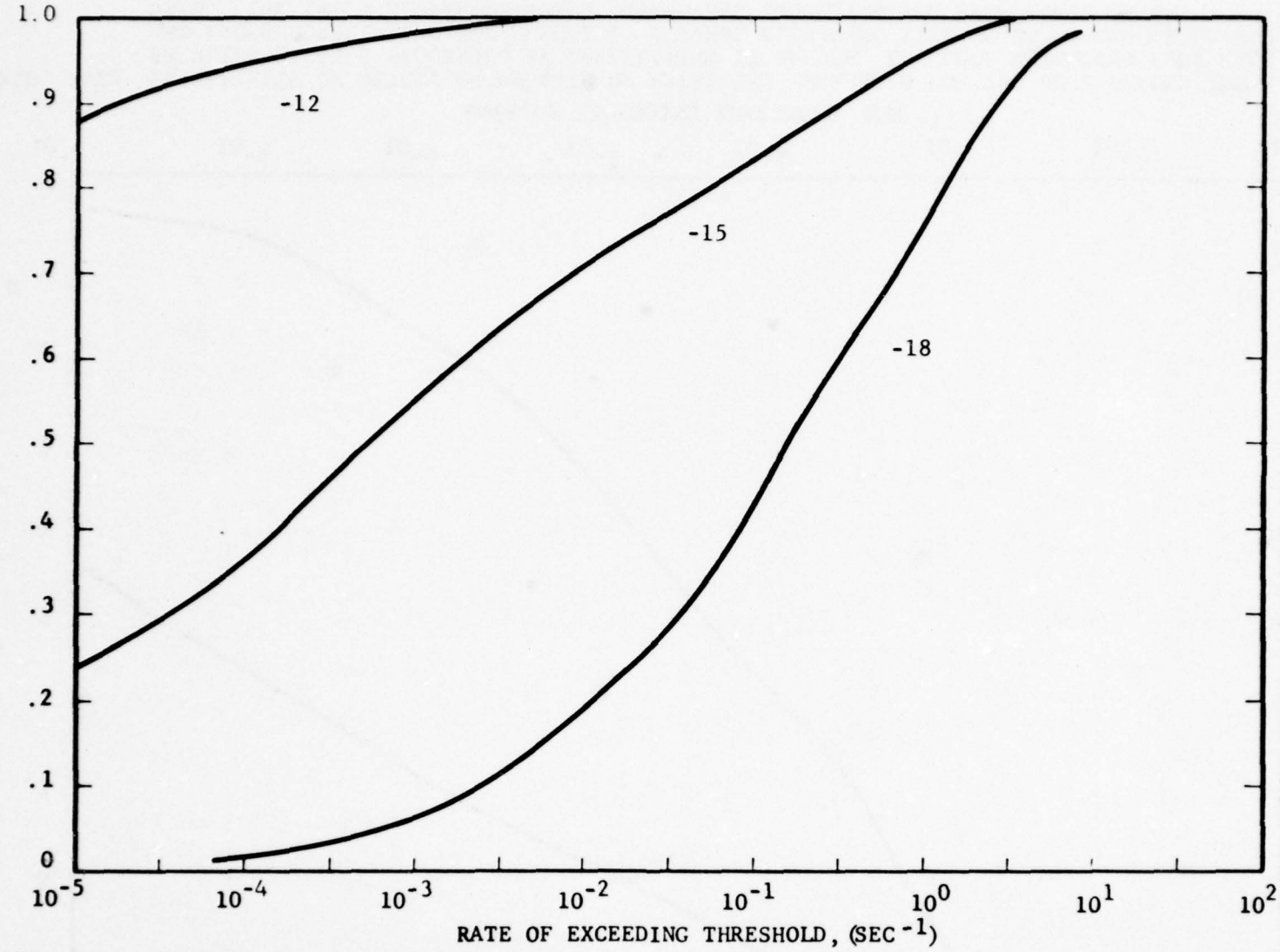

FIG. 2-24 PROBABILITY OF DETECTION VS RATE OF EXCEEDING THRESHOLD FOR 200 HZ 2 SECOND IDEAL FM SLIDE SIGNALS PROCESSED BY CORRELATING IN HALVES, ENVELOPE DETECTING EACH HALF, AND CROSS CORRELATING THE RESULTS. A FINAL AVERAGING TIME OF 10 MILLISECONDS WAS USED. THE INPUT SIGNAL-TO-NOISE RATIOS ARE INDICATED FOR EACH CURVE IN dB.

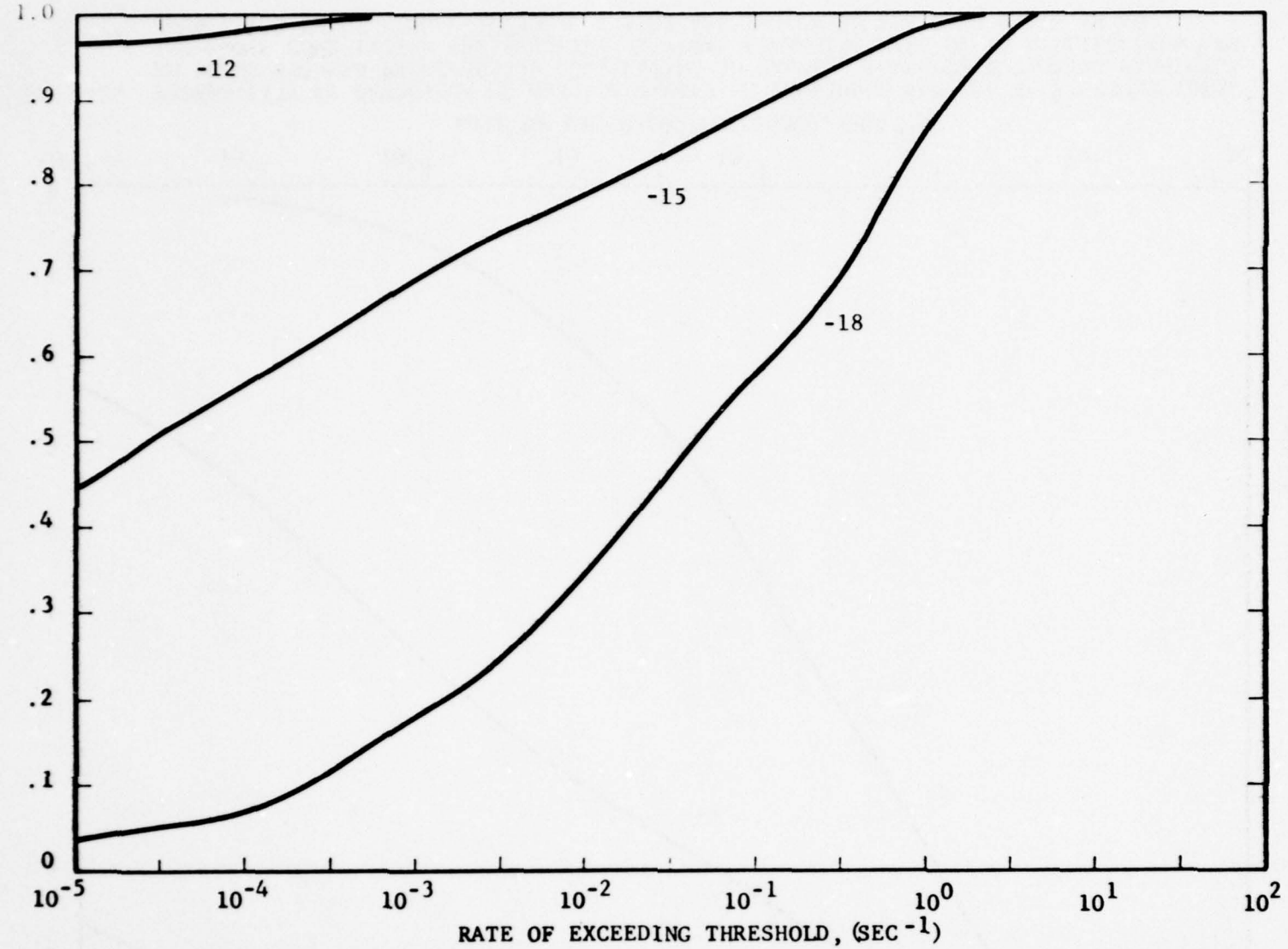

TRACOR, INC. AUSTIN, TEXAS 1 DWG 6-13-315 5-16-68 BROWN/BL

FIG. 2-25 PROBABILITY OF DETECTION VS RATE OF EXCEEDING THRESHOLD FOR 200 HZ 2 SECOND IDEAL FM SLIDE SIGNALS PROCESSED BY CORRELATING IN HALVES, ENVELOPE DETECTING EACH HALF, AND CROSS CORRELATING THE RESULTS. A FINAL AVERAGING TIME OF 20 MILLISECONDS WAS USED. THE INPUT SIGNAL-TO-NOISE RATIOS ARE INDICATED FOR EACH CURVE IN dB.

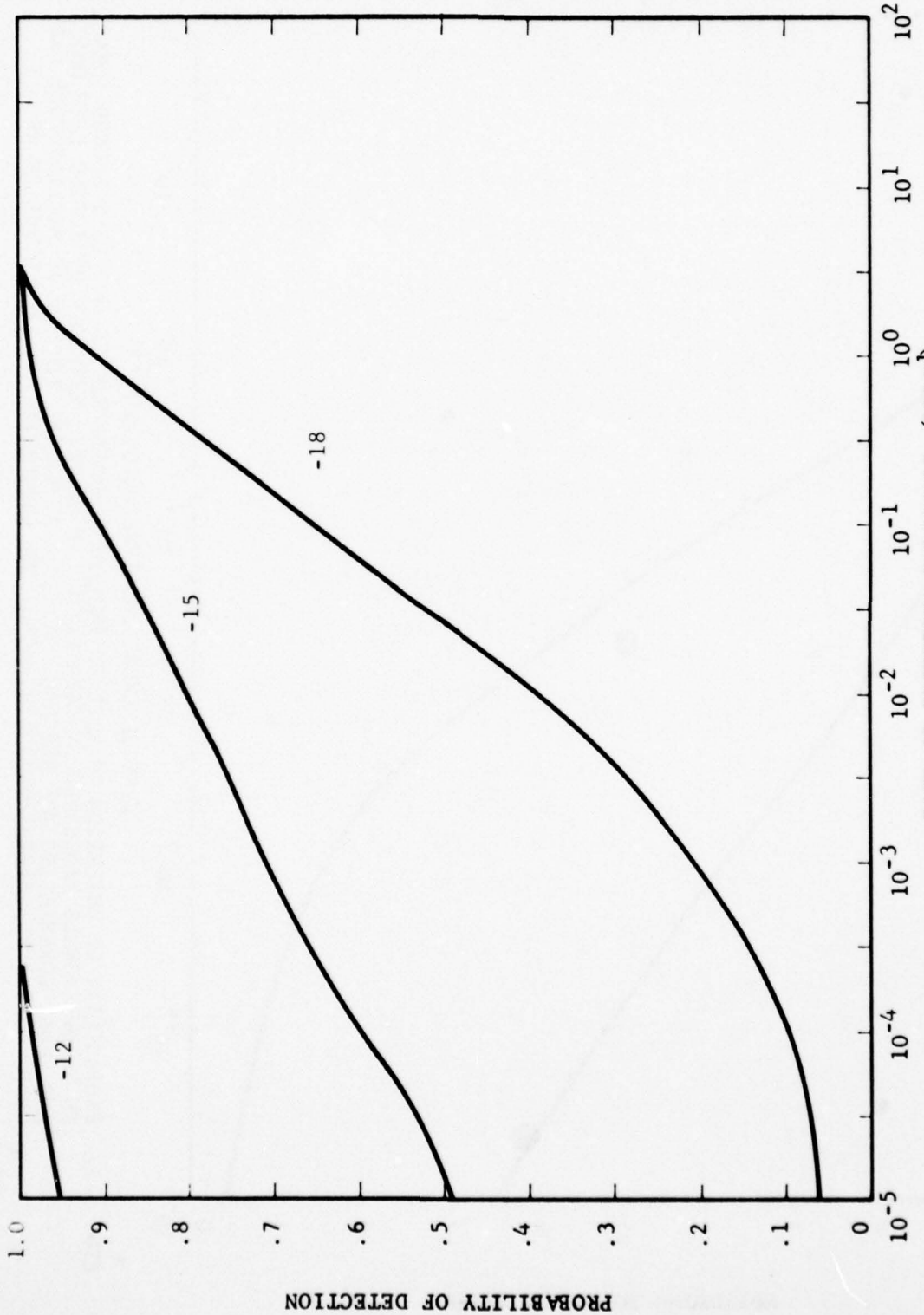

FIG. 2-26 PROBABILITY OF DETECTION VS RATE OF EXCEEDING THRESHOLD FOR 200 HZ 2 SECOND IDEAL FM SLIDE SIGNALS PROCESSED BY CORRELATING IN HALVES, ENVELOPE DETECTING EACH HALF, AND CROSS CORRELATING THE RESULTS. A FINAL AVERAGING TIME OF 40 MILLISECONDS WAS USED.. THE INPUT SIGNAL-TO-NOISE RATIOS ARE INDICATED FOR EACH CURVE IN dB.

TRACOR, INC. AUSTIN, TEXAS | 1 DWG 6-13-314 | 3-16-66 BROWN/SL

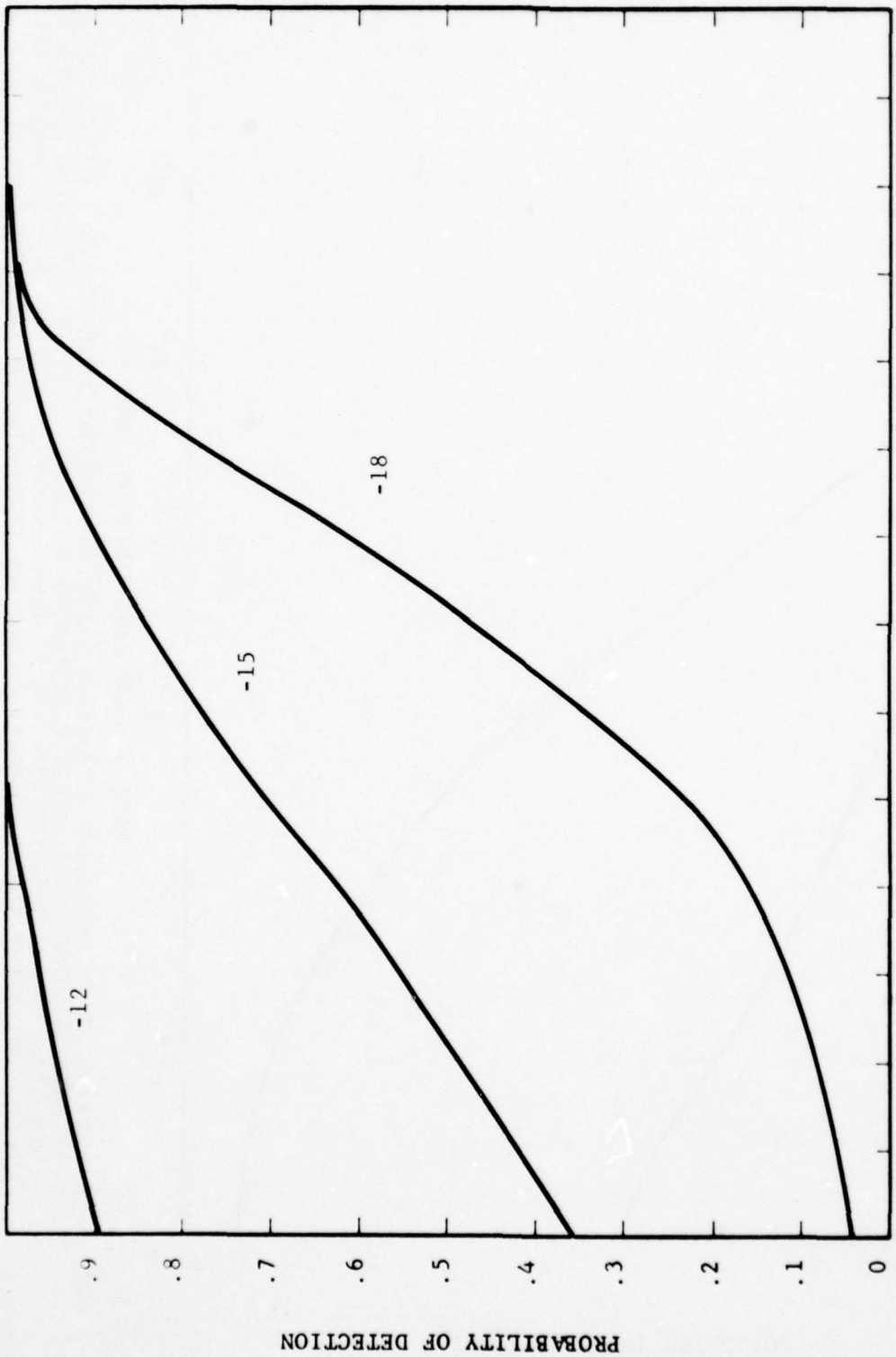

FIG. 2-27 PROBABILITY OF DETECTION VS RATE OF EXCEEDING THRESHOLD FOR 200 HZ 2 SECOND IDEAL FM SLIDE SIGNALS PROCESSED BY CORRELATING IN HALVES, ENVELOPE DETECTING EACH HALF, AND CROSS CORRELATING THE RESULTS. A FINAL AVERAGING TIME OF 80 MILLISECONDS WAS USED. THE INPUT SIGNAL-TO-NOISE RATIOS ARE INDICATED FOR EACH CURVE IN dB.

TRACOR, INC | 1 DWG 6-13-312
AUSTIN, TEXAS | 3-16-66 | BROWN/SL

FIG. 2-28 REQUIRED INPUT SIGNAL-TO-NOISE RATIO FOR 0.5 PROBABILITY OF DETECTION VS RATE OF EXCEEDING THRESHOLD FOR 2 SECOND, 200 HZ IDEAL FM SLIDE SIGNALS PROCESSED BY CORRELATING IN HALVES, ENVELOPE DETECTING EACH HALF, AND CROSS CORRELATING THE RESULTS. FOUR FINAL AVERAGING TIMES ARE USED AS SHOWN.

TRACOR, INC. AUSTIN, TEXAS | DWG 6-13-297 | 3-15-66 | BROWN/SL

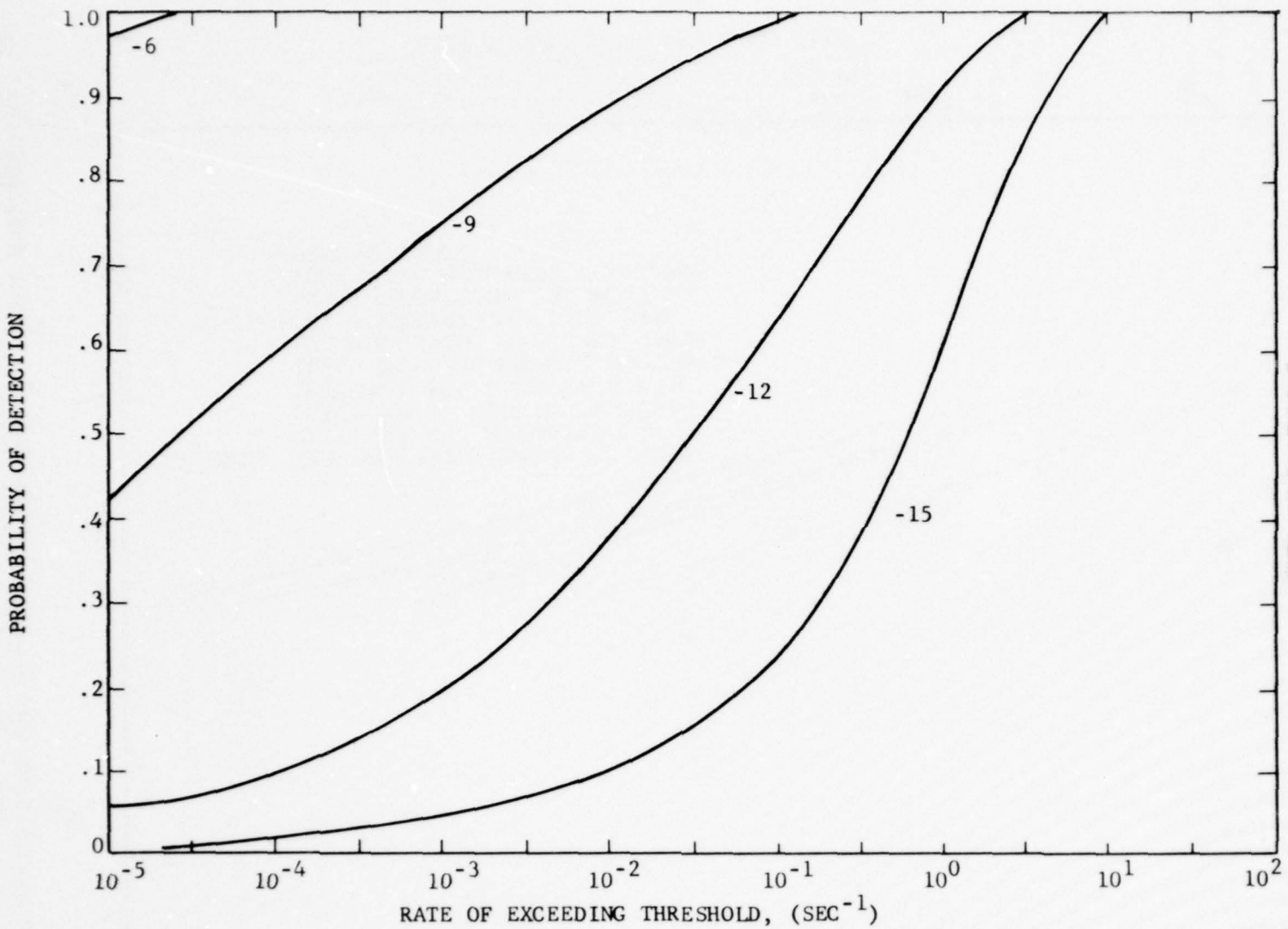

FIG. 2-29 PROBABILITY OF DETECTION VS RATE OF EXCEEDING THRESHOLD FOR 200 HZ 2 SECOND JITTERED FM SLIDE SIGNALS PROCESSED BY CORRELATING IN HALVES, ENVELOPE DETECTING EACH HALF, AND CROSS CORRELATING THE RESULTS. A FINAL AVERAGING TIME OF 10 MILLISECONDS WAS USED. THE INPUT SIGNAL-TO-NOISE RATIOS ARE INDICATED FOR EACH CURVE IN dB.

TRACOR, INC. AUSTIN, TEXAS | DWG 6-13-307 | 4-12-66 | BROWN/SL

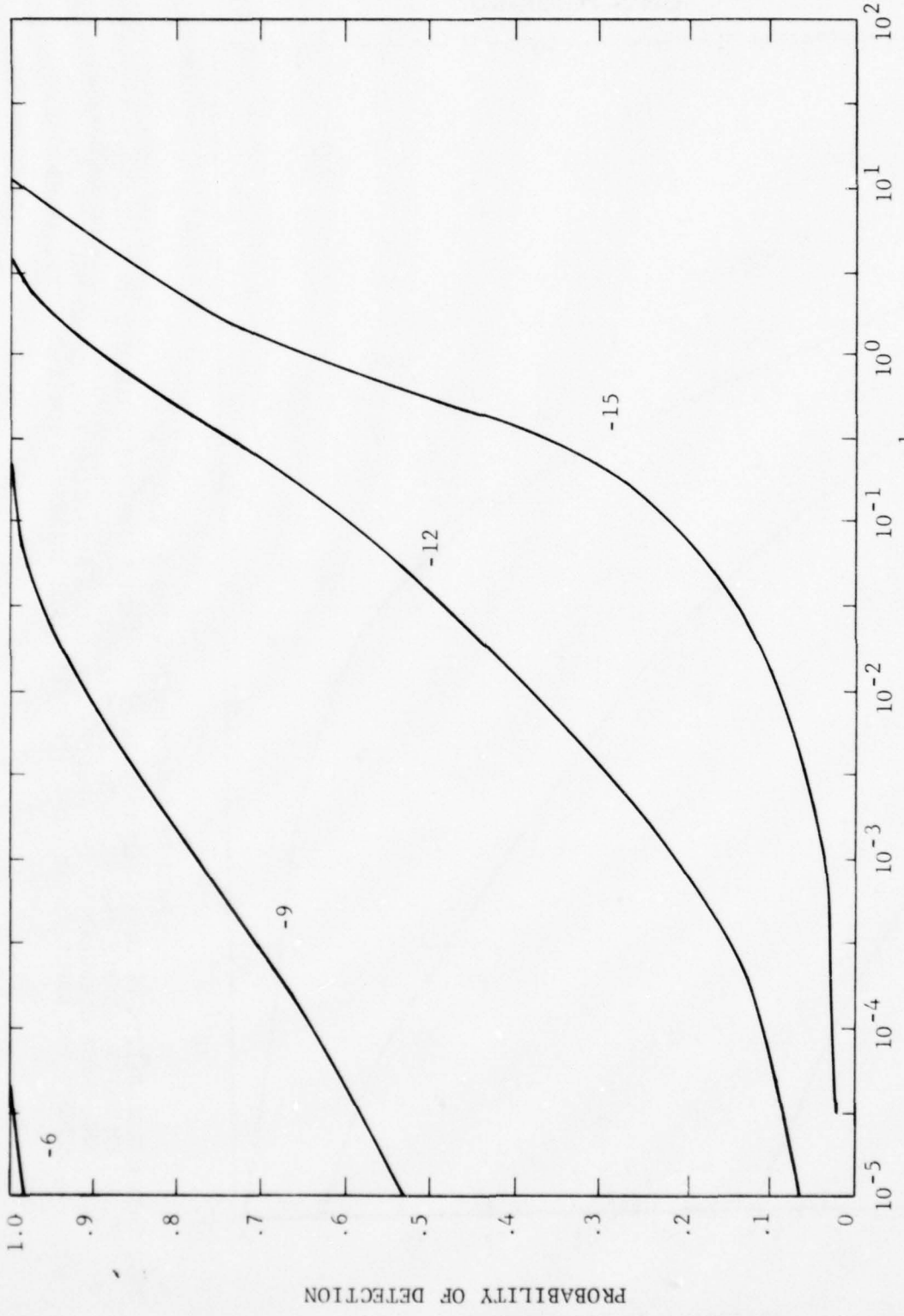

FIG. 2-30 PROBABILITY OF DETECTION VS RATE OF EXCEEDING THRESHOLD FOR 200 HZ 2 SECOND JITTERED FM SLIDE SIGNALS PROCESSED BY CORRELATING IN HALVES, ENVELOPE DETECTING EACH HALF, AND CROSS CORRELATING THE RESULTS. A FINAL AVERAGING TIME OF 20 MILLISECONDS WAS USED. THE INPUT SIGNAL-TO-NOISE RATIOS ARE INDICATED FOR EACH CURVE IN dB.

TRACOR, INC — DWG 6-13-313
AUSTIN, TEXAS — 4-12-66 BROWN/SL

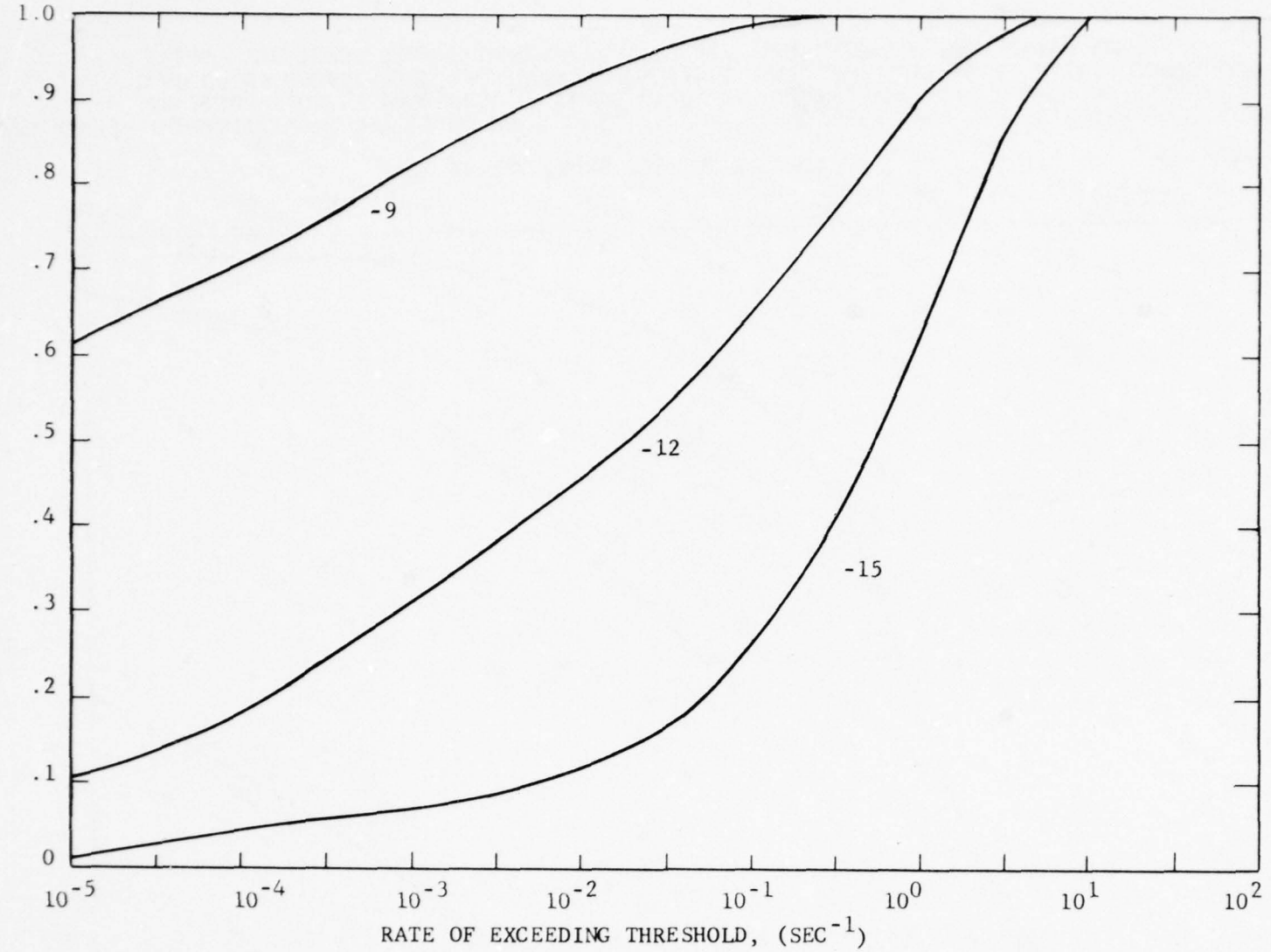

FIG. 2-31 PROBABILITY OF DETECTION VS RATE OF EXCEEDING THRESHOLD FOR 200 HZ 2 SECOND JITTERED FM SLIDE SIGNALS PROCESSED BY CORRELATING IN HALVES, ENVELOPE DETECTING EACH HALF, AND CROSS CORRELATING THE RESULTS. A FINAL AVERAGING TIME OF 40 MILLISECONDS WAS USED. THE INPUT SIGNAL-TO-NOISE RATIOS ARE INDICATED FOR EACH CURVE IN dB.

TRACOR, INC
AUSTIN, TEXAS
1 DWG 6-13-316
4 12 66 BROWN/SL

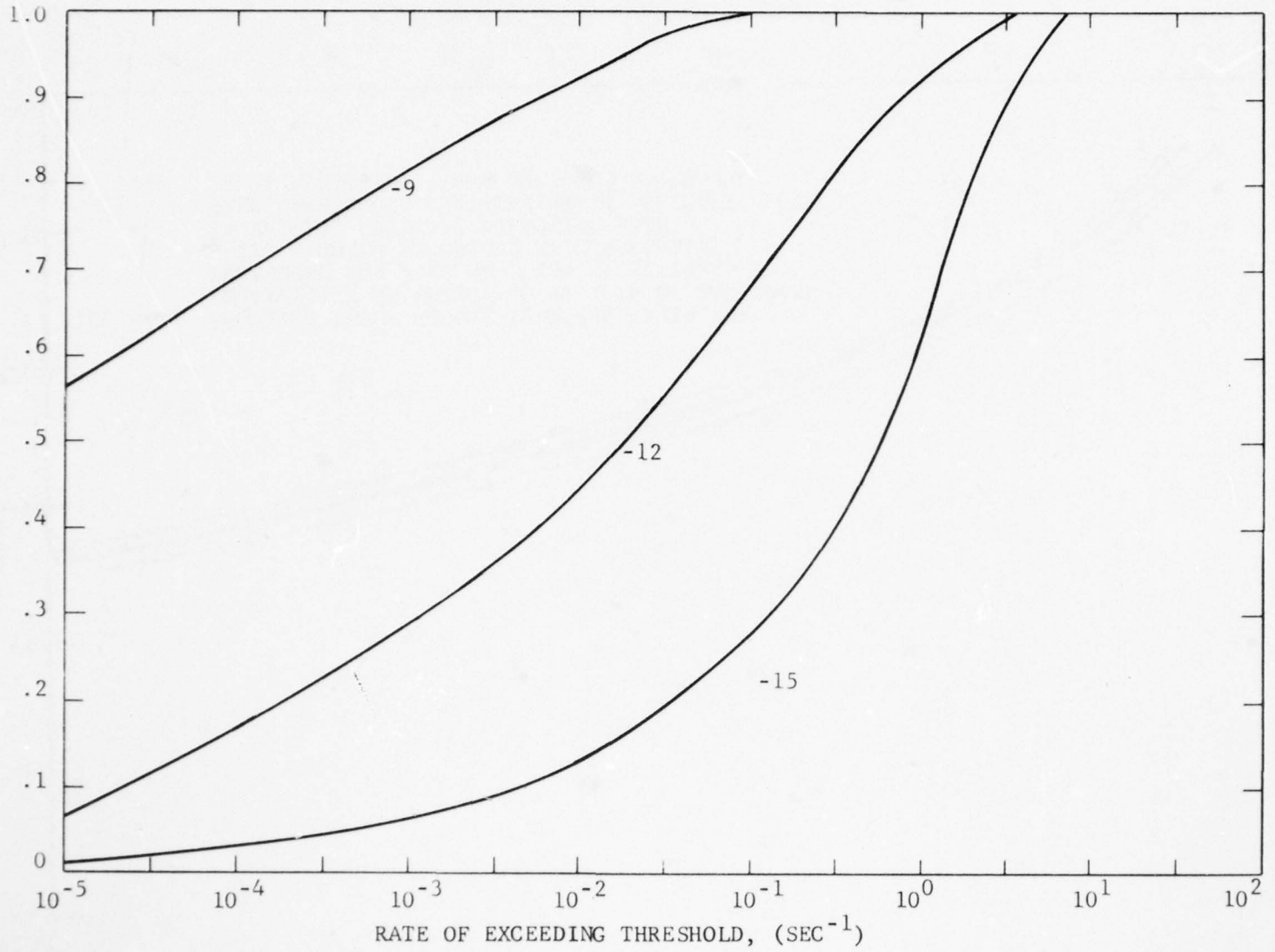

FIG. 2-32 PROBABILITY OF DETECTION VS RATE OF EXCEEDING THRESHOLD FOR 200 HZ 2 SECOND JITTERED FM SLIDE SIGNALS PROCESSED BY CORRELATING IN HALVES, ENVELOPE DETECTING EACH HALF, AND CROSS CORRELATING THE RESULTS. A FINAL AVERAGING TIME OF 80 MILLISECONDS WAS USED. THE INPUT SIGNAL-TO-NOISE RATIOS ARE INDICATED FOR EACH CURVE IN dB.

UNCLASSIFIED

TRACOR, INC. AUSTIN, TEXAS | DWG 6-13-311
4 12 66 BROWN/SL

FIG. 2-33 REQUIRED INPUT SIGNAL-TO-NOISE RATIO FOR 0.5 PROBABILITY OF DETECTION VS RATE OF EXCEEDING THRESHOLD FOR 2 SECOND, 200 HZ JITTERED FM SLIDE SIGNALS PROCESSED BY CORRELATING IN HALVES, ENVELOPE DETECTING EACH HALF, AND CROSS CORRELATING THE RESULTS. FOUR FINAL AVERAGING TIMES ARE USED AS SHOWN.

TRACOR, INC. AUSTIN, TEXAS | DWG 6-13-295 4-12-66 BROWN/SL

2.5.4 Summary of Processor Performances

Figure 2-34 gives required input signal-to-noise ratio for 0.5 probability of detection as a function of threshold crossing rate for the ideal signals and ideal triplets processed as described above. As a general statement, the fully coherent correlation of the FM slides performed best, and the correlation by partial sums of FM slides performed nearly as well.

Figure 2-35 is a plot of required input signal-to-noise ratio for 0.5 probability of detection vs threshold crossing rate for the various processors operating on the jittered signals. The full correlation and the correlation by partial sums in two pieces gave practically the same performance. It is not too surprising that two-piece correlation by partial sums did not have any advantage over the full correlation since the range and Doppler resolutions remaining in the 1 sec, 100 Hz half-signals were still quite adequate to resolve each of the peaks in most of the signals. In the case of the eight-piece partial sums correlation, however, definite improvement is apparent. The cross correlation of the two correlator outputs showed a slight improvement over the full correlation.

2.6 ADAPTIVE RECOMBINATION

Another method of coping with energy-split signals is to measure the energy splitting factor previously described, and to apply an appropriate correction to the output signal-to-noise ratio. This is equivalent to "unsplitting" each signal; that is, the output signal-to-noise ratio is adjusted to that of an ideal signal of the same energy content.

The steps involved in adaptive recombination are illustrated in Fig. 2-36. The energy splitting factor of the output correlogram is continuously measured. If the peak signal-to-noise ratio of the energy-split correlogram is o_1 (Fig. 2-36A), then a corrected value o_2 is derived by use of the energy splitting factor as follows. The processing

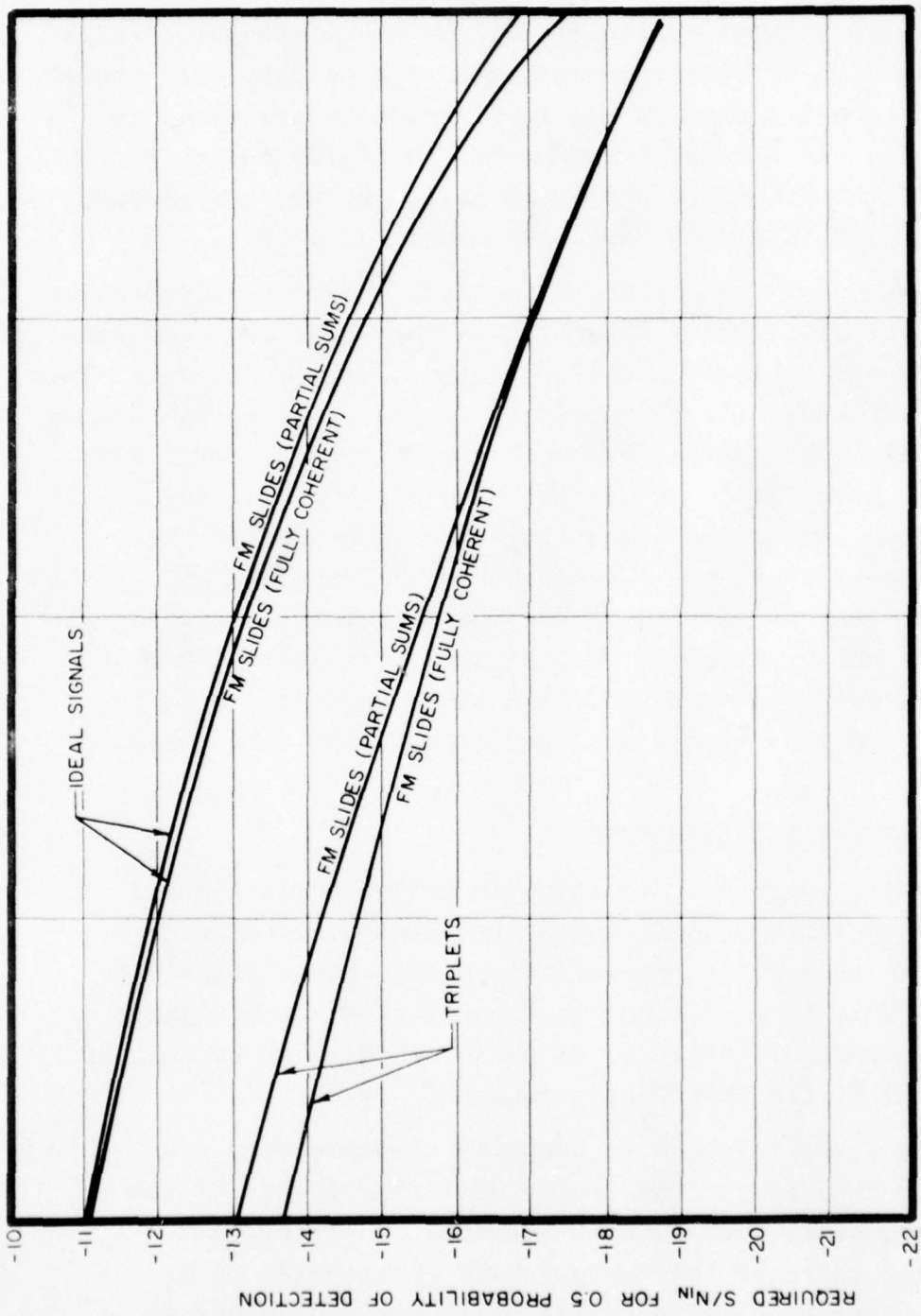

FIG. 2-34 – REQUIRED INPUT SIGNAL-TO-NOISE RATIO FOR 0.5 PROBABILITY OF DETECTION VS RATE OF EXCEEDING THRESHOLD FOR 2 SEC 200 Hz SIGNALS. THE SPECIFIC SIGNAL IS INDICATED ON EACH CURVE

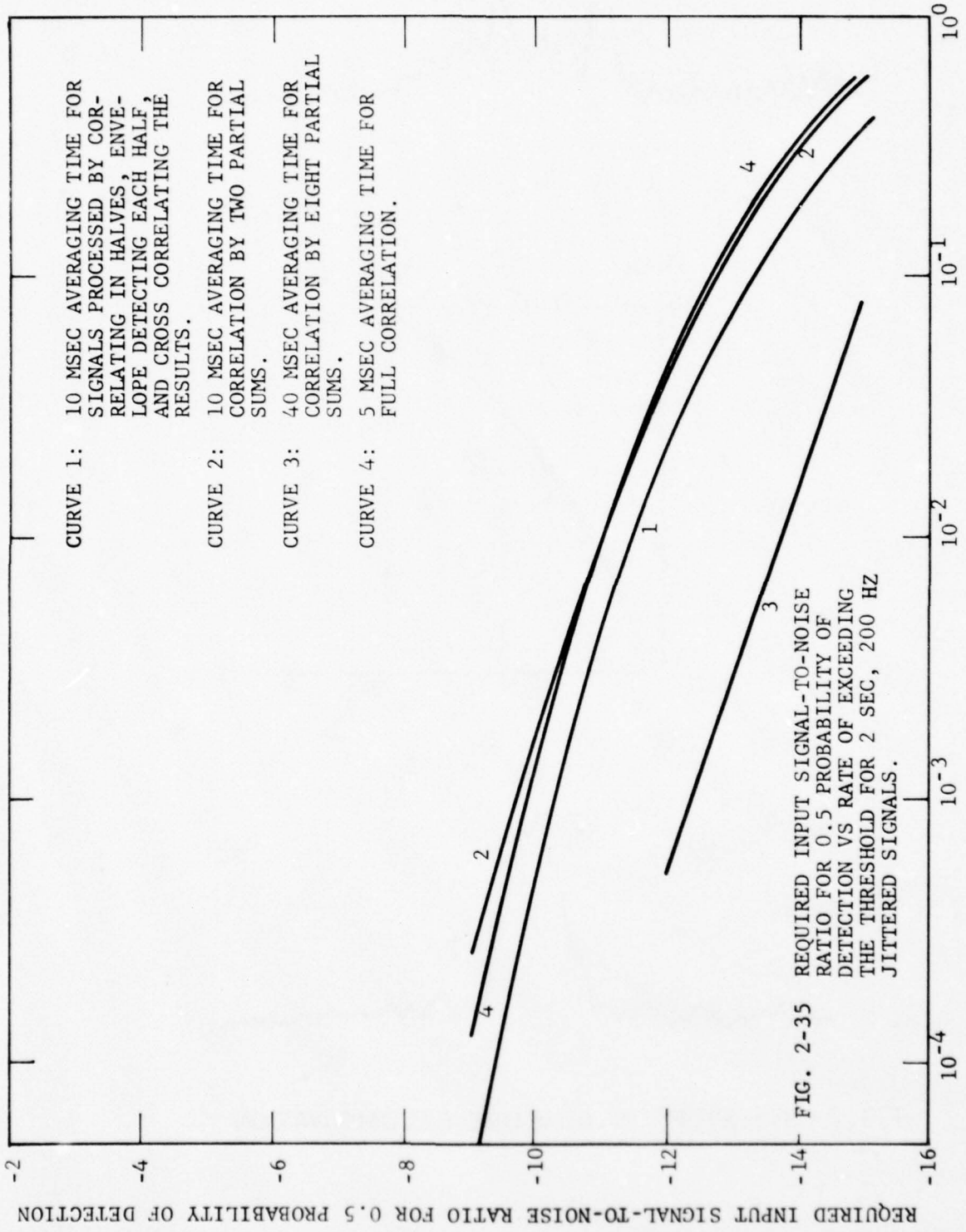

FIG. 2-35 REQUIRED INPUT SIGNAL-TO-NOISE RATIO FOR 0.5 PROBABILITY OF DETECTION VS RATE OF EXCEEDING THE THRESHOLD FOR 2 SEC, 200 HZ JITTERED SIGNALS.

TRACOR, INC. DWG. A6-13-2009
AUSTIN, TEXAS 1-26-67 BROWN/BL

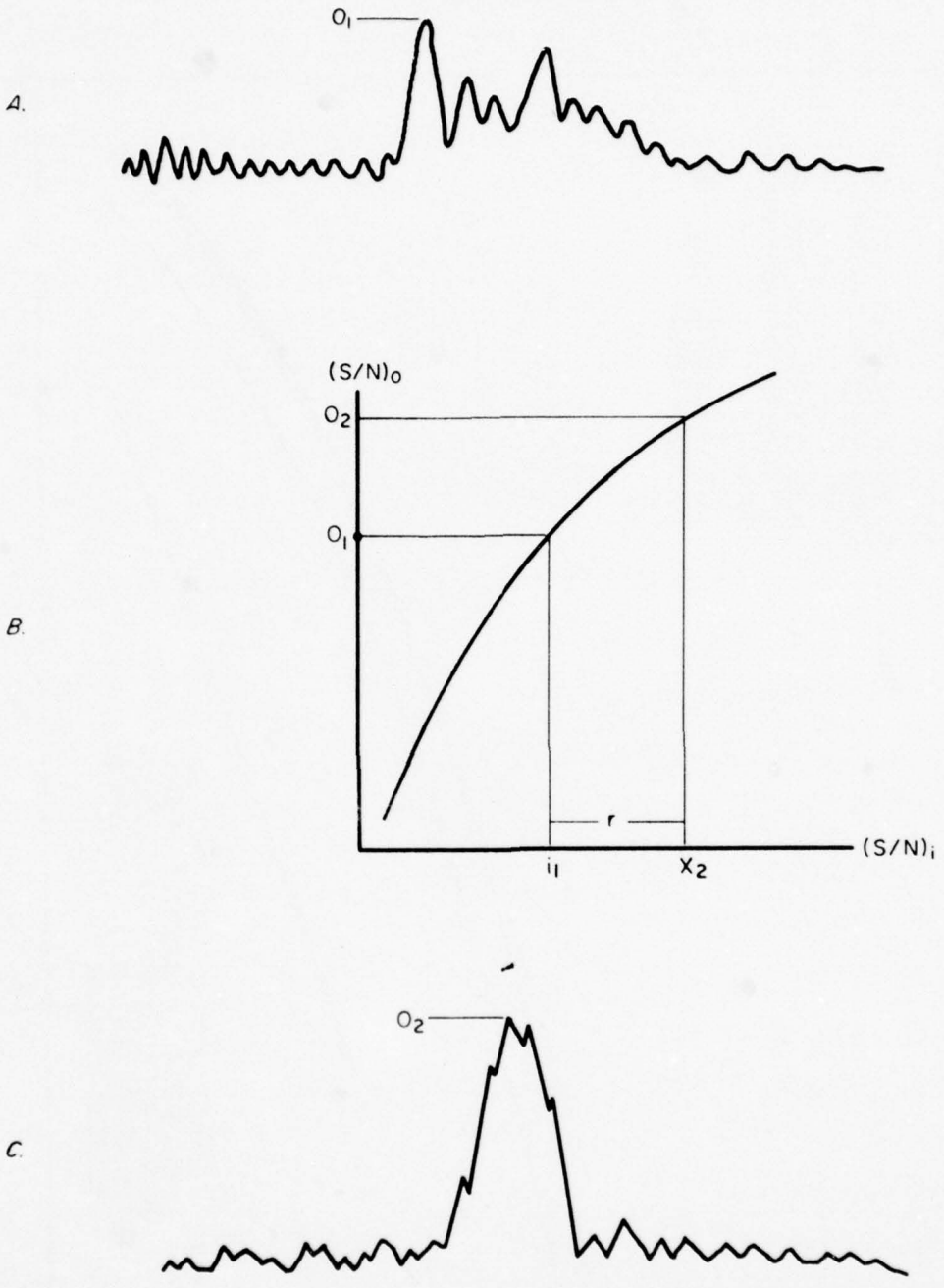

FIG. 2-36 —STEPS IN ADAPTIVE RECOMBINATION

TRACOR DWG. A6-13-2201
9/6/67 HAYES/SL

gain characteristics of the correlator (Fig. 2-36B) are used to find the input signal-to-noise ratio, i_1, of an ideal signal that would give the same output signal-to-noise ratio, o_1, found for the energy-split signal. The measured energy splitting factor, r, is then added to i_1 to obtain a corrected input signal-to-noise ratio, i_2. The processing gain characteristics are then used to find the output signal-to-noise ratio, o_2, corresponding to the corrected input signal-to-noise ratio, i_2. The correlogram output is then adjusted to the corrected value, o_2. For noise alone, o_2 will be practically the same as o_1, but for an energy-split signal, the result is the same as if an ideal signal with input signal-to-noise ratio i_2 had been received and the corresponding output signal-to-noise ratio o_2 recorded (Fig. 2-36C).

This technique was applied to sea data containing echoes from targets at different aspect angles. Its advantages over simple linear correlation are shown in Figs. 2-37 through 2-40. However, the computer simulations used to produce these figures did not operate in real time. The practical application of this method to real time shipboard equipments has not yet been investigated.

2.7 SUMMARY

When real sonar echoes are processed by a linear correlator, a time spreading is observed in the output in excess of that produced by a perfectly coherent, single signal of the same energy. Although this phenomenon is frequently called "correlation loss", it is entirely explainable in terms of multiple returns and does not occur in the correlation process. The energy contained in a real echo is divided among many Doppler-shifted and time-delayed components. This division is termed "echo energy splitting" in this report. When all the effects of echo energy splitting are taken into account, the actual processing gain of the linear correlator agrees with the theoretically expected value.

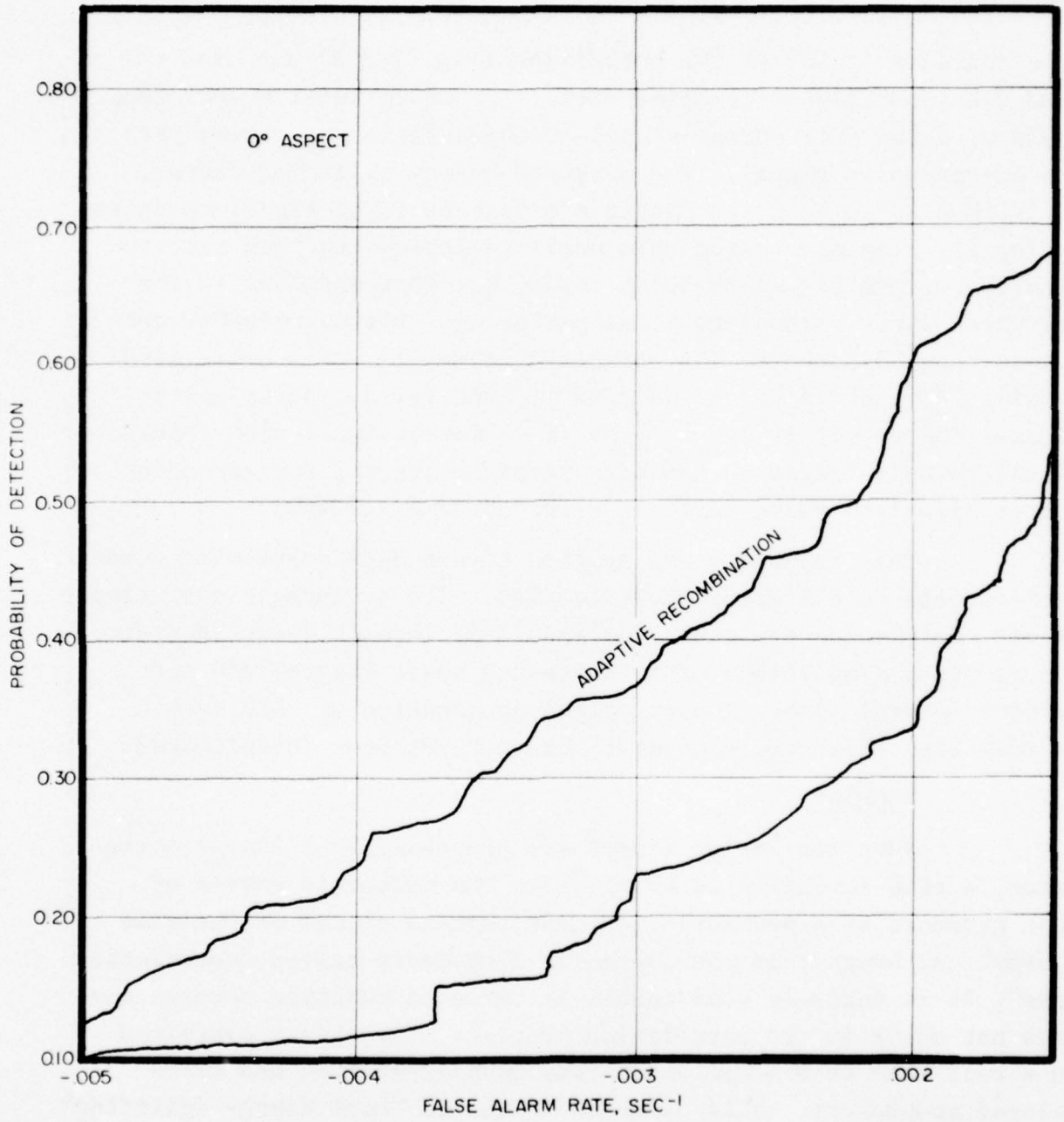

FIG. 2-37 — ADAPTIVE RECOMBINATION COMPARED TO STANDARD LINEAR CORRELATION FOR SEA DATA WITH TARGET AT 0° ASPECT

TRACOR, INC. DWG A6-B-2185
AUSTIN, TEXAS 9-5-67 HAYES/SL

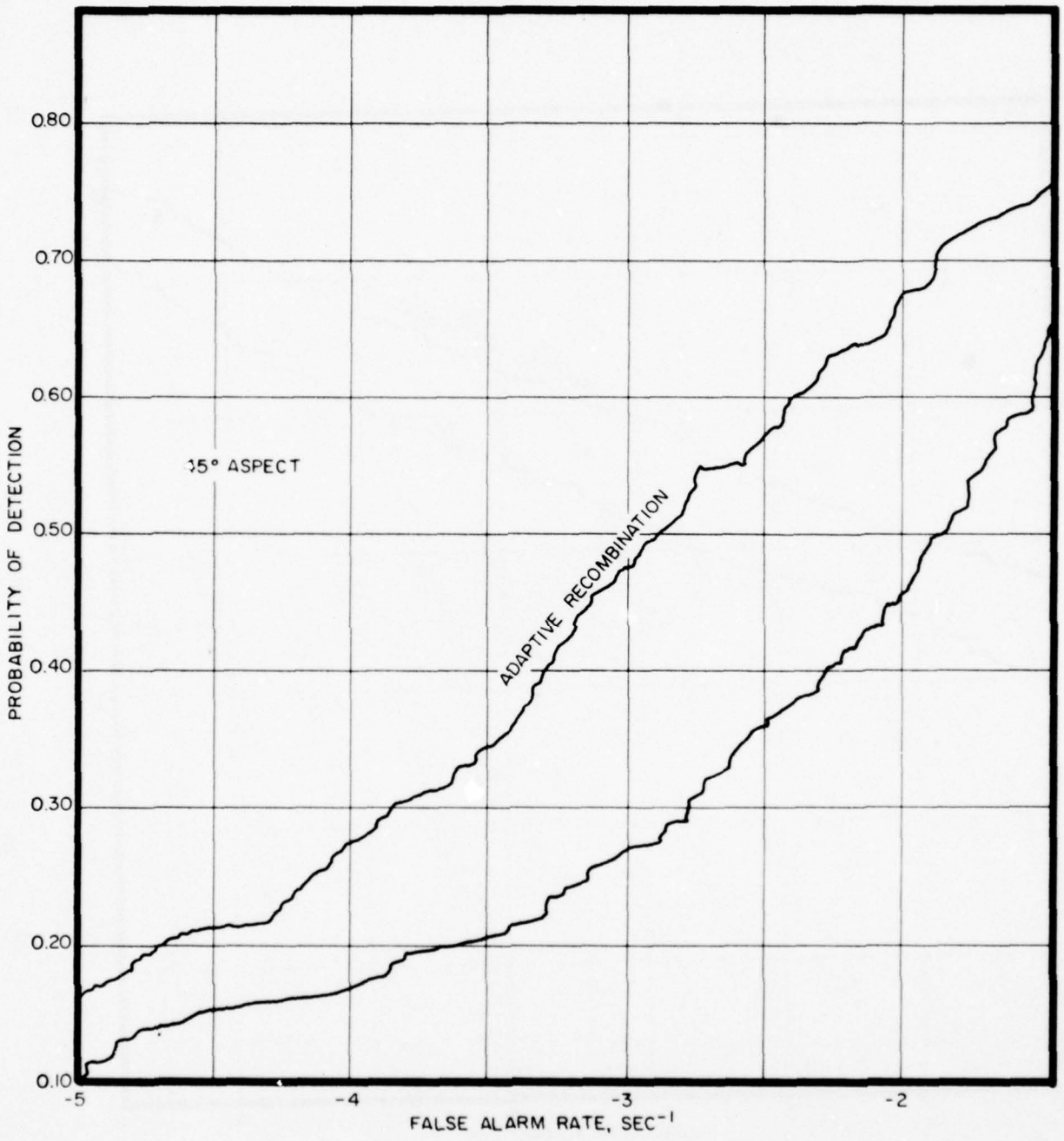

FIG. 2-38 – ADAPTIVE RECOMBINATION COMPARED TO STANDARD LINEAR CORRELATION FOR SEA DATA WITH TARGET AT 45° ASPECT

TRACOR, INC. AUSTIN, TEXAS 9-5-67 DWG A6-13-2187 HAYES/SL

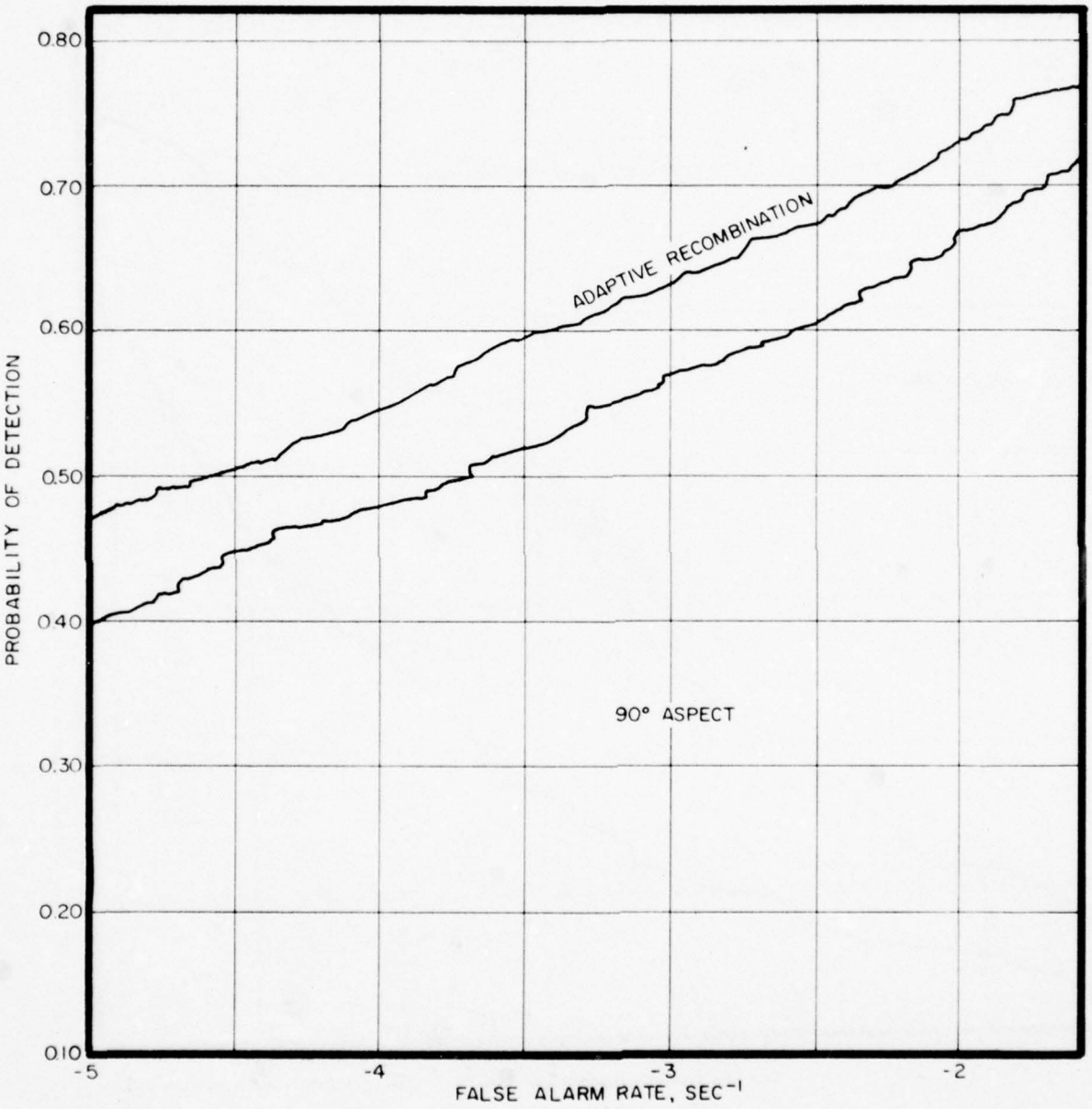

FIG. 2-39 – ADAPTIVE RECOMBINATION COMPARED TO STANDARD LINEAR CORRELATION FOR SEA DATA WITH TARGET AT 90° ASPECT

TRACOR, INC. DWG A6-13-2186
AUSTIN, TEXAS 9-5-67 HAYES/SL

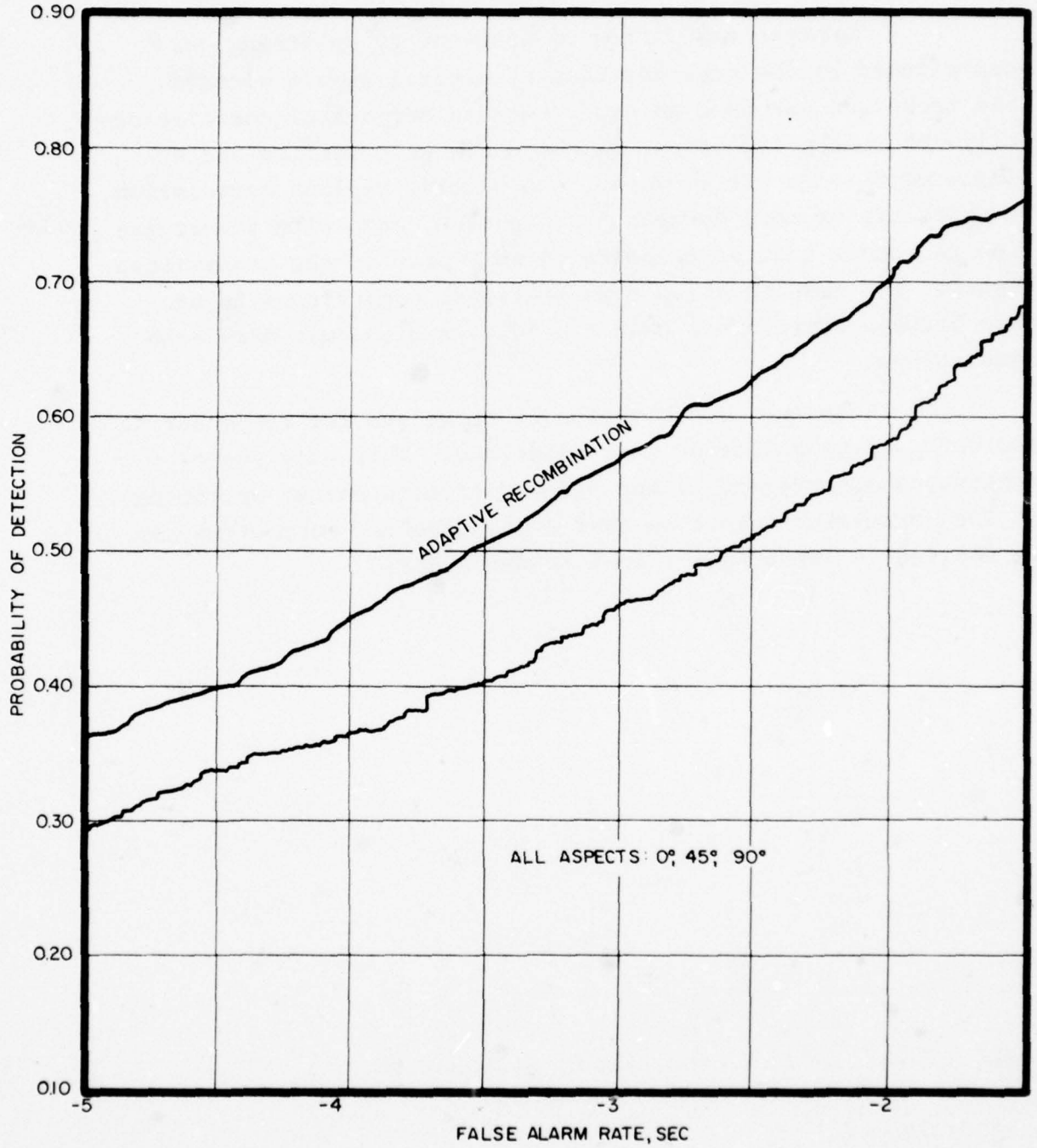

FIG. 2-40 —ADAPTIVE RECOMBINATION COMPARED TO STANDARD LINEAR CORRELATION FOR SEA DATA FOR ALL TARGET ASPECTS

TRACOR, INC. AUSTIN, TEXAS DWG. A6-13 -2188 9-5-67 HAYES/SL

Computer simulation of echo energy splitting was accomplished by the superposition of several simple signals. This technique was used to study two basic types of correlation: fully coherent correlation, in which a single replica and a single correlator are employed, and partial replica correlation, in which two or more correlators are used, each with a correlation reference that corresponds to only part of the transmitted signal. The results allow more realistic comparisons to be made between correlators than can be done with customary echo simulations.

Adaptive recombination, a technique for compensating for echo energy splitting, was described. This consists of a continuous measurement of the effects of echo energy splitting in the correlator output so that a commensurate correction can be applied to the output signal-to-noise ratio.

3. POST CORRELATION NORMALIZATION

3.1 GENERAL DISCUSSION OF NORMALIZATION

In modern sonar systems one of the large remaining problems is that of obtaining a well normalized output from the temporal processor without sacrificing processing gain By a normalized output is meant that in the absence of signal the output from the processor will possess a stationary statistic, which in turn implies that the mean and standard deviation of the output will be time-invariant. This normalization is required to obtain optimum performance from existing sonar displays due to their limited dynamic range. There are several ways to obtain normalization in the output from the temporal processor. One of these is by the well-known technique of hard-clipping. Unfortunately, performance degradations are inherent in this approach. The conventional AGC is another method to achieve normalization. When the AGC is applied before the temporal processor, time constants which are large compared to the signal duration must be used in order not to degrade the signal return. This restriction places a limit on the degree of normalization which may be achieved.

The use of linear matched filter techniques provides an opportunity to do further normalization after the temporal processor. This is due to the time compression of the signal which occurs in such a device. The nominal pulse length from the matched filter is given by the reciprocal of the pulse bandwidth. For example, if 100 Hz bandwidth FM slide signals of $\frac{1}{2}$ sec duration are processed through a linear replica correlator, the pulse length expected in the output is 10 ms. A process similar to AGC may be implemented on this output, but the time constant must now be long relative to 10 ms rather than to $\frac{1}{2}$ sec.

This chapter presents the results of some investigations of techniques for effecting post-correlation normalization of the output of a specific processor, a linear replica correlator followed by an envelope detector with a 10 ms time constant operating on 100 Hz FM slide signals of 0.5 sec duration.

3.2 NORMALIZATION TECHNIQUES

Normalization was performed in three ways according to the following formulas:

$$y = \frac{x-\bar{x}}{\sigma} , \qquad (3.2\text{-}1)$$

$$y = \frac{x-\bar{x}}{\bar{x}} , \qquad (3.2\text{-}2)$$

$$y = \frac{x}{\bar{x}} , \qquad (3.2\text{-}3)$$

where y represents normalized output, x represents the input sample to the normalizer, and σ and $\bar{x}$ are the standard deviation and the mean of the input computed in a region in the vicinity of x.

The mean and standard deviation of the unnormalized output were examined for AN/SQS-26 sea data representing the annulus of bottom-bounce transmission with a depression angle of 30^{o}. The mean and standard deviation of the output were calculated for each sequential 100 ms interval of the input data. The input data were recorded at the input to the clipper amplifier so that the AGC circuits of the system were used.

TRACOR 6500 TRACOR LANE, AUSTIN, TEXAS 78721

The first curve of Fig. 3-1 shows sequential values of the mean values for a typical echo cycle. For this cycle the mean value of these numbers is 0.042 and the standard deviation of the numbers is 0.014. For a total of 16 echo cycles investigated the average mean value and standard deviation of the mean value were 0.043 and 0.014, respectively.

The second curve of Fig. 3-1 shows sequential values of the standard deviations calculated from the 100 ms intervals of the same echo cycle. The mean value for these numbers is 0.017 and their standard deviation is 0.006. The average mean and standard deviation for the 16 echo cycles were 0.018 and 0.007, respectively.

The third curve of Fig. 3-1 shows the standard deviation divided by the mean. This ratio was calculated for each of the 100 ms intervals described above. The mean value for these numbers is 0.404 and their standard deviation is 0.083. Average values for the 16 echo cycles are 0.411 and 0.093.

When the above described experiments were repeated using a 200 ms interval instead of a 100 ms interval, the results given in Table 3-I were obtained.

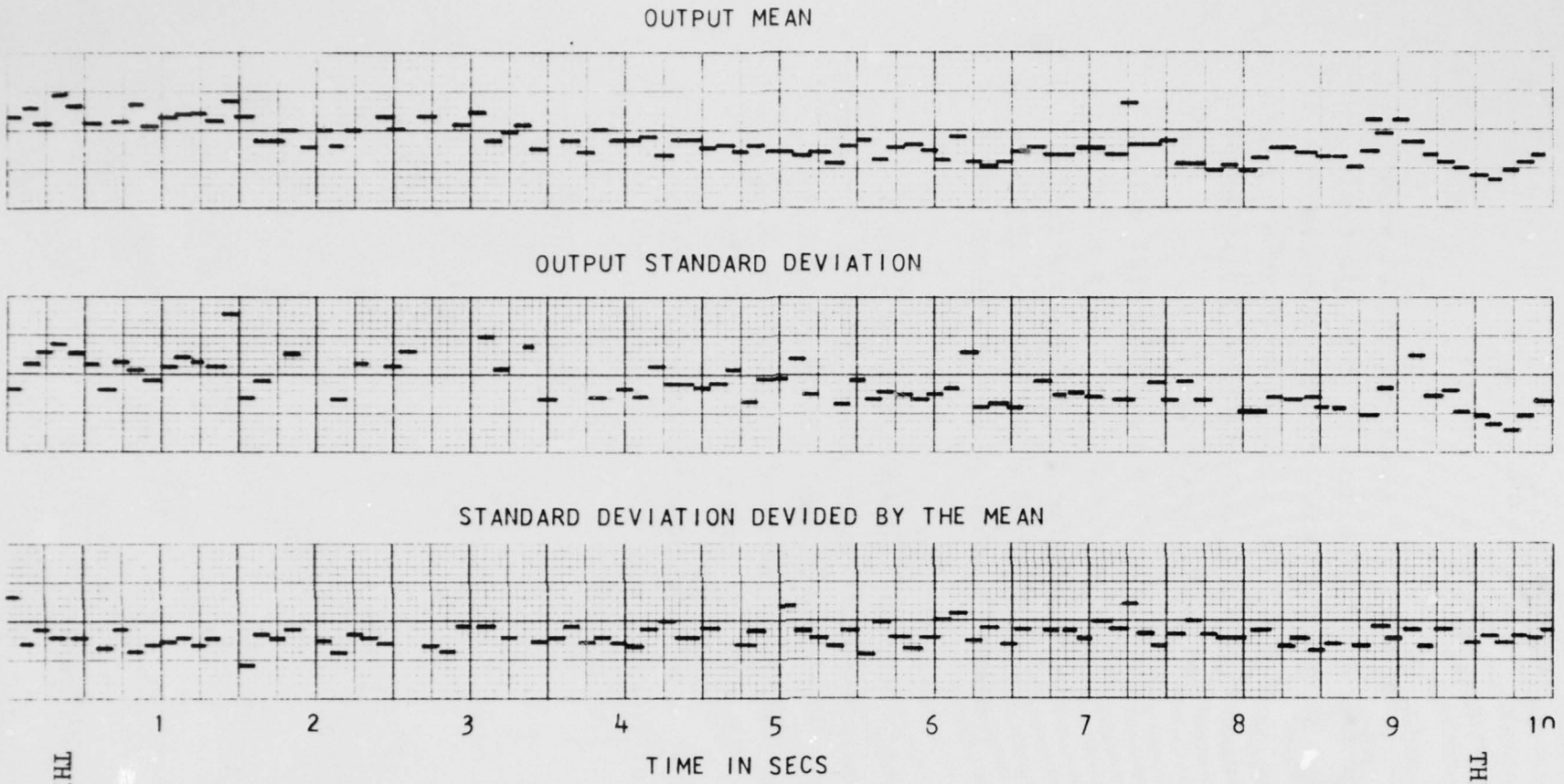

FIG 3-1 - MEAN AND STANDARD DEVIATION FOR 100 MS INCREMENTS OF A TYPICAL ECHO CYCLE

60

CONFIDENTIAL
THIS DRAWING IS UNCLASSIFIED

TRACOR, INC. | DWG A6-13-2090
AUSTIN, TEXAS 5-4-67 C. HAYES S.D.

TRACOR 6500 TRACOR LANE, AUSTIN, TEXAS 78721

TABLE 3-I

DATA COMPUTED FROM SEQUENTIAL 200 MS SECTIONS FROM TYPICAL BOTTOM BOUNCE ANNULI

	For One Typical Echo Cycle	Average for 16 Echo Cycles
Mean Values		
mean	0.042	0.041
standard deviation	0.013	0.012
Standard Deviations		
mean	0.018	0.019
standard deviation	0.006	0.007
Ratio of Standard Deviation to the Mean		
mean	0.426	0.435
standard deviation	0.071	0.078

These data carry certain implications with regard to the three normalization formulas previously listed. From Fig. 3-1 it can be seen that both the output mean and the standard deviation change with time, but that their quotient is approximately time-invariant. Equation (3.2-1) will yield an output function which is directly relatable to output signal-to-noise ratio defined by

$$\left(\frac{S}{N}\right)_o = \frac{(P-\bar{x})^2}{\sigma^2},$$

where P is the peak value of the signal. Equation (3.2-1) should give the closest approximation to an output function having a zero mean and unity standard deviation. Since the ratio of standard deviation to the mean is nearly time stationary, Eq. (3.2-2) should give a result equivalent to Eq. (3.2-1) except for a constant factor. Since Eq. (3.2-3), written in terms of voltage, varies from Eq. (3.2-2) only by the additive constants of one, its effect on the relative peak heights should be identical to that of Eq. (3.2-2). This is verified in the following data.

For each of the three normalizing equations two basically different techniques were used to obtain the required values of mean and standard deviation.

In the first method, three consecutive windows, as shown in Fig. 3-2, were established in the data record. The first and third windows, each of 100 ms duration, made up the region from which the noise mean and standard deviation were calculated. The center window, initially of 100 ms duration, provided the value of x used in the normalization formulas. After each measurement of x, $\bar{x}$, and σ, the correlator output was advanced one sample and the process was repeated.

The 100 ms duration used initially for the signal window gave erroneous results because, in the data used, the signal structures trailed out beyond the largest peak by more than 50 ms. As a result, some of the signal structure occurred within the second region in which the mean and standard deviation were measured so that excessively large values were measured for these quantities. Using a window duration of 200 ms eliminated this problem.

The second basic technique for obtaining the required values consisted of measuring the mean and standard deviation in a single section of noise which preceded the sample value x

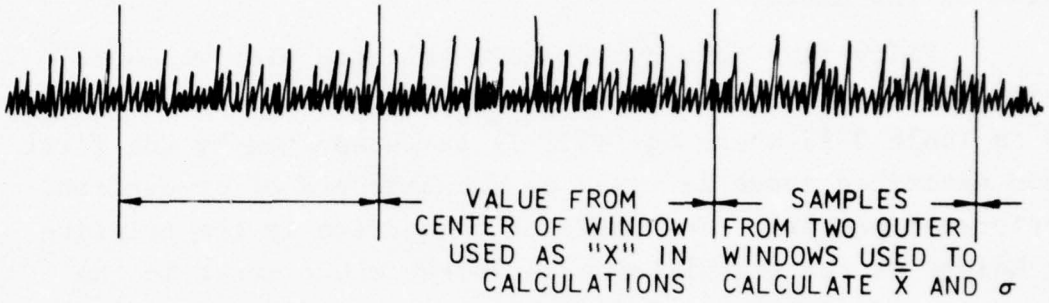

FIG. 3-2 - FIRST METHOD OF OBTAINING MEAN AND STANDARD DEVIATION

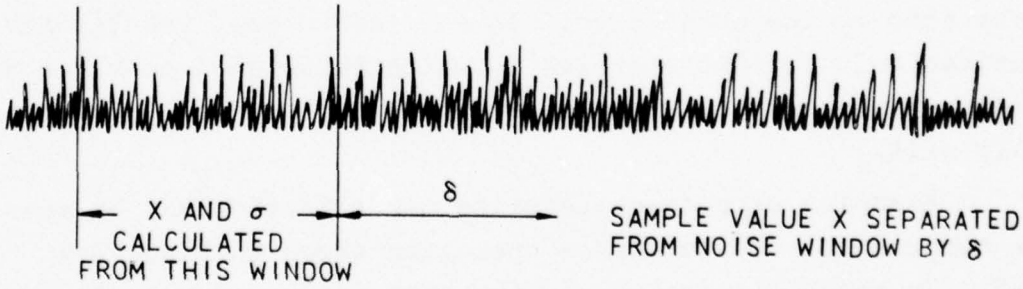

FIG. 3-3 - SECOND METHOD OF OBTAINING MEAN AND STANDARD DEVIATION

by a given amount δ (Fig. 3-3). Two different intervals, 100 ms and 200 ms, were used for obtaining the mean and standard deviation of the noise.

Fifty-five echo cycles were selected over which to compare the three normalization schemes. The results are summarized in Table 3-II where Eq. (3.2-1) as determined by the first method described above is taken as the standard of comparison, or reference process. The basis of comparison is the relative peak height of the signal compared to the other peaks in the echo cycle. For example if, for the reference process, the signal peak were the second largest peak in the echo cycle and another process resulted in making the signal peak the largest, this latter process would win over the reference process. However, if the signal peak dropped to third position or lower, the process would lose. The table lists the number of echo cycles in which each process performed better than the reference process, the number for which it tied, and the number for which it lost.

In Table 3-II, the first row summarizes the results for all the echo cycles considered. In the second row, results are summarized only for those cycles in which the signal peak was not the largest peak value. As expected, Eqs. (2) and (3) performed equally well.

Examples of post-correlation normalization may be seen in the outputs for bottom bounce operation shown in Figs. 3-4 and 3-5. In these figures the entire echo cycle was used instead of just the annulus. In Fig. 3-4, the upper graph shows unnormalized output of a linear correlator that had input from the beamformer, and the lower graph shows the same output normalized according to Eq. (3.2-1). The graphs in Fig. 3-5 show linear correlator output for input that had been through the AGC. The unnormalized correlator output shown in the upper graph as compared to the upper graph of Fig. 3-4 demonstrates that the AGC has partially normalized the output. The further effect of normalization according to Eq. (3.2-1) is shown in the lower graph of Fig. 3-5.

Table 3-II

	MEAN AND STANDARD DEVIATION COMPUTED IN REGION CONSISTING OF TWO SECTIONS EACH 100 MS LONG, ONE BEFORE AND ONE AFTER THE PEAK VALUE			MEAN AND STANDARD DEVIATION COMPUTED IN REGION CONSISTING OF ONE SECTION 200 MS LONG AHEAD OF PEAK VALUE ENDING 50 MS BEFORE THE PEAK VALUE			MEAN AND STANDARD DEVIATION COMPUTED IN REGION CONSISTING OF ONE SECTION 100 MS LONG AHEAD OF PEAK VALUE ENDING 50 MS BEFORE THE PEAK VALUE			
	EQ. 1	EQ. 2	EQ. 3	EQ. 1	EQ. 2	EQ. 3	EQ. 1	EQ. 2	EQ. 3	NO NORMALIZATION
WON	0	10	10	9	6	6	7	4	4	
TIED	55*	33	33	23	8	8	17	10	10	1
LOST	0	12	12	23	41	41	31	41	41	11
AVERAGE SIGNAL POSITION IN RANK	2.95	3.25	3.25	2.4	4.72	4.72	6.1	6.68	6.68	12.26

The following columns are a result of selecing echo cycles such that the signal peak is not the largest peak value in the echo cycle

WON	0	3	3	5	4	4	2	1	1	
TIED	15*	5	5	3	1	1	1	1	1	
LOST	0	7	7	7	10	10	12	13	13	
AVERAGE SIGNAL POSITION IN RANK	7.26	8.6	8.6	7.23	9.96	9.96	13.66	15.63	15.63	16.20

*Reference performance to which other results were compared

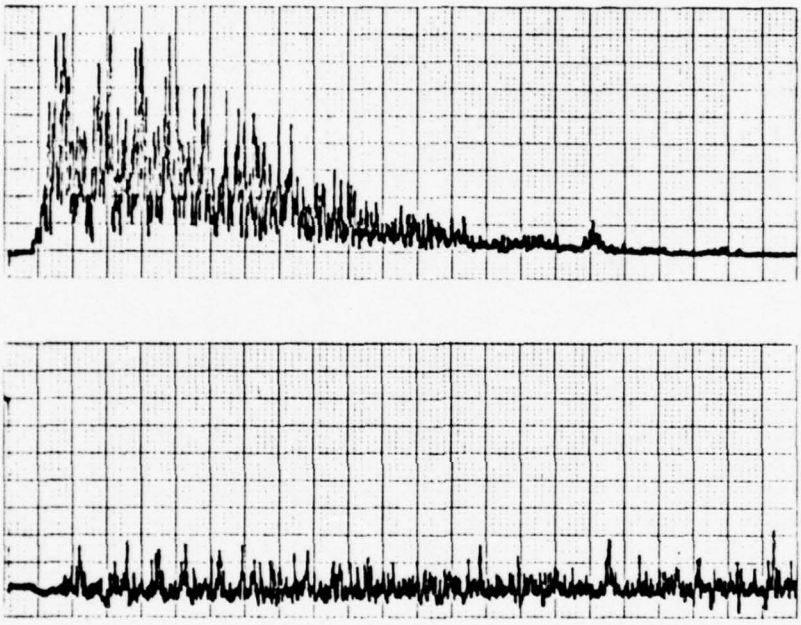

FIG. 3-4 - THE OUTPUT OF A LINEAR CORRELATOR WITHOUT AGC BEFORE AND AFTER NORMALIZATION

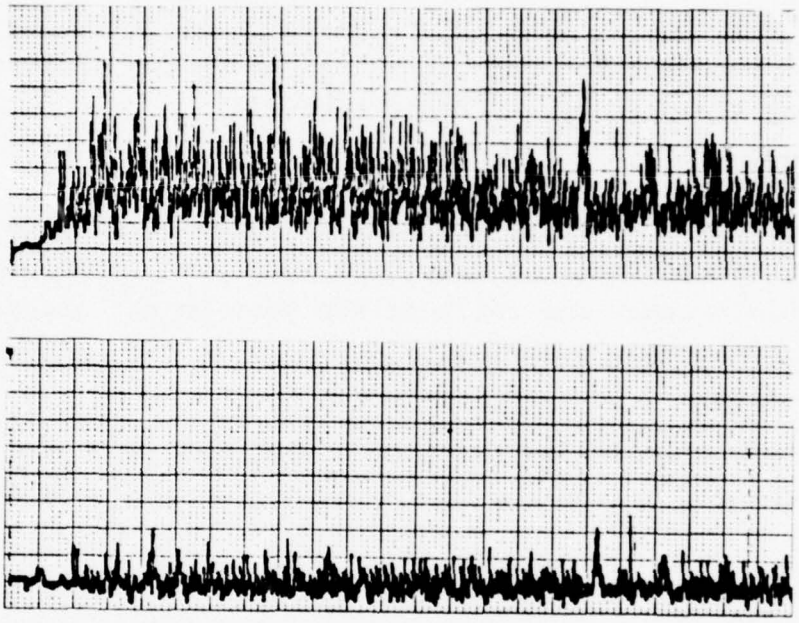

FIG. 3-5 - THE OUTPUT OF A LINEAR CORRELATOR WITH AGC BEFORE AND AFTER NORMALIZATION

From Figures 3-4 and 3-5 one might conclude that the AGC before the processor is unnecessary since the post correlation normalization appears to do an adequate job. From a practical point of view, however, the best approach could well be to use both the AGC and the post correlation normalizer. The AGC would control the dynamic range at the input to the processor thereby making the processor cheaper to build.

3.3 SUMMARY

The output of a linear correlator was normalized by each of three techniques. It was found that such techniques are practicable because the ratio of the mean to the standard deviation is apparently relatively invariant in the unnormalized correlator output.

Of the normalizing techniques employed, the best results were achieved by the one characterized by the formula

$$y = \frac{x - \bar{x}}{\sigma}$$

where y is the normalized output, x is the input sample to the normalizer, $\bar{x}$ is the mean value of the input in the vicinity of x, and σ is the corresponding standard deviation.

4. SIGNAL PROCESSING APPLIED TO A SECTOR SCAN INDICATOR

Much of the improvement in sonar performance so far achieved has been by the application of signal processing techniques that enhance the signal-to-noise ratio of the return prior to its display. But these signal processing techniques have not been explited for precision bearing measurements on the Sector Scan Indicator (SSI).

SSI displays the output of a phase measuring device as a function of range for a chosen section of bearing angle. Essentially no signal processing is done to enhance the signal-to-noise ratio. This chapter investigates a coded pulse SSI that employes signal processing by a linear replica correlator.

4.1 BEARING INFORMATION FROM PHASE MEASUREMENTS

On search and initial detection, fixed receiving beams are used and the output of each beam is subjected to separate signal processing. Equipment and space requirements limit the number of beams which, in turn, limits bearing accuracy. Since receiving beams are formed from the output of several adjacent transducer staves, the receiving array may be divided into two parts to form a split beam. Each of these beams may then be processed and phase differences measured to obtain bearing. This accomplishes interpolation between the receiving beams.

A small bearing deviation from the center of the receiving beam can cause a significant phase difference between the two split beams. For the geometry and frequency of the SQS-26 sonar system for example, one degree of bearing deviation would cause about 27 degrees of phase difference in the outputs from correlators processing FM slide signals running from 100 → 200 Hz.

4.2 PHASE MEASUREMENTS PROCEDURE

A simulation analysis was performed to determine whether sufficient accuracy could be obtained from phase difference measurements in the output of a correlator. An analog device was constructed to measure the time difference between positive going axis crossings in the two channels from which the phase difference could be computed. The output of this device was analyzed on a digital computer. This particular device was somewhat inflexible and, in later investigations, the phase measurements were accomplished on a digital computer directly from the sampled time function.

4.3 PHASE MEASUREMENT ACCURACIES

4.3.1 Ideal Signals

Since the signal is added to noise, the time difference between channels can be expected to vary statistically. The first part of this study investigated the accuracy that can be expected in phase measurements as a function of signal-to-noise ratio.

The analog device was tested with a simulated CW signal and found to give accuracies that agree with theoretical predictions. Correlograms of 100 Hz FM slides were processed. The procedure for measuring phase differences of correlograms utilized a synchronization channel so that phase measurements were taken only when correlogram peaks were expected. The standard deviation of phase measurements is plotted as a function of rms output signal-to-noise ratio in Fig. 4-1. The solid curve is the theoretically predicted standard deviation. Phase measurements that would correspond to bearing deviations of targets in other beams have been eliminated in this plot.

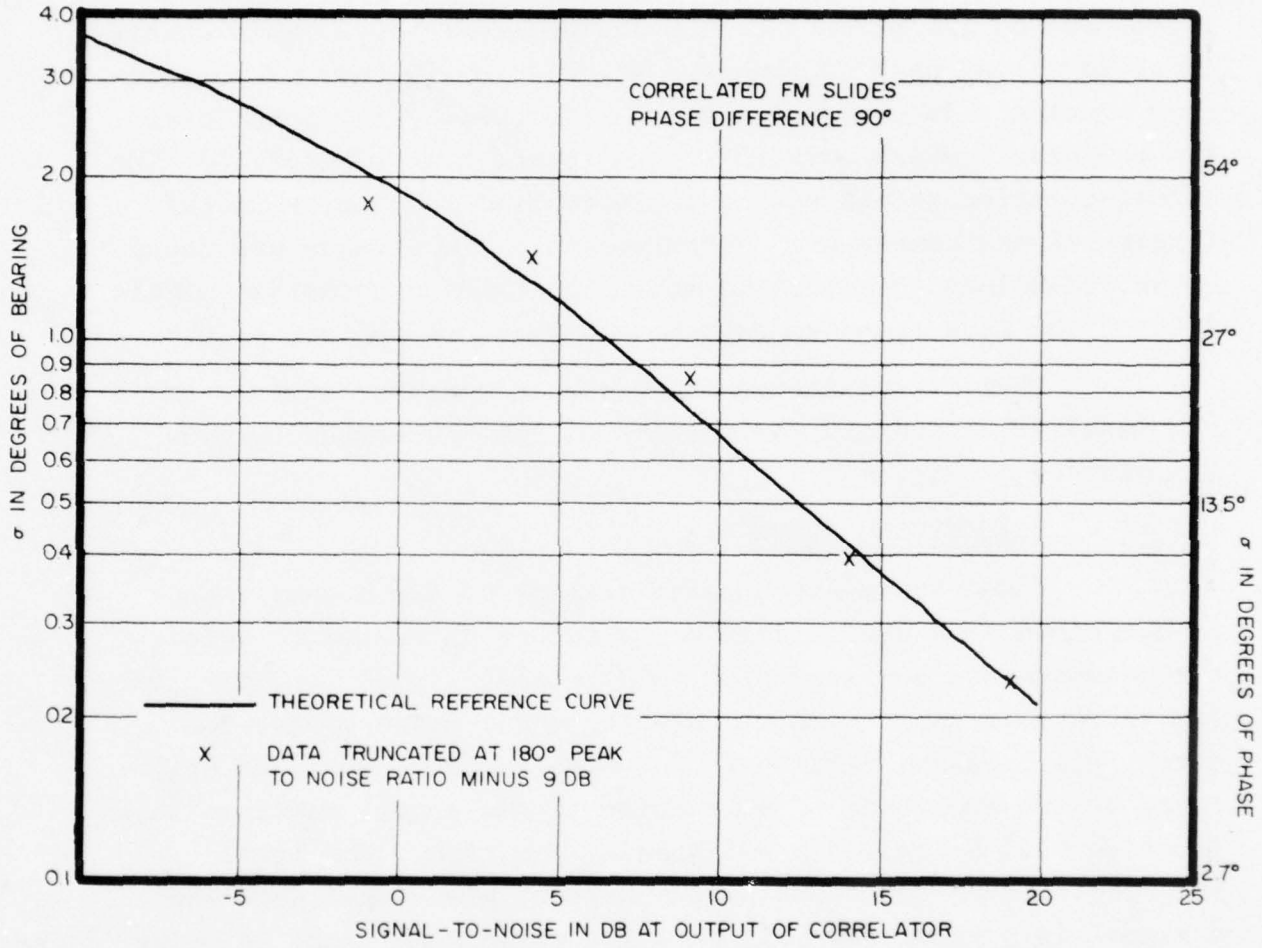

FIG. 4-1 –STANDARD DEVIATION OF PHASE DIFFERENCE VS SIGNAL-TO-NOISE RATIO FOR SPLIT BEAM SIGNALS

TRACOR, INC. AUSTIN, TEXAS 9-5-67 DWG. A6-13-2196 HAYES/SL

4.3.2 Simulated Structured Signals

In Section 2 a statistical model for signals was described that is representative of time and frequency spreading introduced by the effects of the medium and target. This statistical model was used to generate signals for further phase accuracy studies. In these signals the energy is distributed over six components which vary in frequency and time of arrival. The signal-to-noise ratios were calculated from the energy in the largest signal component. Measurement on 100 signals was found to be sufficient to place the measured standard deviation within ±20% of the true standard deviation with a probability of 0.8.

These signals were processed in a manner similar to the ideal FM slides and the results of the phase measurements are plotted in Fig. 4-2.

4.4 BRIGHTENING FUNCTIONS

Since the exact time of arrival of the signal peak is not known in a real situation, a method is needed to select the measurements corresponding to promising signal returns. One way to do this is to make the display phase measurements for every axis crossing detected. The display trace would be brightened by the amplitude of a function of the signal return. This function will be called a brightening function. The ideal brightening function would have a narrow, pronounced peak when a signal is present and fall to a low value when there is noise alone. There are several possible functions to consider:

1. The correlated signal from one channel.
2. The envelope of the correlated signal from one channel.
3. The coherent sum of both channels.
4. The envelope of the coherent sum of both channels.
5. The incoherent sum of both channels formed by adding the envelopes of each of the channels.

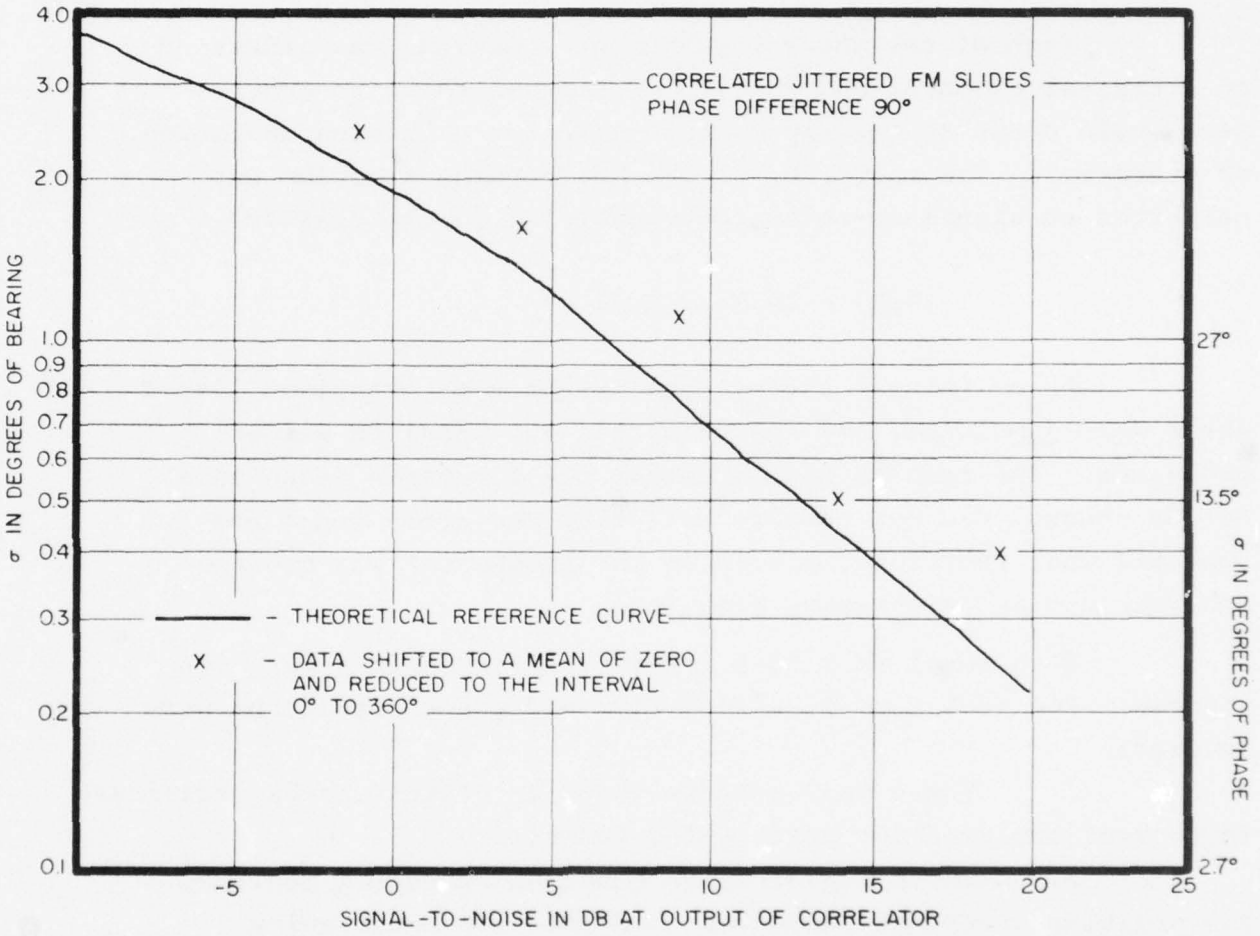

FIG. 4-2 — STANDARD DEVIATION OF PHASE DIFFERENCE VS SIGNAL-TO-NOISE RATIO FOR SPLIT BEAM SIGNALS

TRACOR, INC. AUSTIN, TEXAS 9-5-67 DWG A6-13-2195 HAYES/SL

TRACOR 6500 TRACOR LANE, AUSTIN, TEXAS 78721

6. The coherent sum with peak holding accomplished by averaging the magnitudes of the negative and positive peaks of the coherent sum previous to the crossings.

Each of the above brightening functions was generated on a digital computer and shifted in time so that its central peak would occur at the appropriate time for a bearing deviation of 0 degrees. The value, B, of the brightening function was converted to signal-to-noise (dB) according to the relation

$$(S/N) = 20 \log[(B-m)/\sigma] \quad .$$

As an initial survey, the brightening functions listed above were simulated, and approximately 100 ideal FM slides processed. The results indicate that the functions based on a single channel did not compare well with the other functions. Emphasis was, therefore, placed on the incoherent sum and the coherent sum as brightening functions.

Both ideal FM slides and jittered FM slides were considered. For each type of signal five different situations were covered:

1. Phase measurements based on positive axis crossing incoherent sum used for brightening function.
2. Phase measurements based on averaging positive and negative crossings-incoherent sum used for brightening function.
3. Phase measurement based on positive crossings-coherent sum used for brightening function.
4. Phase measurement based on averaging positive and negative crossings - coherent sum used as brightening function
5. Phase measurements based on averaging positive and negative crossings - coherent sum with peak holding used as brightening function.

TRACOR 6500 TRACOR LANE, AUSTIN, TEXAS 78721

4.5 RESULTS

In order to display the phase measurement data in a readable, condensed form, thresholds of 10, 15, and 20 dB were set on the brightening functions. The standard deviation of all phase measurements corresponding to brightening function values above these thresholds were found. Figures 4-3 through 4-8 show the standard deviations associated with each threshold as a function of rms $(S/N)_{out}$ of the correlogram for both the coherent and incoherent sum brightening functions. In each case both the positive and negative crossings were used to determine the phase measurement. Graphs for 0, 2, and 4 degrees bearing deviation are presented for both ideal and jittered signals. The measurements utilizing only positive going crossings gave standard deviations from 1 to 4 phase degrees higher than the corresponding positive and negative crossings. The coherent sum with peak holding gave performance equivalent to the coherent sum except in the 4 degree bearing deviation case where it was slightly better. There are some anomalies in the graphs; for example, in Fig. 4-3, the 20 dB threshold curve for the incoherent sum increases with increasing output S/N. This is caused by the rather broad peak of the incoherent sum allowing phase measurements to be taken from crossings associated with secondary peaks of the correlogram.

In general, the coherent sum selects the good correlogram crossings when the bearing deviation is small; however, for larger bearing deviations destructive adding becomes important and its performance is degraded. The incoherent sum has the disadvantage of a broad peak that allows some phase measurements in regions where accurate measurements cannot be made. Its performance does not change significantly with bearing deviation. If the maximum bearing deviation could be limited to about two degrees, the coherent sum seems to be the best brightening function, combining a sharp peak with good processing gain. Otherwise, the best compromise is the incoherent sum with excellent processing gain but a rather broad peak.

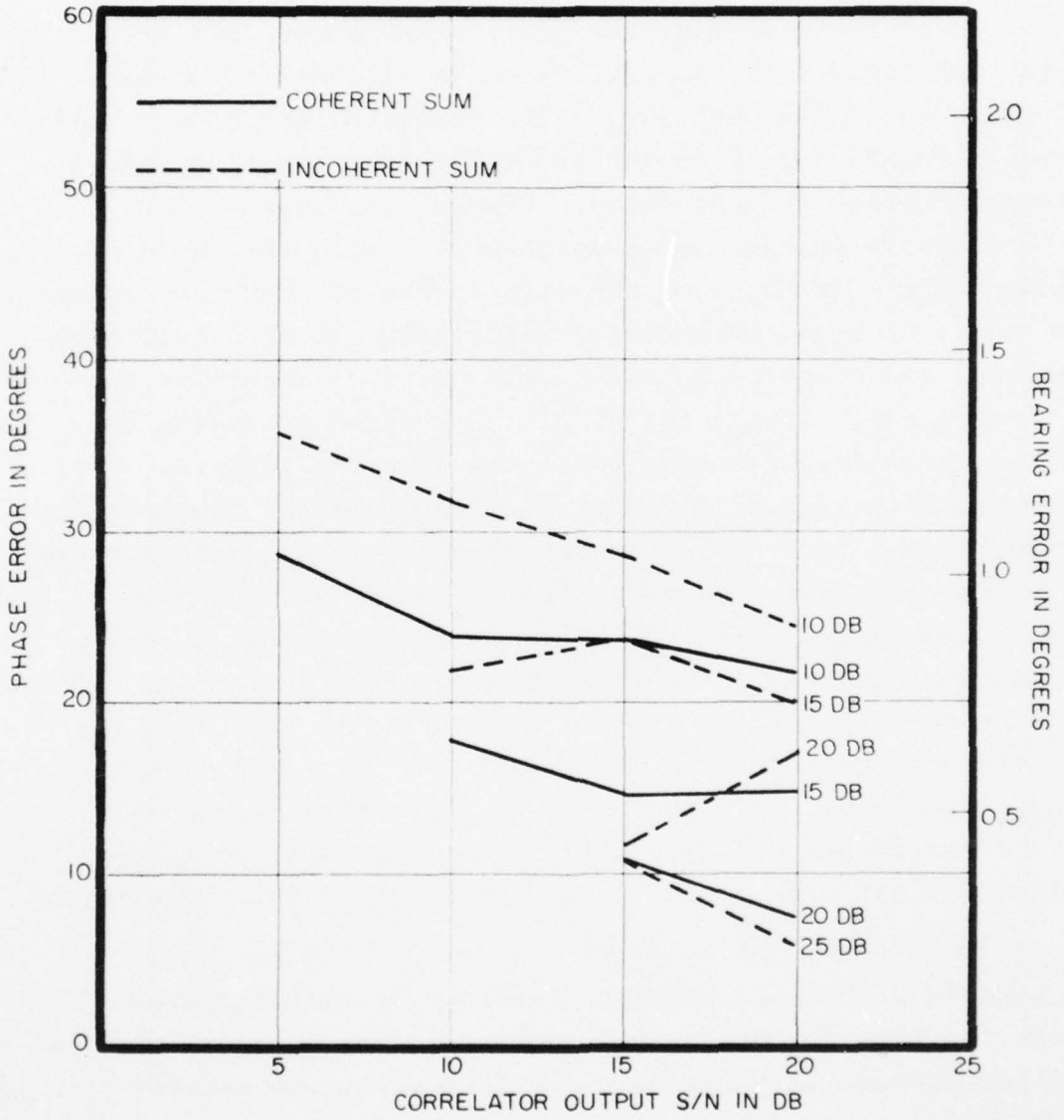

FIG. 4-3 - STANDARD DEVIATION OF PHASE ERRORS FOR VARIOUS BRIGHTENING FUNCTION THRESHOLDS. COHERENT AND INCOHERENT SUMS WITH POSITIVE AND NEGATIVE CROSSINGS IDEAL SIGNALS, 0° BEARING

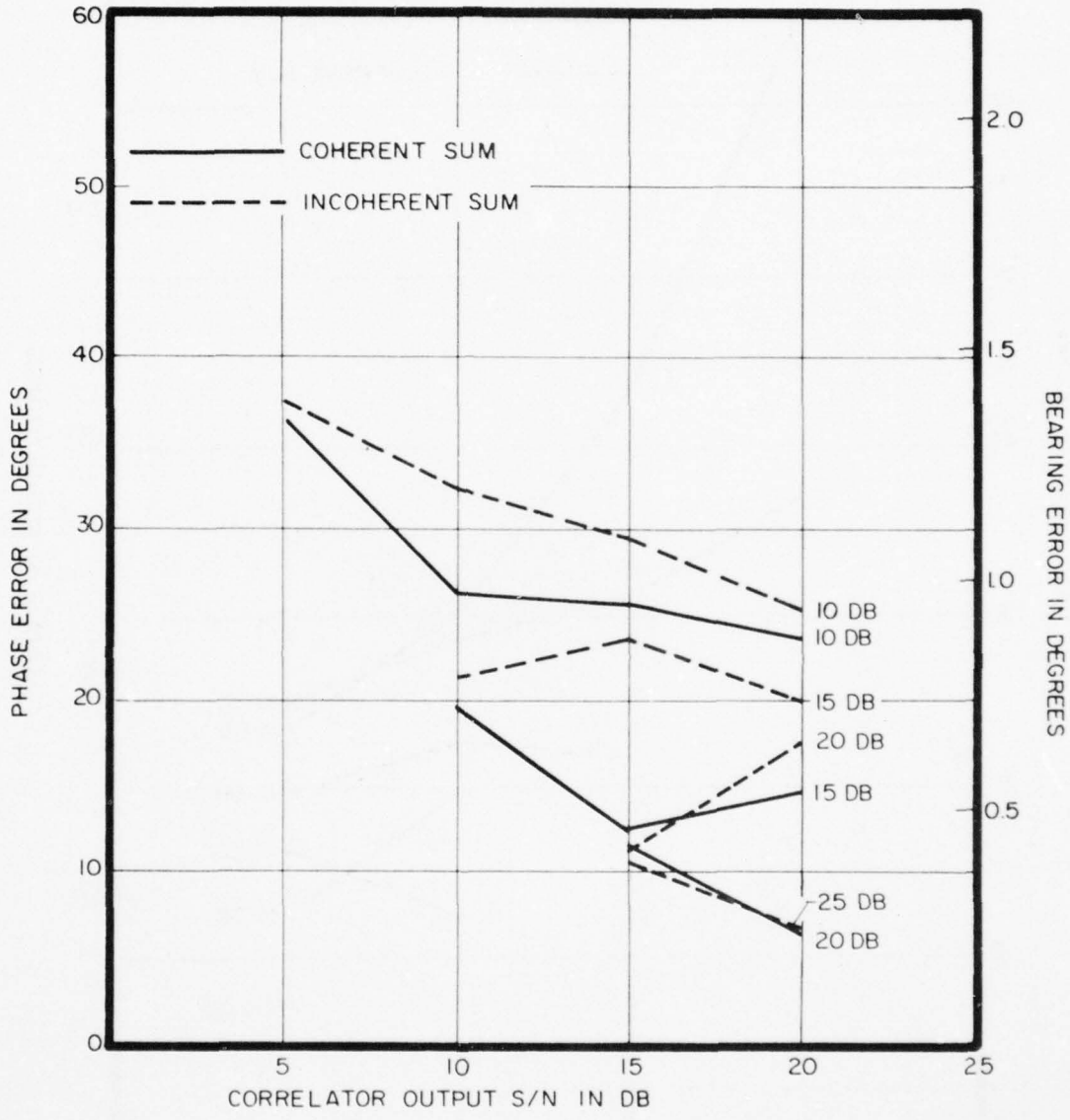

FIG. 4-4 — STANDARD DEVIATION OF PHASE ERRORS FOR VARIOUS BRIGHTENING FUNCTION THRESHOLDS. COHERENT AND INCOHERENT SUMS WITH POSITIVE AND NEGATIVE CROSSINGS IDEAL SIGNALS, 2° BEARING

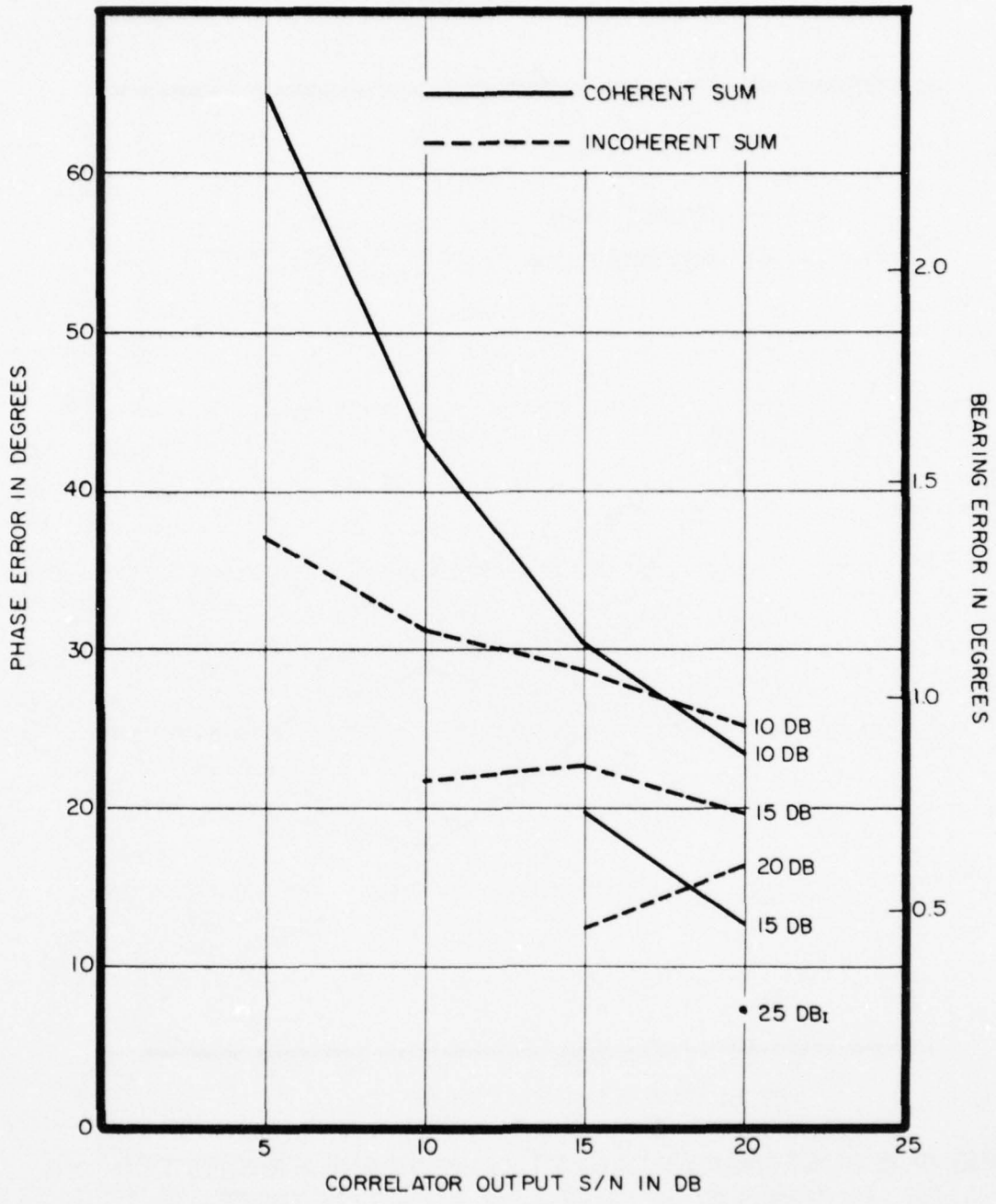

FIG. 4-5 — STANDARD DEVIATION OF PHASE ERRORS FOR VARIOUS BRIGHTENING FUNCTION THRESHOLDS. COHERENT AND INCOHERENT SUMS WITH POSITIVE AND NEGATIVE CROSSINGS IDEAL SIGNALS, 4° BEARING

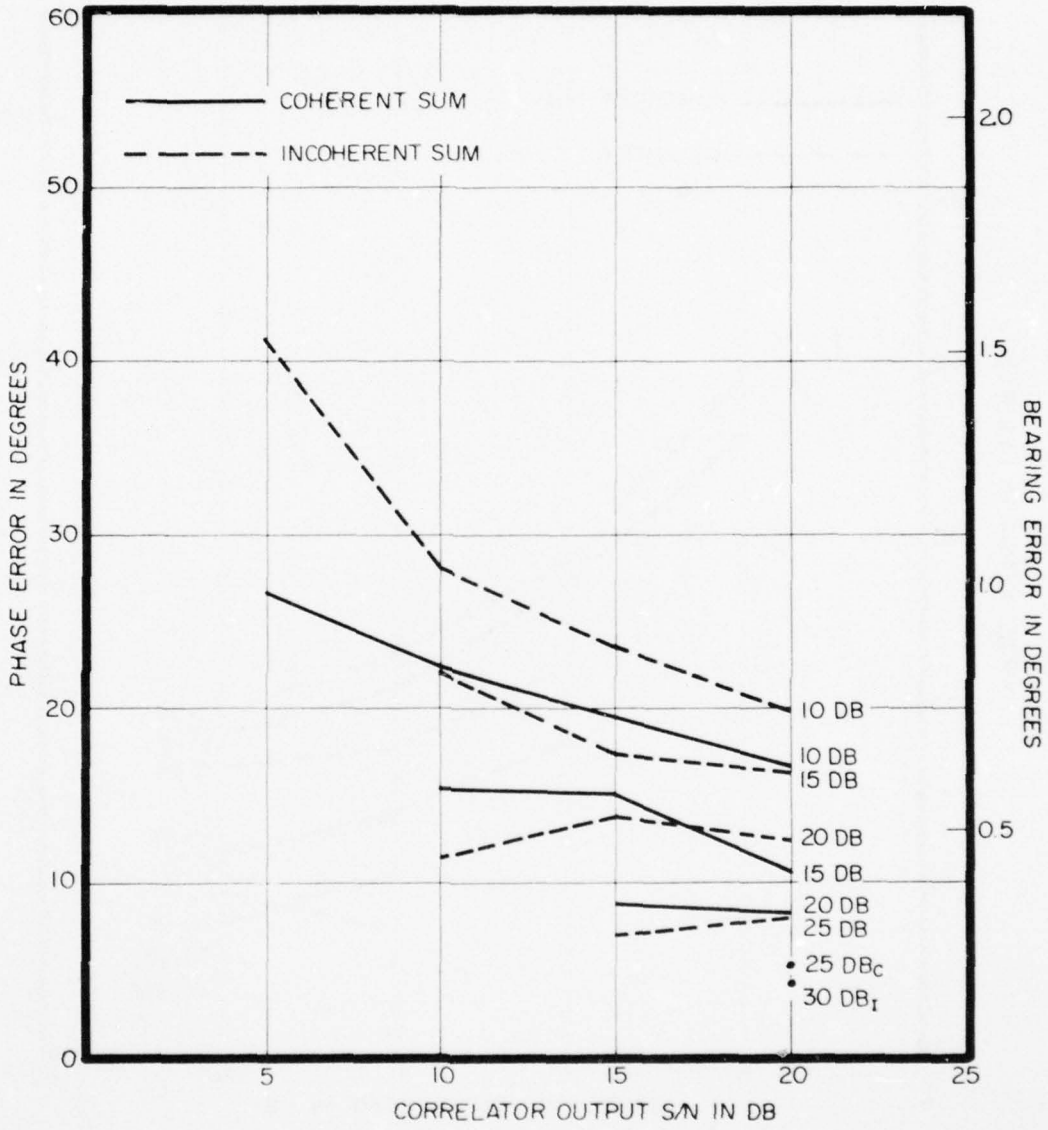

FIG. 4-6 — STANDARD DEVIATION OF PHASE ERRORS FOR VARIOUS BRIGHTENING FUNCTION THRESHOLDS. COHERENT AND INCOHERENT SUMS WITH POSITIVE AND NEGATIVE CROSSINGS JITTERED SIGNALS, 0° BEARING

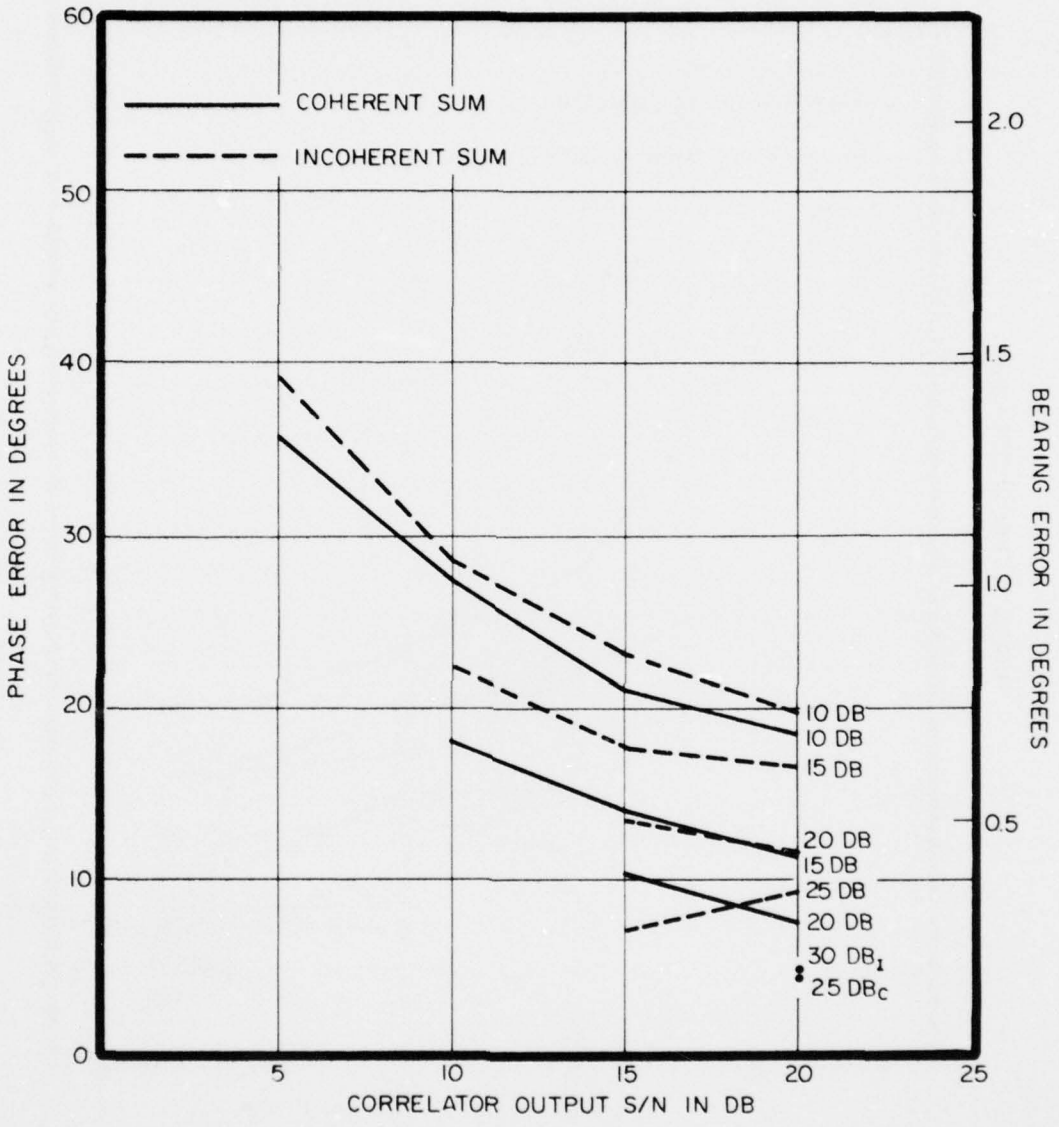

FIG. 4-7 —STANDARD DEVIATION OF PHASE ERRORS FOR VARIOUS BRIGHTENING FUNCTION THRESHOLDS. COHERENT AND INCOHERENT SUMS WITH POSITIVE AND NEGATIVE CROSSINGS JITTERED SIGNALS, 2° BEARING

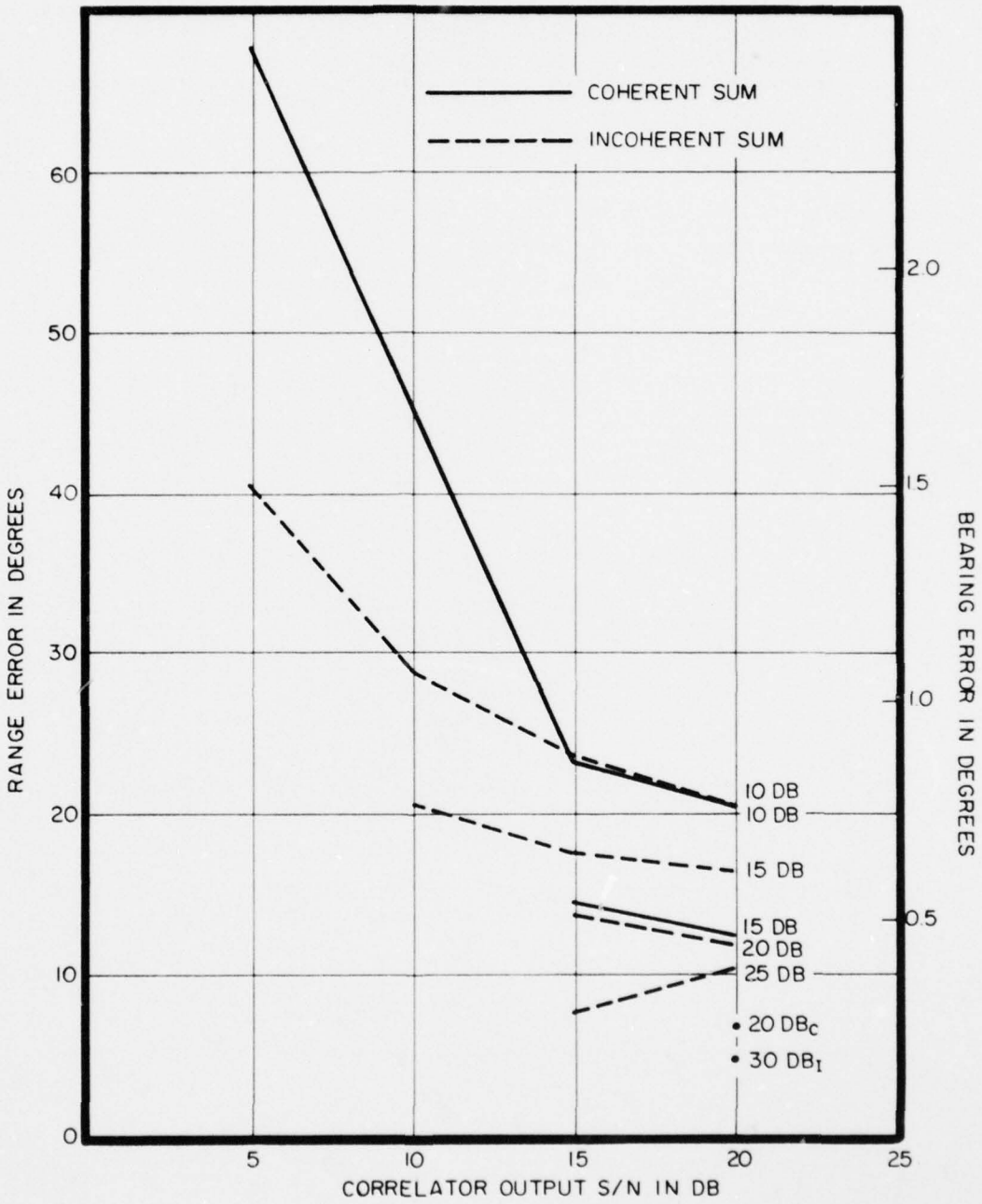

FIG. 4-8 – STANDARD DEVIATION OF PHASE ERRORS FOR VARIOUS BRIGHTENING FUNCTION THRESHOLDS. COHERENT AND INCOHERENT SUMS WITH POSITIVE AND NEGATIVE CROSSINGS JITTERED SIGNALS, 4° BEARING

TRACOR 6500 TRACOR LANE, AUSTIN, TEXAS 78721

5. THE AN/SQS-26(BX) CLIPPED CORRELATOR

Most of the attention given to long range upgrading of the AN/SQS-26 sonar system has been directed toward further improvements in the system. Certain specific problems which have arisen in existing hardware have been investigated, however. The present chapter describes work that was directed toward specific problems associated with the BX system.

Prior to the model CX, AN/SQS-26 systems employed delay line time-compressed (Deltic) clipped correlation. The advantages of such polarity correlation over complete amplitude correlation include the normalizing effect of hard-clipping and the use of digital storage and shift register time delay techniques. Disadvantages appear in the variations in correlation output due to the clipping, especially for structured signals.

The problems considered in this chapter relate to two tests, the first conducted at the EDO Corporation and the second aboard the USS WAINWRIGHT (DLG 28).

5.1 THE EDO TESTS

A brief test of the AN/SQS-26(BX) clipped correlator signal processor and display was conducted 2-4 February 1966 in cooperation with the EDO Corporation at their plant in College Point, N. Y. The purpose of these tests was to check the processing gain of the deltic correlator processor using both controlled signals and noise and sea test data on magnetic tape as input. The same data were input to a computer-simulated clipped correlator which acted as the performance reference. Further comparisons were made with a computer-simulated linear correlator. The uniformity of the "A" scan display of the coded channel outputs was checked by photographing the display output while using the same input signal data on each of the 12 channels of the processor. The photographs show qualitatively the degree of channel equivalence.

Analog data from magnetic tapes were used as input to the system. The test results indicate that the hardware processor performs in accordance with theoretical processing gain design criteria and that the display is normalized across the twelve beams processed in the system. The average difference between the theoretical and the actual gain in output signal-to-noise ratio is less than 1 dB, which is within the range of statistical measurement error for these data.

5.1.1 Generated Signal Input

Figure 5-1 shows oscilloscope photographs made at the test site comparing the computer simulated and AN/SQS-26(BX) processor outputs displayed as "A" scans for several levels of output signal-to-noise ratio. The input data and reference pulse are also shown. A sea test echo with very little energy splitting is shown in the lower right corner of the figure. In each case the hardware correlator outputs were equivalent to those of the simulated correlator reference.

Figure 5-2 gives a comparison of threshold crossing rate vs threshold for the processor output sets. Since sufficiently large noise set was not available, the curves are extrapolated beyond a threshold of four units of standard deviation relative to the mean. The difference between the two noise sets is due to the difference in the computer-simulated and hardware detector-averager processes that follow the clipped correlators.

The difference between the curves shown in Fig. 5-2 may be used to determine the line of equivalent performance based on equivalent false alarm rates. Figure 5-3 gives a plot of output signal-to-noise ratio for the computer-simulated processor vs output signal-to-noise ratio for the AN/SQS-26(BX) processor on a point for point basis, using generated signal input. The line of equivalent performance fits through these points well, showing less than 1 dB greater processing gain for the computer simulated processor.

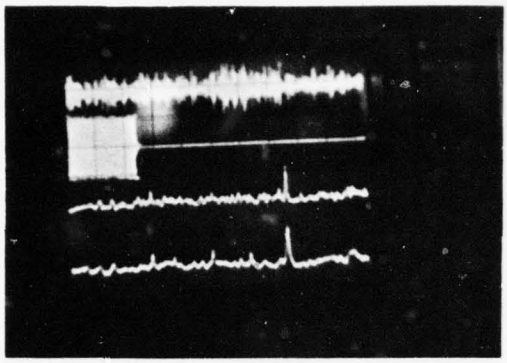

1.
2.
3.
4.

23 dB

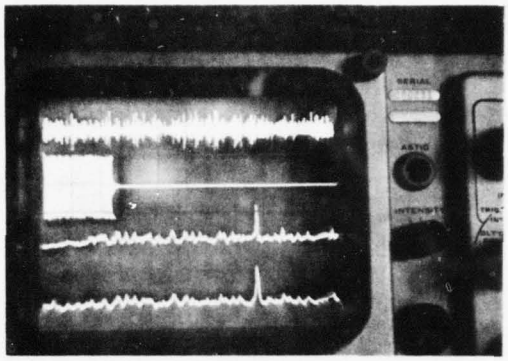

1.
2.
3.
4.

19 dB

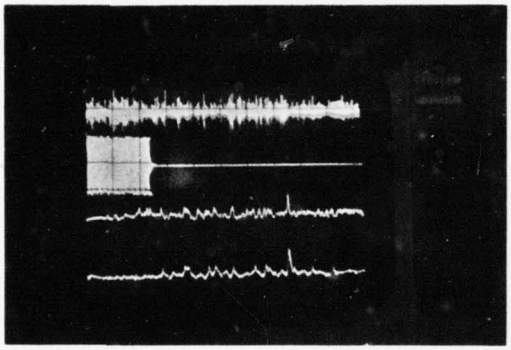

1.
2.
3.
4.

17 dB

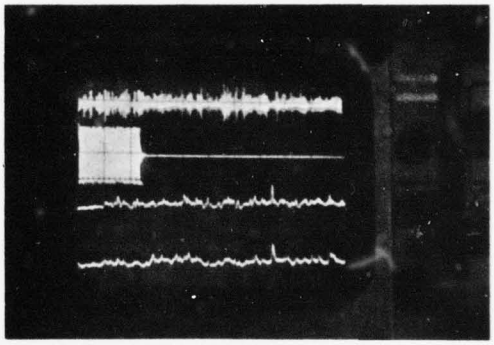

1.
2.
3.
4.

13 dB

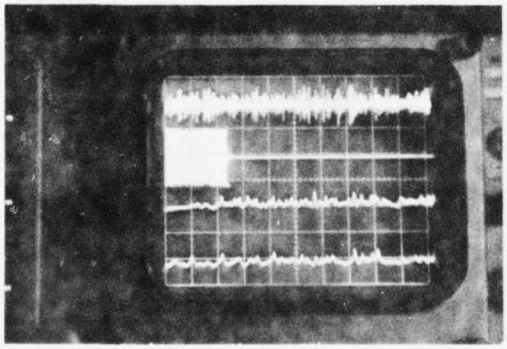

1.
2.
3.
4.

9 dB

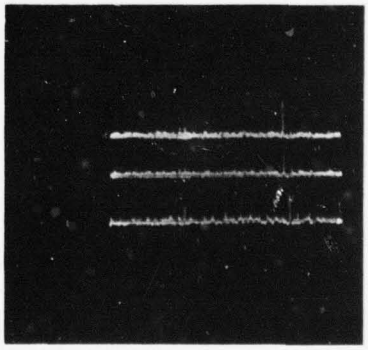

5.
6.
7.

SEA TEST ECHO

Figure 5-1 OSCILLOSCOPE PHOTOGRAPHS COMPARING COMPUTER SIMULATED AND AN/SQS-26(BX) CLIPPED CORRELATOR PROCESSORS.

1. Raw Data
2. Correlator Reference
3. Computer Simulated Processor Output
4. AN/SQS-26(BX) Clipped Correlator Output
5. Computer Simulated Linear Correlator Output
6. Computer Simulated Clipped Correlator Output
7. AN/SQS-26(BX) Clipped Correlator Output

Fig. 5-2 RATE OF EXCEEDING THRESHOLD VS THE THRESHOLD AT THE OUTPUT OF THE AN/SQS-26(BX) AND COMPUTER SIMULATED CLIPPED PROCESSORS.

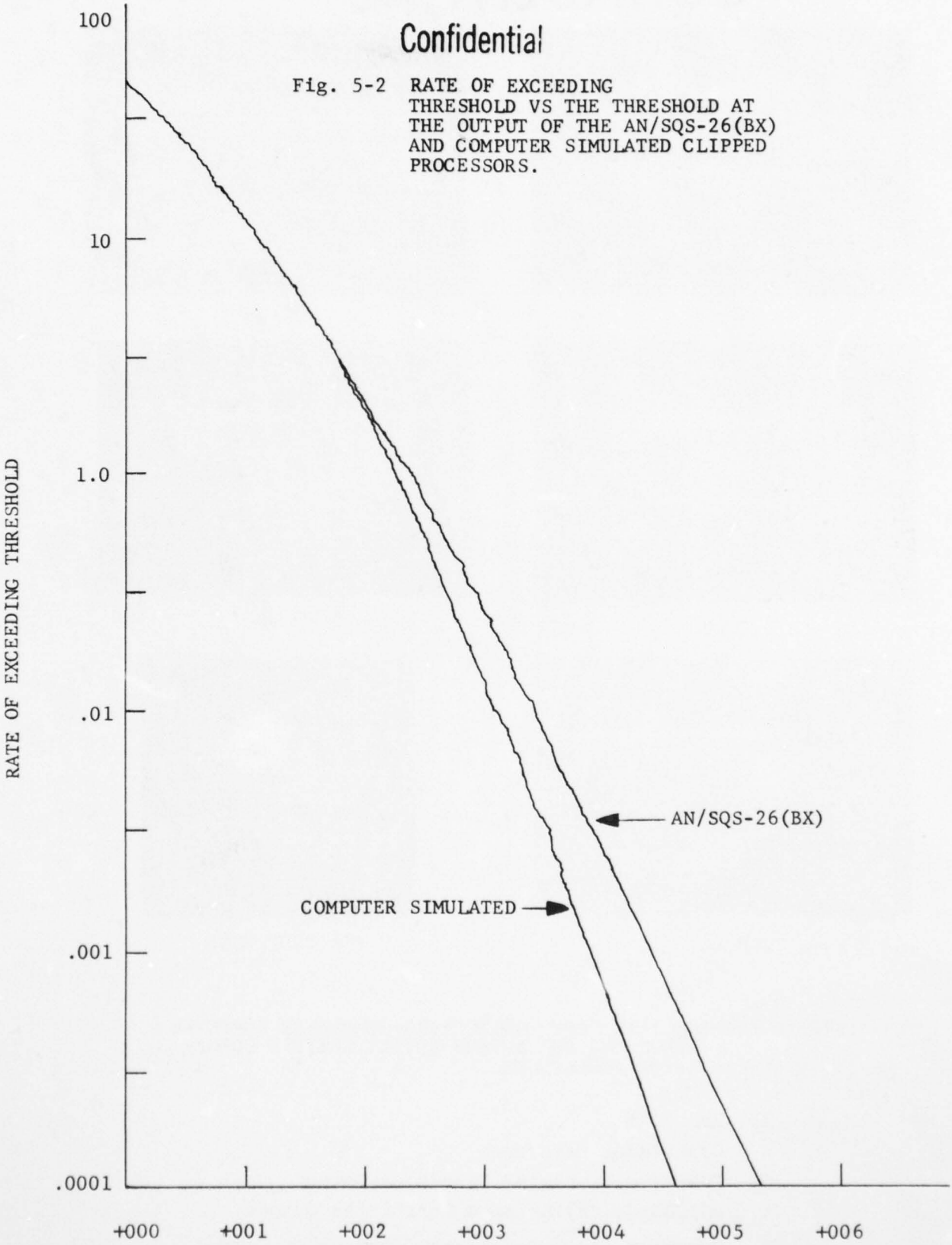

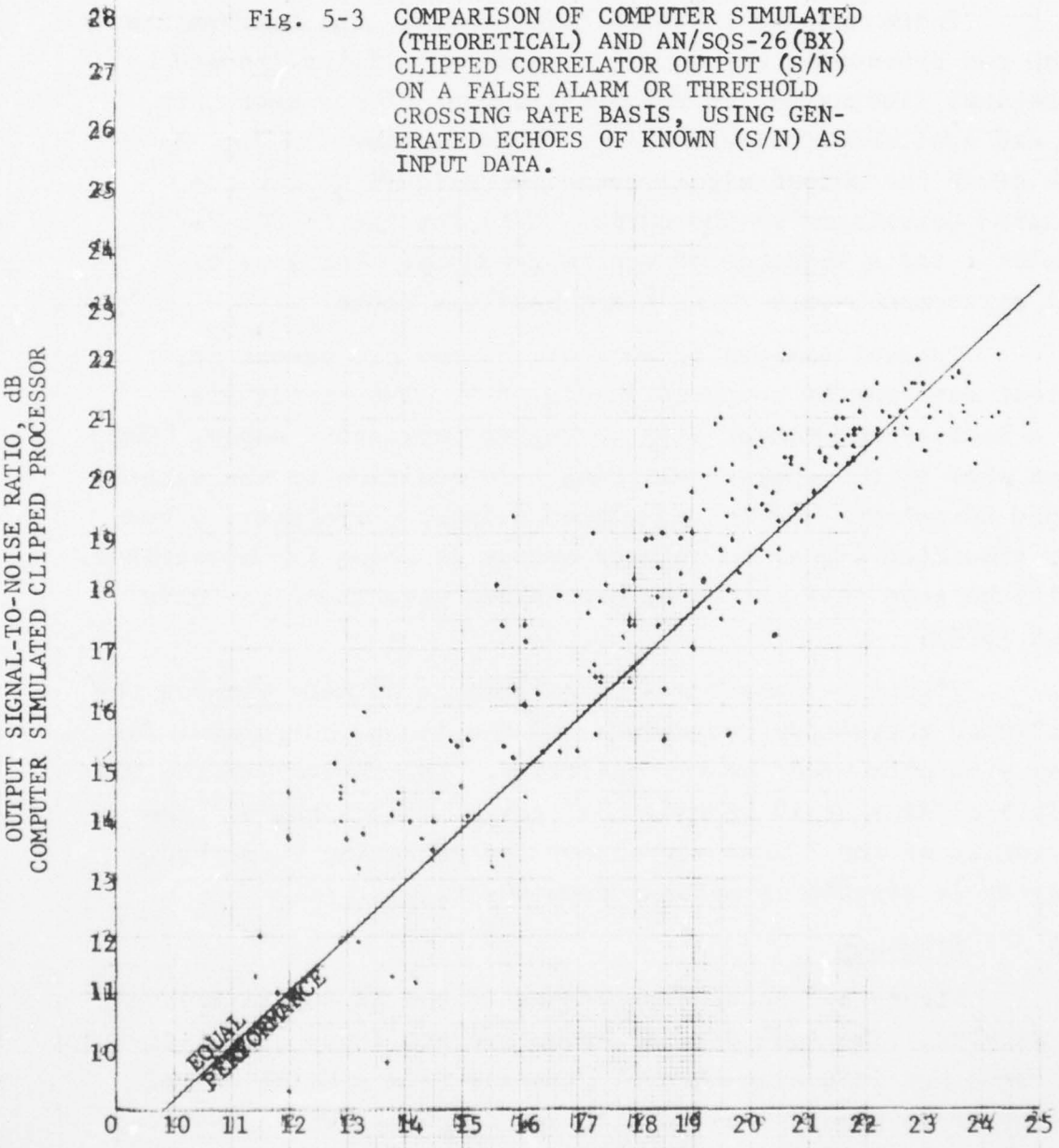

Fig. 5-3 COMPARISON OF COMPUTER SIMULATED (THEORETICAL) AND AN/SQS-26(BX) CLIPPED CORRELATOR OUTPUT (S/N) ON A FALSE ALARM OR THRESHOLD CROSSING RATE BASIS, USING GENERATED ECHOES OF KNOWN (S/N) AS INPUT DATA.

5.1.2 Sea Test Data Input

There appears to be no difference in the performance of the two processors within the measurement limits imposed by statistical fluctuation in the small amount of sea test data that was available for processing. This is shown in Fig. 5-4 which gives the output signal-to-noise ratio (S/N) for the simulated correlator vs the output (S/N) for the AN/SQS-26(BX) correlator for a sequence of sea test echoes. The line of equal performance on a false alarm basis is shown.

Typical Sanborn outputs of the two processors for sea test data may be compared in Fig. 5-5. The echoes are from a beam aspect target at a 15 degree depression angle. The echoes show little energy splitting. In addition to the actual clipped correlator and the simulated clipped correlator, a computer simulated linear correlator output is shown for comparison. It will be seen that the three processors give about the same output (S/N).

Figure 5-6 enables a comparison to be made between the two clipped correlator processors and the linear correlator for echoes with pronounced energy splitting. The target was the USS NAUTILUS closing at 10 knots at 34^{o} target aspect angle. The superiority of the linear correlator for detecting these badly energy-split signals is evident from the figure.

5.1.3 Displays

Figure 5-7 shows photographs of the AN/SQS-26(BX) "A" scan display. The same data of known average input signal-to-noise ratio were put into each channel by means of a special set of transformer coupled "signal splitting" circuits, which assured inter-channel isolation. The display traces are twenty seconds long with signals spaced three seconds apart. The signals are displayed with both amplitude and intensity modulation. Inter-channel normalization is evident by the constancy of length and

AD-A067 035 TRACOR INC AUSTIN TEX F/G 17/1
LONG RANGE UPGRADING OF THE AN/SQS-26.(U)
AUG 67 C H HAYES NOBSR-95149
UNCLASSIFIED TRACOR-67-693-C NL

2 OF 2
AD A
067035

END
DATE
FILMED
6-79
DDC

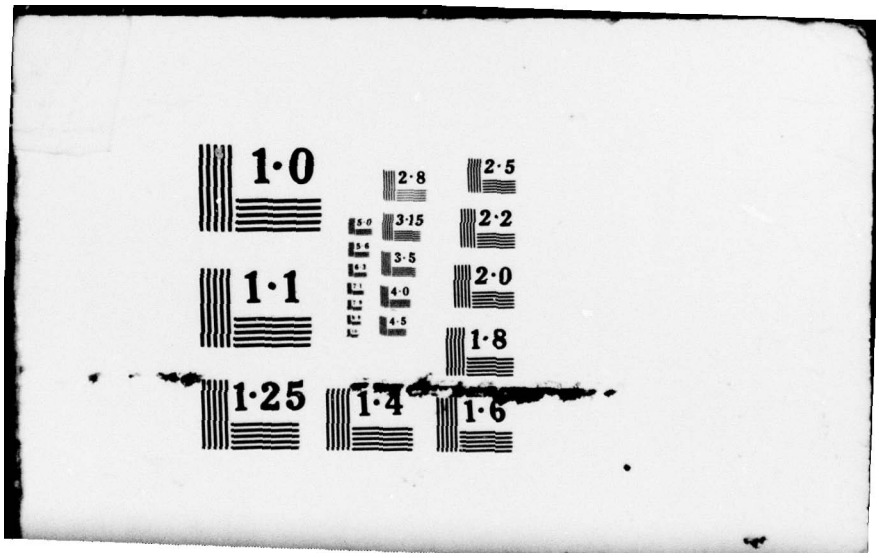
1·0
1·1
1·25
1·4
1·6
2·8
3·15
3·5
4·0
4·5
2·5
2·2
2·0
1·8

FIG. 5-4 COMPARISON OF COMPUTER SIMULATED (THEORETICAL) AND AN/SQS-26(BX) CLIPPED CORRELATOR OUTPUT (S/N) ON A FALSE ALARM OR THRESHOLD CROSSING RATE BASIS, USING SEA TEST DATA ECHOES AS INPUT.

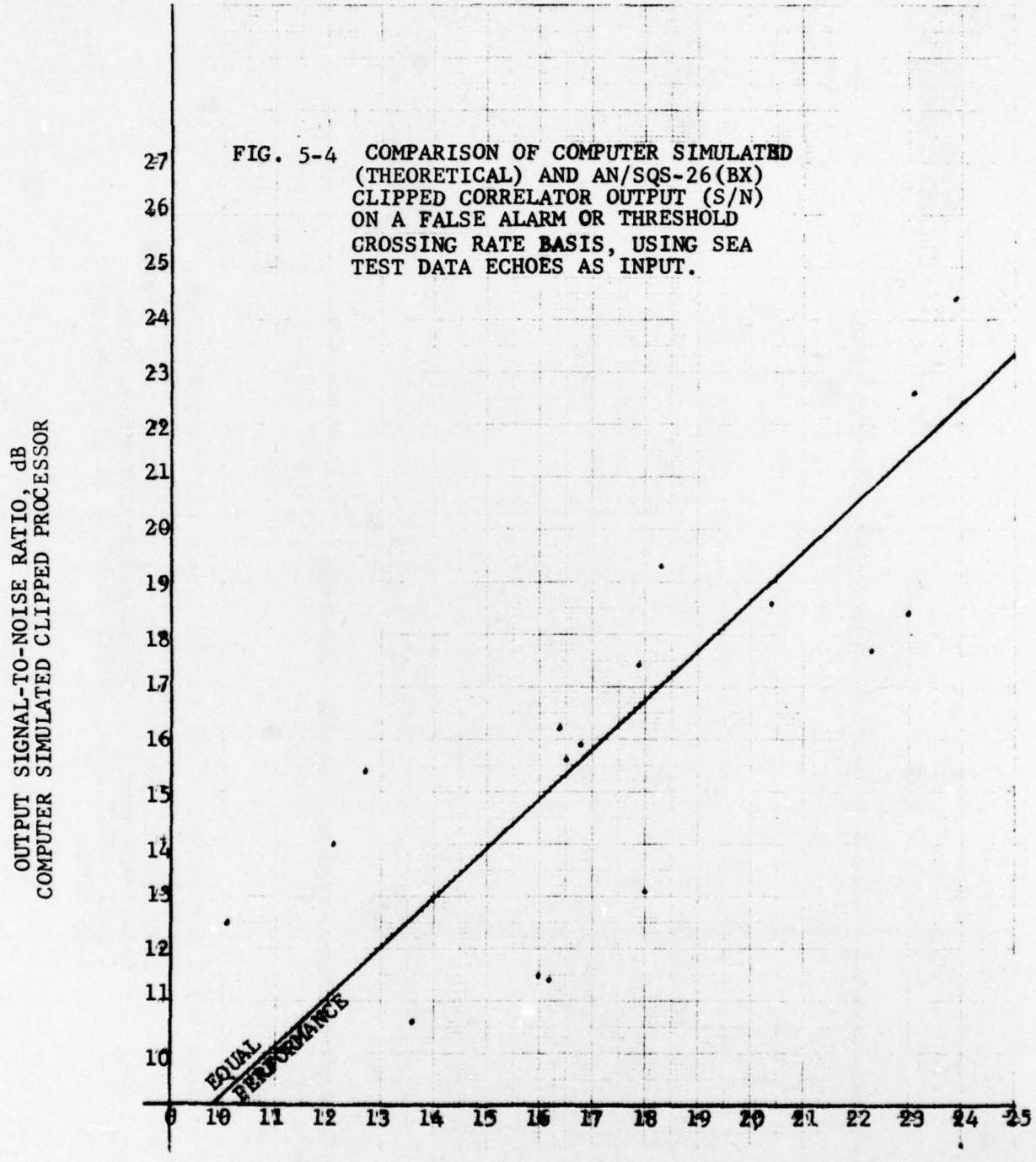

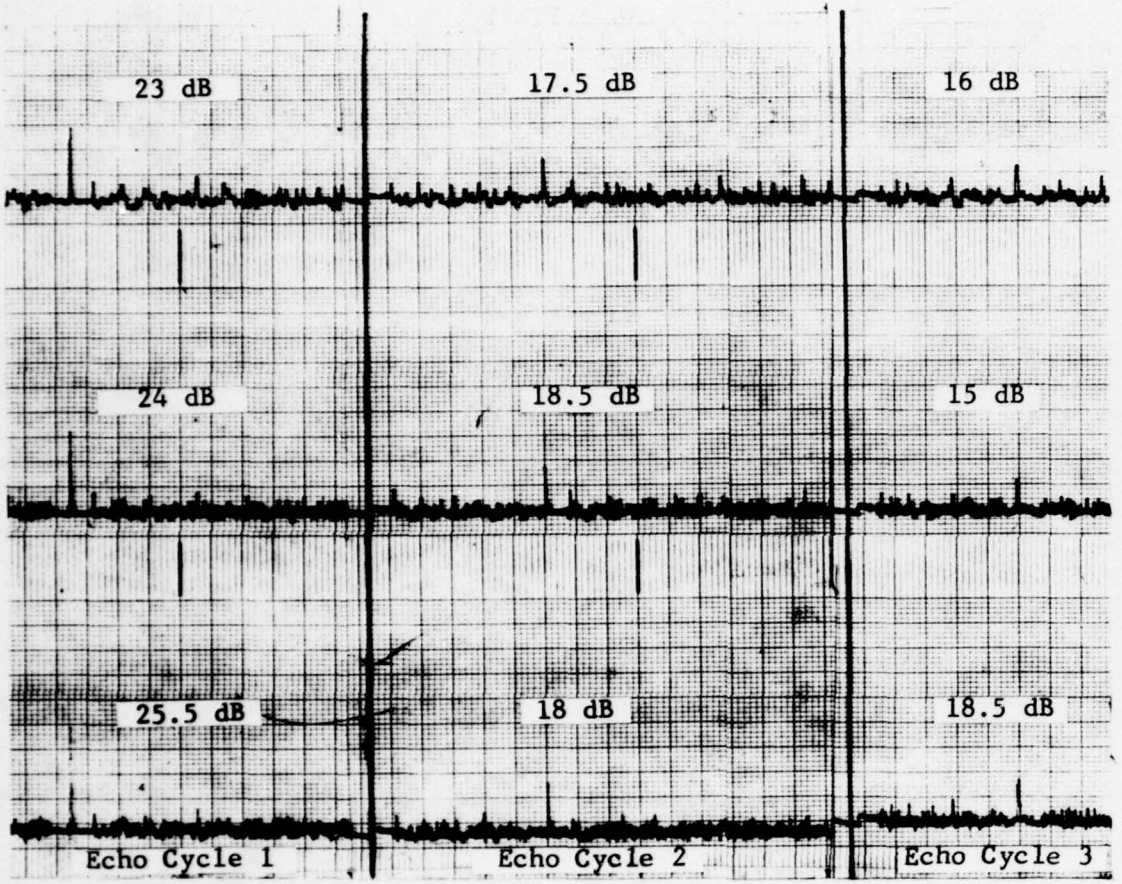

Figure 5-5 A COMPARISON OF THE AN/SQS-26(BX) CLIPPED CORRELATOR, COMPUTER SIMULATED CLIPPED CORRELATOR, AND COMPUTER SIMULATED LINEAR CORRELATOR USING SEA TEST DATA INPUT. DATA TAKEN FROM A 15 DEGREE DEPRESSION ANGLE, BEAM TARGET ASPECT RUN. OUTPUT (S/N) IN dB IS SHOWN FOR EACH ECHO.

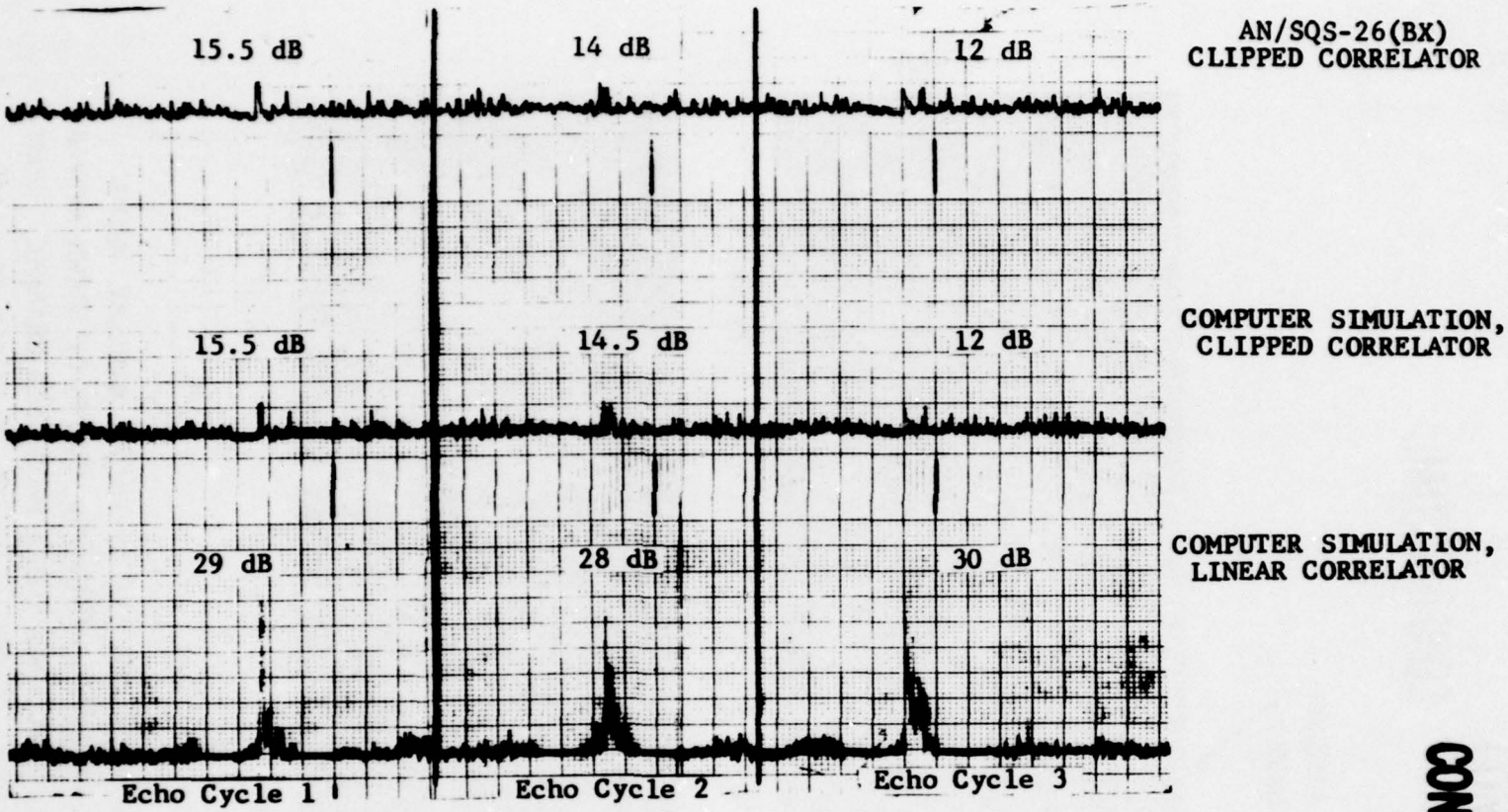

Figure 5-6 A COMPARISON OF THE AN/SQS-26(BX) CLIPPED CORRELATOR, COMPUTER SIMULATED CLIPPED CORRELATOR, AND COMPUTER SIMULATED LINEAR CORRELATOR USING SEA TEST DATA INPUT. DATA TAKEN FROM A CLOSING TARGET (10 KNOT), 34° ASPECT RUN.

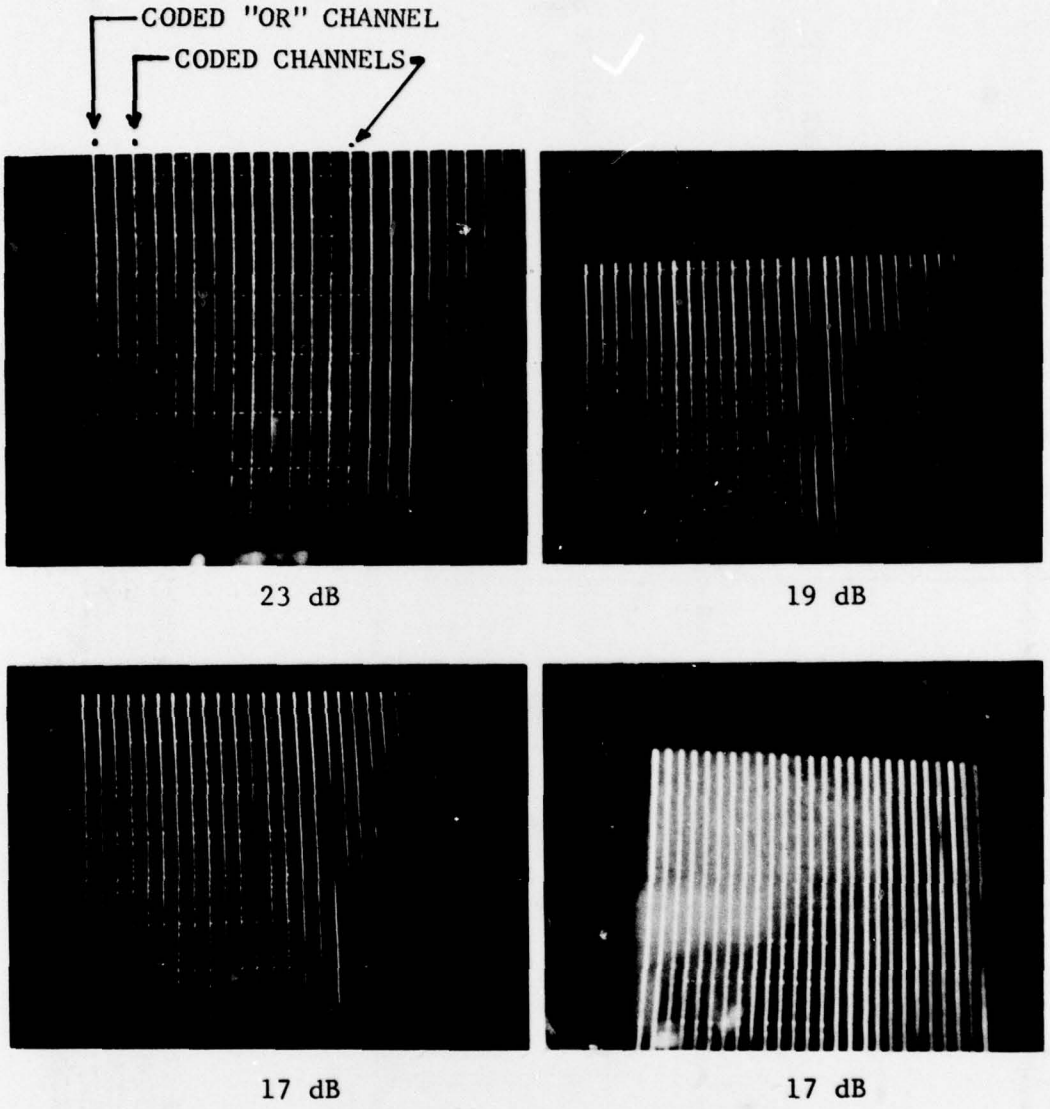

Figure 5-7 PHOTOGRAPHS OF THE AN/SQS-26(BX) DISPLAY USING THE SAME COMPUTER GENERATED INPUTS OF KNOWN AVERAGE INPUT (S/N) TO EACH CODED PROCESSOR CHANNEL. NOMINAL PROCESSOR OUTPUT (S/N) IS INDICATED FOR EACH DISPLAY. TOTAL DISPLAY SWEEP IS 20 SECONDS WITH SIGNALS 3 SECONDS APART.

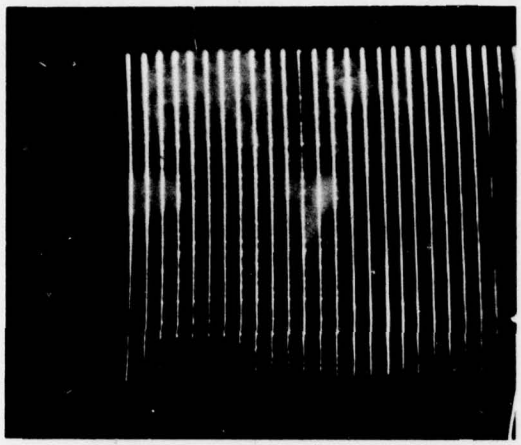

13 dB

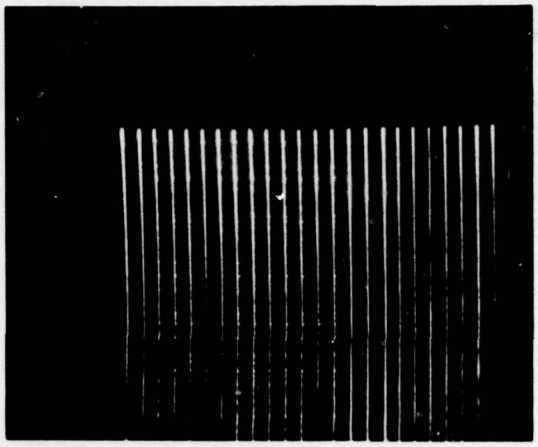

13 dB

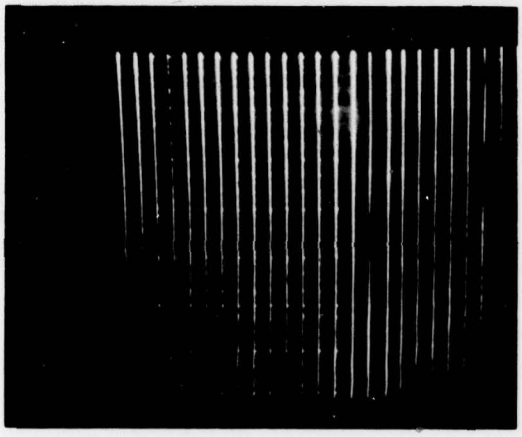

13 dB

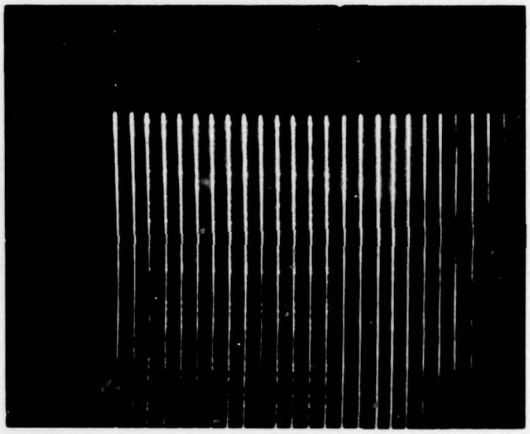

13 dB

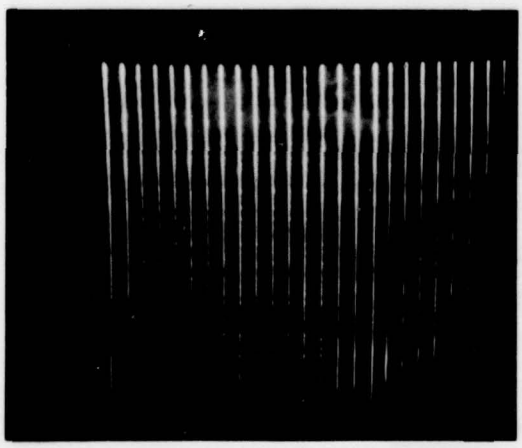

9 dB

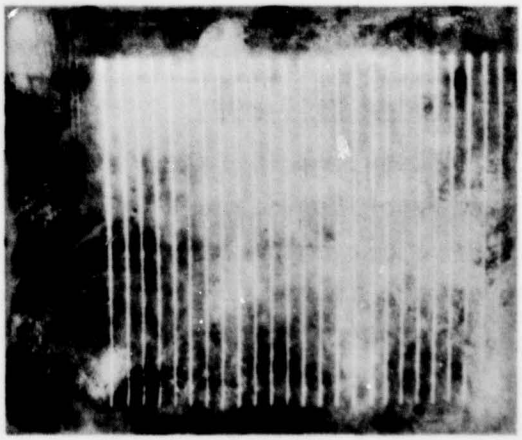

9 dB

Figure 5-7 (continued)

intensity across the twelve channels. The difference in intensity from the top to the bottom of each channel trace shown in the photographs actually appeared in the display. This difference in intensity was independent of the amplitude modulation and did not greatly affect the ability to see the signals.

5.2 THE WAINWRIGHT TESTS

This section discusses the analysis of AN/SQS-26(BX) data from the USS WAINWRIGHT (DLG 28) sea test conducted during the period 28 May through 23 June 1966 to investigate the causes and extent of system performance degradation observed intermittently during the tests for closing target runs.

The method of approach to the problem was to investigate those system areas which would normally be suspect from the symptoms exhibited in the loss of performance. Experimental work subsequent to the sea test consisted of dockside and limited checks at sea of the USS WAINWRIGHT (DLG 28) system, various checks on the barge system, and analysis of tape recorded data. Tests on the barge and shipboard systems were unable to duplicate the system performance degradation problem that existed during the sea trials. The analysis of the sea test data at TRACOR did not yield a clear cut determination of any specific system failure that could cause a loss in performance to the 5 dB extent indicated from the MDL measurements made at sea. The following items were investigated by TRACOR with the results indicated.

5.2.1 Coded Processor

Tape-recorded data at the SSI output, input to AGC, and coded processor input were analyzed using a computer simulated processor to determine whether more echoes were present at these earlier points in the system than in the hardware coded processor output. No additional echoes were found to be present at these earlier points in the system, indicating that the hardware processor was performing properly on the runs checked.

5.2.2 ODN Frequency

The ODN frequency was checked using the transponder return on closing and parallel runs. The ODN frequency error was found to be 10 Hz or less, which would cause no more than 1 dB loss in coded processing gain.

5.2.3 Echo Observations

The number and strength of echo observations by TRACOR from paper recordings of the processor output were in agreement with those of shipboard observers at the display, indicating that the display was not likely at fault.

5.2.4 Search vs Track Mode

The percentage of returns was better for the track mode than for the search mode of operation for both closing and parallel runs. MDL measurements in the track mode were roughly 3 dB better on the average than in the search mode. In the data there is apparently a higher reverberation level in the search mode than in the track mode. It is felt that this higher reverberation level is a contributing factor in the observed difference between the two modes with respect to percentage of returns and MDL measurements.

5.2.5 Target Tracking Considerations

There were 25 parallel and 11 closing runs in the AREA BRAVO data considered here. The runs were made as shown in Fig.5-8.

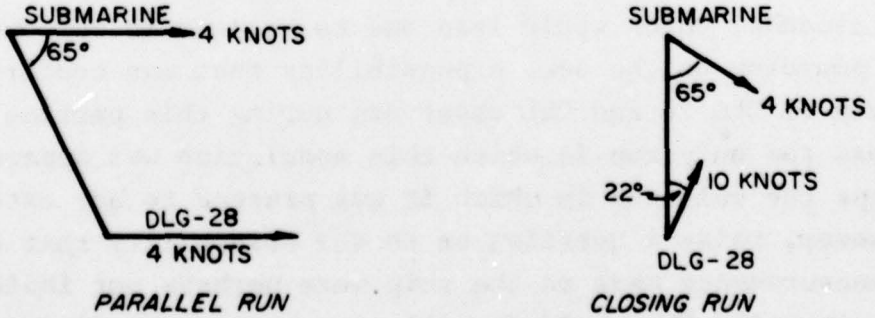

FIG. 5-8 – TARGET TRACKING GEOMETRY

As a practical matter, one would expect that it would be more difficult to maintain position and track the target on the closing runs. In addition to this the target is moving through the annulus during the closing runs, which would lead to changes in echo strength not expected in parallel runs.

In an attempt to establish the existence of a target tracking problem the levels of the transponder returns were examined for closing and for parallel runs. The transponder return levels vary greatly from one ping to the next on both types of runs, but the levels appear generally higher on parallel than on closing runs.

The above observations lend credence to the idea that inability to track the target accurately through the annulus on beam 6 (since observations and recordings were made only on beam 6) is at least a contributing factor to the decrease in percent returns for the closing runs.

5.2.6 Self-Noise

Closing runs were conducted at a speed of 10 knots, and parallel runs at 4 knots. The increase of own ship's speed from 4 to 10 knots was reported not to affect the background level measured at sea. This is mentioned in order to call attention to Run 6A, a closing run, which exhibited a varying modulation that consistently appeared from the front end of the system to the input to the coded processor. The period of this modulation was about three seconds, which would lead one to believe it was due to the seas pounding on the bow, a possibility that was confirmed by the captain of DLG 28 and USL observers during this particular run. This was the only run in which this modulation was apparent and is perhaps the only one in which it was present to any extent. It does, however, raise a question as to the possibility that the self-noise measurements made on the ship were perhaps not indicative of the situation that held for all time periods or directions of listening beam training during the tests.

For closing runs, the expected strength of echo returns was somewhat lower than for parallel runs. Normally, the search mode of operation was employed in closing runs, thus increasing the reverberation level by some 3 dB over the parallel runs which employed the track mode. The expected strength of echo returns was thus in the region of 14-16 dB output (S/N). In the region of 14-16 dB output (S/N) a threshold setting which results in 50-60% probability of detection at a given input (S/N) will yield only 30-40% probability of detection if the input (S/N) is reduced by only 2 dB. Difficulty in tracking the target might have provided a degradation of from one to three dB, depending on how far the target varied off beam 6. This degradation, coupled with higher reverberation levels during closing runs, would have drastically affected the expected detection probability. This comment is based upon observations of strip chart recordings and measurements of changes in probability of detection at constant false alarm rates and constant thresholds. Although this effect may not apply identically to the operator and display in the shipboard environment, the possibility that a similar effect may occur should be considered.

5.2.7 Conclusions Regarding Performance Degradation

The analysis of the tape-recorded data does not indicate that a system failure caused the system performance degradation experienced at sea. The observations made in the analysis of the problem lead to the conclusion that the poor performance on closing runs relative to the parallel runs may be caused by a combination of interrelated incremental "1 dB" effects, which add up to significantly degraded performance.

It is doubtful that subsequent analysis of the sea test data presently available will pinpoint the source of the problem that existed on this sea test or aid quantitatively in the prediction of the effectiveness of the operational performance of

the AN/SQS-26(BX). This was a limited test with a minimal amount of instrumentation; the resultant data were not intended to do much more than demonstrate the operation of the system at sea. Many items of data and useful channels of recorded information necessary for the analysis of a subtle performance degradation problem were not planned for, and are consequently not available. It is recommended that any future tests be planned around a meticulous instrumentation and data-taking scheme capable of both recording data and making at-sea checks that would aid in pinpointing the problem, or problems, if the situation repeats itself.

6. SUMMARY AND CONCLUSIONS

Some of the more important conclusions to be drawn from the investigations reported in the previous chapters are summarized below.

A major portion of this report concerns echo energy splitting. The importance of this topic is based on the fact that actual sea echoes are energy-split to varying degrees, that is, they are made up of many signals with different Doppler shifts and time delays. For computer simulations, echo energy splitting therefore presents a problem of realism. Processor simulations using ideal signals have been useful in the past and are still suitable for some purposes; but more realistic simulations are required in increasingly many cases as more subtle differences between processors are investigated. Simulations of energy-split signals such as described in Section 2 should be used for future processor comparisons.

In addition to its importance to simulation techniques, echo energy splitting presents a challenge to processor design. One method of nullifying the effects of energy splitting was investigated in Section 2. This method, adaptive recombination, was effective as a computer simulation without real time requirements. The possible application of such techniques to real time shipboard equipments should be considered.

The importance of normalizing the output of the signal processor is due to the fact that, if the processor output is not kept within the range of the display, performance degradation will result. Effective normalization techniques must involve time constants that are long with respect to the signal. Because the correlation process results in a time compression, the output of a correlator is particularly amenable to normalization procedures. This characteristic of correlation combined with the fact that unnormalized correlator output was found to have a relatively invarient

ratio of mean and standard deviation, permitted an effective normalization technique to be employed in a computer program. The development of similar techniques for hardware applications is suggested in Section 3.

In Section 4 an investigation was made of the application of advanced signal processing techniques to enhance signal-to-noise ratio prior to the SSI display. Quantitative comparisons with other SSI techniques would be necessary before recommendations could be made in regard to the different methods employed in this study.

The problems treated in Section 5 relating to the AN/SQS-26(BX) are illustrative of both the usefulness of simulation techniques in performance evaluation and the need of extending testing instrumentation as more subtle problems are encountered.

UNCLASSIFIED

DOCUMENT CONTROL DATA - R&D

(Security classification of title, body of abstract and indexing annotation must be entered when the overall report is classified)

1. ORIGINATING ACTIVITY (Corporate author)	2a. REPORT SECURITY CLASSIFICATION
TRACOR, Inc. 6500 TRACOR Lane Austin, Texas 78721	CONFIDENTIAL
	2b. GROUP 4

3. REPORT TITLE

LONG RANGE UPGRADING OF THE AN/SQS-26(U)

4. DESCRIPTIVE NOTES (Type of report and inclusive dates)

Summary Report

5. AUTHOR(S) (Last name, first name, initial)

Hayes, Charles H.

6. REPORT DATE	7a. TOTAL NO. OF PAGES	7b. NO. OF REFS
30 August 1967	106	-

8a. CONTRACT OR GRANT NO.	9a. ORIGINATOR'S REPORT NUMBER(S)
NObsr-95149	67-693-C
b. PROJECT NO SS041-001	
c. 8156, 8193	9b. OTHER REPORT NO(S) (Any other numbers that may be assigned this report) --
d.	

10. AVAILABILITY/LIMITATION NOTICES

11. SUPPLEMENTARY NOTES	12. SPONSORING MILITARY ACTIVITY
	Naval Ship Systems Command Department of the Navy Washington, D. C. 20360

13. ABSTRACT A major portion of this report concerns echo energy splitting. Actual sea echoes are energy-split to varying degrees, therefore, echo energy splitting presents a problem of realism in computer simulations. More realistic simulations will be required as more subtle differences between processors are investigated.

Echo energy splitting also presents a challenge to processor design. One method of nullifying the effects of energy splitting, adaptive recombination, was investigated.

Because the correlation process results in a time compression, the output of a correlator is particularly amenable to normalization procedures. This characteristic of correlation permits an effective normalization technique to be employed in a computer program.

An investigation was also made of the application of advanced signal processing techniques to enhance signal-to-noise ratio prior to the SSI display.

The problems relating to the AN/SQS-26(BX) are illustrative of both the usefulness of simulation techniques in performance evaluation and the need of extending testing instrumentation as more subtle problems are encountered.

DD FORM 1 JAN 64 1473

UNCLASSIFIED

Security Classification

14 KEY WORDS	LINK A		LINK B		LINK C	
	ROLE	WT	ROLE	WT	ROLE	WT
Echo Energy Splitting (Sonar)						
Signal Simulation (Sonar)						
Signal Processor Comparison (Sonar)						
Adaptive Recombination (Sonar)						
Normalization (Sonar)						
Correlation Loss (Sonar)						
AN/SQS-26						
AN/SQS-26(BX)						

INSTRUCTIONS

1. ORIGINATING ACTIVITY: Enter the name and address of the contractor, subcontractor, grantee, Department of Defense activity or other organization *(corporate author)* issuing the report.

2a. REPORT SECURITY CLASSIFICATION: Enter the overall security classification of the report. Indicate whether "Restricted Data" is included. Marking is to be in accordance with appropriate security regulations.

2b. GROUP: Automatic downgrading is specified in DoD Directive 5200.10 and Armed Forces Industrial Manual. Enter the group number. Also, when applicable, show that optional markings have been used for Group 3 and Group 4 as authorized.

3. REPORT TITLE: Enter the complete report title in all capital letters. Titles in all cases should be unclassified. If a meaningful title cannot be selected without classification, show title classification in all capitals in parenthesis immediately following the title.

4. DESCRIPTIVE NOTES: If appropriate, enter the type of report, e.g., interim, progress, summary, annual, or final. Give the inclusive dates when a specific reporting period is covered.

5. AUTHOR(S): Enter the name(s) of author(s) as shown on or in the report. Enter last name, first name, middle initial. If military, show rank and branch of service. The name of the principal author is an absolute minimum requirement.

6. REPORT DATE: Enter the date of the report as day, month, year, or month, year. If more than one date appears on the report, use date of publication.

7a. TOTAL NUMBER OF PAGES: The total page count should follow normal pagination procedures, i.e., enter the number of pages containing information.

7b. NUMBER OF REFERENCES: Enter the total number of references cited in the report.

8a. CONTRACT OR GRANT NUMBER: If appropriate, enter the applicable number of the contract or grant under which the report was written.

8b, 8c, & 8d. PROJECT NUMBER: Enter the appropriate military department identification, such as project number, subproject number, system numbers, task number, etc.

9a. ORIGINATOR'S REPORT NUMBER(S): Enter the official report number by which the document will be identified and controlled by the originating activity. This number must be unique to this report.

9b. OTHER REPORT NUMBER(S): If the report has been assigned any other report numbers *(either by the originator or by the sponsor)*, also enter this number(s).

10. AVAILABILITY/LIMITATION NOTICES: Enter any limitations on further dissemination of the report, other than those imposed by security classification, using standard statements such as:

(1) "Qualified requesters may obtain copies of this report from DDC."

(2) "Foreign announcement and dissemination of this report by DDC is not authorized."

(3) "U. S. Government agencies may obtain copies of this report directly from DDC. Other qualified DDC users shall request through _____."

(4) "U. S. military agencies may obtain copies of this report directly from DDC. Other qualified users shall request through _____."

(5) "All distribution of this report is controlled. Qualified DDC users shall request through _____."

If the report has been furnished to the Office of Technical Services, Department of Commerce, for sale to the public, indicate this fact and enter the price, if known.

11. SUPPLEMENTARY NOTES: Use for additional explanatory notes.

12. SPONSORING MILITARY ACTIVITY: Enter the name of the departmental project office or laboratory sponsoring *(paying for)* the research and development. Include address.

13. ABSTRACT: Enter an abstract giving a brief and factual summary of the document indicative of the report, even though it may also appear elsewhere in the body of the technical report. If additional space is required, a continuation sheet shall be attached.

It is highly desirable that the abstract of classified reports be unclassified. Each paragraph of the abstract shall end with an indication of the military security classification of the information in the paragraph, represented as *(TS)*, *(S)*, *(C)*, or *(U)*.

There is no limitation on the length of the abstract. However, the suggested length is from 150 to 225 words.

14. KEY WORDS: Key words are technically meaningful terms or short phrases that characterize a report and may be used as index entries for cataloging the report. Key words must be selected so that no security classification is required. Identifiers, such as equipment model designation, trade name, military project code name, geographic location, may be used as key words but will be followed by an indication of technical context. The assignment of links, rules, and weights is optional.